Delft University of Technology

Towards environmentally friendly autonomous swarm sailing for environmental monitoring

L.D. Korvemaker

TU Delft

Towards environmentally friendly autonomous swarm sailing for environmental monitoring

by

L.D. Korvemaker

to obtain the degree of Master of Science
at the Delft University of Technology,
to be defended publicly on Wednesday April 30th, 2025 at 13:45.

Student number: 4359550
Project duration: June 20th, 2024 - April 24th, 2025
Thesis committee: Dr. J.H. Boyle, TU Delft, chair
Z.P. Oikonomou, TU Delft, mentor

TU Delft

Summary

Autonomous sailboats (ASBs) have been researched since the early 2000s. Despite their theoretical advantages in autonomous data gathering, especially in the form of swarms, successful real-world deployment remains rare. Many ASBs still fail during deployments in the harsh marine environment, often as a result of structural failures due to their small size and prototype-nature. This thesis began with the observation that small vessels are hard to get right and fail over time. The aim was to explore how to design ASBs with minimal environmental impact, without compromising basic functionality, when embracing the inevitable failure of small ASBs.

Two research questions were addressed: (1) Which low-impact solutions are suitable for use in an autonomous sailboat? (2) How would the design of a low environmental impact autonomous sailboat look?

The methodology involved two complementary tracks. First, a theoretical exploration examined how environmental impact could be reduced by optimizing the swarm system and better material selection. Through a dimensional analysis of naval parameters it was concluded that small ASBs travel more slowly, but collectively in a swarm, achieve higher data collection for the same total material cost as a single large vessel. For a similar material cost, a swarm of smaller ASBs could thus outperform larger vessels in data gathering and less ASBs would be needed to curb environmental impact, so long as the smaller size does not compromise operational reliability.

Material selection was evaluated both from a production and end-of-life perspective. For durable, scalable production, glass fibre composites and steel were identified as relatively low-impact options when balanced against performance needs. A more radical approach explored biodegradable structural materials, particularly flax fibre-reinforced bioplastics. Two resin options, polyglycerol citrate and polyvinyl alcohol, were identified for their environmental degradability and non-toxicity, although practical fabrication challenges limited their evaluation. The total life cycle cost of both approaches cannot yet be known, as the environmental cost of marine litter is not yet quantifiable.

In parallel, a practical design study led to the SDC25 prototype: a small ASB which naval parameters were set using a statistical design approach. These statistics were based on a comprehensive overview of existing ASB designs, compiled during this research and stated for future work. The swarm optimisation analysis provided a good argument to design a small ASB with an overall length of 1.36m. The resulting boat includes a self-trimming wingsail that uses no energy except during manoeuvres, to curb the use of electronic components and energy. Initial testing suggested the vessel was very stable, even though testing quality was limited by calm weather conditions.

A custom-built CNC foam cutter machine played a key role in fabricating the complex curvature of the wingsail and hull. The setup consists of two XY gantries holding a tensioned, heated nichrome wire, which cuts through foam by melting it along a programmed path. The machine, and the generation of the G-code, toolpaths directly from Rhino using Grasshopper, are described.

By being a conceptual design, several uncertainties remain: the relative environmental impact of marine litter compared to production impacts, the exact influence of certain design interventions, the minimum feasible vessel size, whether investing in fleet management is worth the added complexity, and the vessels actual working lifetime all remain uncertain. In light of those uncertainties, few definite conclusions could be drawn, and two production pathways were outlined: a durable, low-impact approach and a fully biodegradable concept.

Contents

1

Introduction & motivation

This thesis outlines a roadmap towards environmentally friendly marine monitoring using a swarm of autonomous sailboats. ”Environmentally friendliness” is defined by the total lifecycle costs (LCA) of the vessels together with the environmental impact of their degradation in the marine environment.

After reviewing relevant literature, this work explores solutions and ends with the design, engineering and testing of a small, unmanned, autonomous sailboat, all the while reflecting on gaps in knowledge and challenges encountered along the way.

Examining previous autonomous sailing projects, it is reasonable to assume that these vessels will have a limited lifespan and degrade during deployment, as the marine environment is harsh for small vessels. Despite this, the advantages of small swarm robots could outweigh the drawbacks - provided that their potential to become marine debris is considered during the design phase. Avoiding contribution to marine (plastic) pollution is clearly desirable, as this remains the prevailing reality. In other words, the key question becomes: how can an environmentally friendly sailing drone be designed, given the inevitability that it will eventually become marine debris?

This thesis started as a project exploring the general design of an autonomous sailing vessel for environmental monitoring on inland waters. However, during the first phase of the project, the direction was evaluated and adjusted, as multiple similar research projects had already been conducted. The focus shifted towards the environmental impact of these vessels, particularly because many previous designs failed to survive long-term at sea. The emphasis was on biodegradable structures. Later, this scope expanded to include alternative approaches to environmentally friendly design after testing the selected biodegradable materials proved unfeasible within the time-frame of this thesis. Furthermore, following a thorough analysis of the current state of autonomous sailboats, recommendations are provided for general naval architectural parameters.

The biggest motivation to start this particular project is my interest in multidisciplinary engineering. During my time at Industrial Design Engineering, I opted to broaden my engineering skills during my minor project and by taking courses from Maritime, Mechanical and Aerospace Engineering. Especially during my minor project at Maritime Engineering, and the project Advanced Embodiment Design in the Integrated Product Design master, I discovered my passion for making technically ambitious ideas into reality.

Chapter 2 reviews the state of the art and provides background information. Chapter 3 defines the problem. Chapter 4 then provides insights into challenges assessing the impacts during a life cycle and presents a roadmap towards environmentally friendly saildrones. Chapter 5 details the interventions described in the roadmap. Chapter 6 integrates all learnings into a design concept and evaluates the concept with an integrated prototype. Finally, Chapter 7 discusses and concludes this work.

2

Literature review & background

This chapter provides relevant background information and reviews the state of the art across multiple research fields related to this project.

Section 2.1 explores environmental monitoring. This is followed by an analysis of swarm robotics in Section 2.2. Moving forward, Section 2.3 addresses autonomous surface vessels. This chapter then moves on to the domain of sailing in Section 2.4, leading to a focused examination of autonomous or robotic sailing in Section 2.5.

For this review, relevant papers were identified by searching article databases using multiple variations of the section titles. Citation searching and the snowball method were also employed, examining both the references cited in the papers and the newer works that referenced those papers.

2.1. Environmental monitoring

Environmental monitoring plays a central role in diagnosing climate impacts on natural systems and is becoming increasingly important due to growing concerns about global climate change and its regional effects (Lin & Yang, 2020; Manfreda et al., 2018). Increasingly, robotic systems are being used to gather data, as understanding and quantifying environmental processes require large amounts of accurate spatial and temporally distributed data (Dunbabin & Marques, 2012). To meet these data requirements, Dunbabin and Marques (2012) further elaborates that remote-sensing satellites are being used at a global scale, fixed monitoring stations for regional scales, and manual and automated sampling for local scales. They note that researchers turn to robotics to overcome the limitations of traditional fixed monitoring points and increase data collection. Their article lists common sensor types and technologies for measuring environmentally relevant variables.

2.2. Swarm robotics

Swarms, composed of multiple simple agents - either homogeneous or heterogeneous - operate without central control, instead relying on simple, local behaviours (Dorigo, 2007). Schranz et al. (2020) then further describes that a collective behaviour emerges through their interactions, enabling the swarm to tackle complex tasks. Swarm systems offer a couple of advantages, also illustrated by figure 2.1:

- Adaptability: a swarm has the ability to adapt to changing environments (Schranz et al., 2021)
- Scalability: adding or removing agents is possible and does not impair the efficient functionality of the collective (Schmickl et al., 2011; Schranz et al., 2021).
- Robustness: swarm systems can achieve their goals despite disturbances and failures, e.g. losing individual agents (Schranz et al., 2021).

In swarm robotics, multiple robots, equipped with local processing, communication, and sensing capabilities, form a swarm that interacts autonomously with each other and their environment. An engineered swarm consists of simple (e.g., artificial ants) to complex (e.g., self-driving cars) autonomous

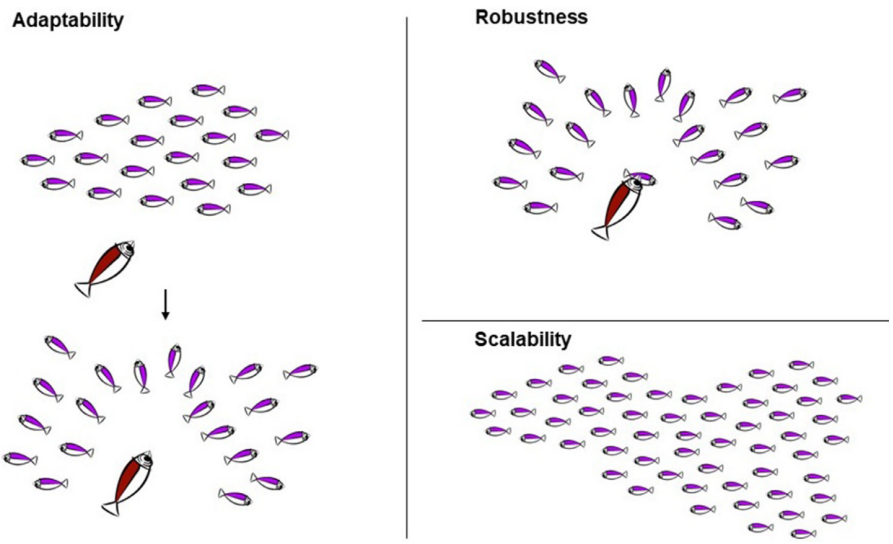

Figure 2.1: A swarm generally offers three key strengths: adaptability to changing environments, robustness against disturbances or failures, and efficient scalability when adding or removing agents. Image from Schranz et al. (2021).

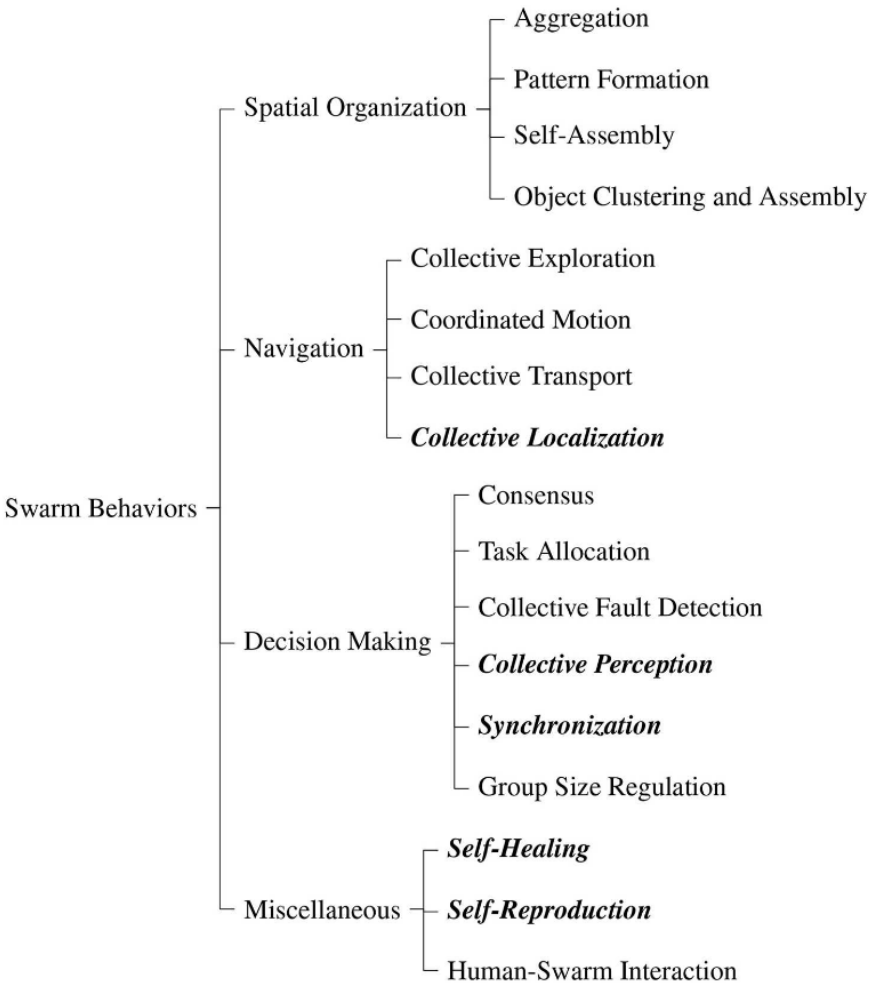

Figure 2.2: Taxonomy of swarm behaviours. The spatial organisation category enables robots in a swarm to arrange themselves or interact with other objects. Navigation facilitates the coordinated movement of agents or the swarm as a whole. Decision-making allows agents to collectively choose a course of action in response to a given issue. The miscellaneous category includes other behaviours that do not fit within these classifications. From Brambilla et al. (2013) and Schranz et al. (2020).

agents (Schranz et al., 2021). Figure 2.2 classifies all swarm behaviours in multiple categories. Collective perception is a good description of the goal of this project. Schranz et al. (2020) describes is as combining locally sensed data from the robots into a big picture.

Critically reflecting on current swarm robotics systems and applications, Schranz et al. (2021) argues that most of the swarm robotics systems to date hardly scale to useful real-world applications in a reliable, predictable and efficient manner. This due to the proof-of-concept nature of most projects and in spite of the interesting swarm behaviour observed. The author further states that current robot swarms are alike toy examples compared to current complex individual robotic systems like self-driving cars and stable quadruped robots. They question if swarm robotics will be able to pass from the stage of studying group behaviours in abstract terms to producing systems that can reliably do useful things in the real world. The authors conclude that it might be necessary to give up some overly restrictive assumptions about swarm robotics and be pragmatic and balance swarms bottom-up design with top-down methods like centralised control, when getting things done in the real world.

2.2.1. Aquatic swarms

This section presents some autonomous aquatic swarms, developed for research or industrial purposes. According to Dunbabin and Marques (2012) there have been many unmanned underwater vehicles (UUV) robots for oceanographic measurements, of which the greatest contribution to spatially distributed robotic monitoring is from the global Argo floater array (“Argo”, n.d.). These floats, deployed in oceans worldwide, drift in ocean currents and are able to dive - to depths from 2000 to 6000m - and resurface, while recording data. Each instrument spends most of its lifetime below the water surface. As of the moment of writing, 4162 robots are deployed (illustrated by figure 2.3) throughout the worlds oceans, its data feeding numerous climate research initiatives, of which an example is shown in figure 2.4. Current floats use GPS to establish their position and the Iridium satellite network to transmit data.

The CoCoRo (Collective Cognitive Robotics) system (Schmickl et al., 2011) is a swarm of UUVs able to explore underwater environments. The swarm consists of exploration UUVs and communication UUVs to relay information to the third robot type: an unmanned surface vehicle (USV) base station. The base station includes communication to researchers and is able the charge the UUVs. The envisioned application is the underwater monitoring of seas and lakes.

In the CORATAM (Control of Aquatic Drones for Maritime Tasks) project, Lyhne Christensen et al. (2015) designed a swarm of relatively simple and inexpensive surface drones for sea patrolling. Drones communicate through an ad-hoc wireless network. Researchers can communicate with the swarm through a subset of drones equipped with long-range communication hardware.

The company “Apium” (n.d.) developed a fleet of both USVs and UUVs. Applications include hydrographic surveying, searching in marine environments and data collection.

Schill et al. (2019) developed UUVs for cooperative environmental sensing. Their Vertex swarm is able to dive to 300m and take water quality measurements. The UUVs are equipped with radio, 3G and acoustic communication protocols. A Vertex robot can be fitted with multiple interchangeable sensors, up to seven simultaneously.

The SWARMs project (“SWARMs”, n.d.) aims to expand the use of underwater and surface vehicles to the conception, planning and execution of offshore operations.

All the stated examples, with the exception of the Argo floaters, use motorised propulsion and are powered by batteries.

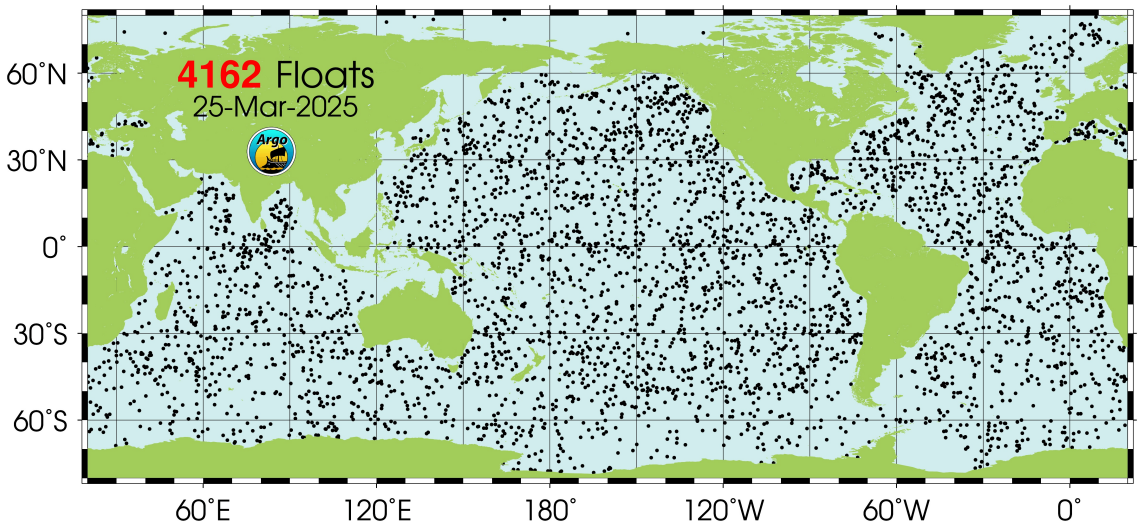

Figure 2.3: As of 2025, 4162 Argo floats are deployed in the worlds oceans. This map shows their locations. (“Argo”, n.d.)

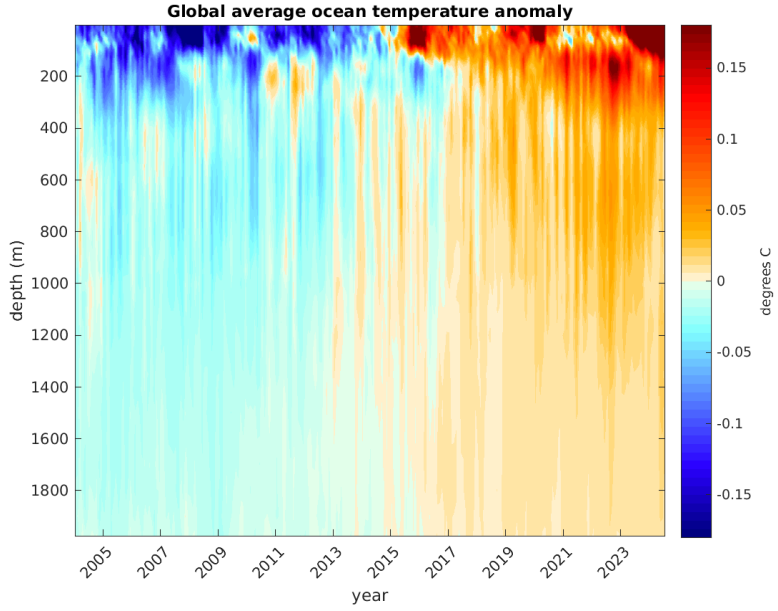

Figure 2.4: Global average ocean temperature anomalies over time and depth, an example of learnings from Argos data (“Argo”, n.d.).

2.3. Autonomous surface vehicles

In recent years, research interest in unmanned and autonomous surface vehicles (USV/ASV) has increased (Ye et al., 2023). The development of autonomous control technologies have gone hand-in-hand with the demand in monitoring climate change, environmental abnormalities, maritime transportation, and military applications (Bai et al., 2022; Liu et al., 2016; X. Sun et al., 2018). The arrival of effective, compact, commercially available and affordable navigation equipment, such as GPS systems and IMUs, combined with developments in wireless communication systems, have given rise to USVs and their applications (Manley, 2008).

Despite all the developments, only semi-autonomous USVs are currently being used rather than fully-autonomous USVs (Liu et al., 2016; X. Sun et al., 2018), their statement however being already 7 and 9 years old. These authors further explain that reliable guidance, navigation and control functions still are beyond current capabilities in the face of complex and hazardous (sea) environments.

Liu et al. (2016), Tipsuwan et al. (2023), and Vagale et al. (2021) explore strategies for guidance, navigation, situational awareness, collision avoidance, and communication. While developments in these areas are extensive and crucial for the successful implementation of USVs, the technical details are beyond the scope of this work.

Bai et al. (2022) state the current USVs are mainly underwater robots, small submarines, or small surface boats, which are used for ocean information collection, sample collection, measurements, or special military missions and have lengths in the range of a couple meters. However, with further development of these technologies, Bai et al. (2022) argues that normal ships will eventually become intelligent USVs and become an important part of the shipping industry.

Fully autonomous USVs offer several advantages and disadvantages compared to conventional crewed vessels, as compiled from Bai et al. (2022), Liu et al. (2016), X. Sun et al. (2018), Vagale et al. (2021), and Ye et al. (2023). USVs can undertake longer and more hazardous missions while significantly improving personnel safety by eliminating the need for onboard crew. Their operational costs are lower, and their lightweight, compact design enhances manoeuvrability and deployability in shallow waters, such as inland and coastal waters, where larger crewed vessels may struggle. Intelligent route design enables precise, automated navigation, reducing energy losses associated with human control. However, the absence of a crew necessitates greater stability at all times and a higher level of intelligent technological support to ensure its safety. Additionally, maybe the biggest challenge is that current regulatory provisions and international maritime conventions were primarily developed for crewed vessels, making them unsuitable for USVs without modification.

2.3.1. Elements of USVs

After reviewing many developments in USV systems, Liu et al. (2016) compiled a list of basic elements that must be present in every USV. Figure 2.5 visualises this list.

1. Hull and auxiliary structural elements. Depending on applications, designers can choose multiple hull variations, typically grouped into one of four different types: rigid inflatable hulls, kayaks (single hulls), catamarans (twin hulls), and trimarans (triple hulls).

2. Propulsion and power system. Most USVs are propelled by propellers or water jets and steered by rudder. Others are steered only by differential thrust.

3. Guidance, navigation and control (GNC) systems. GNC systems are generally composed of onboard computers and software, which manages all systems. The three subsystems are tightly integrated; imperfections in one may degrade the performance as a whole. The guidance system continuously generates trajectory commands to the control system according to information from the mission, navigation system, capabilities from the vehicle and environmental conditions. The navigation system identifies the current state (position, velocity, attitude) of the USV as well as environmental conditions. The control system determines and feeds the correct control inputs to the USVs propulsion system (Liu et al., 2016; Vagale et al., 2021).

4. Communication systems. Includes wireless connectivity with ground stations and other vehicles. Furthermore, these systems also include the communication with onboard sensors, actuators and other equipment.

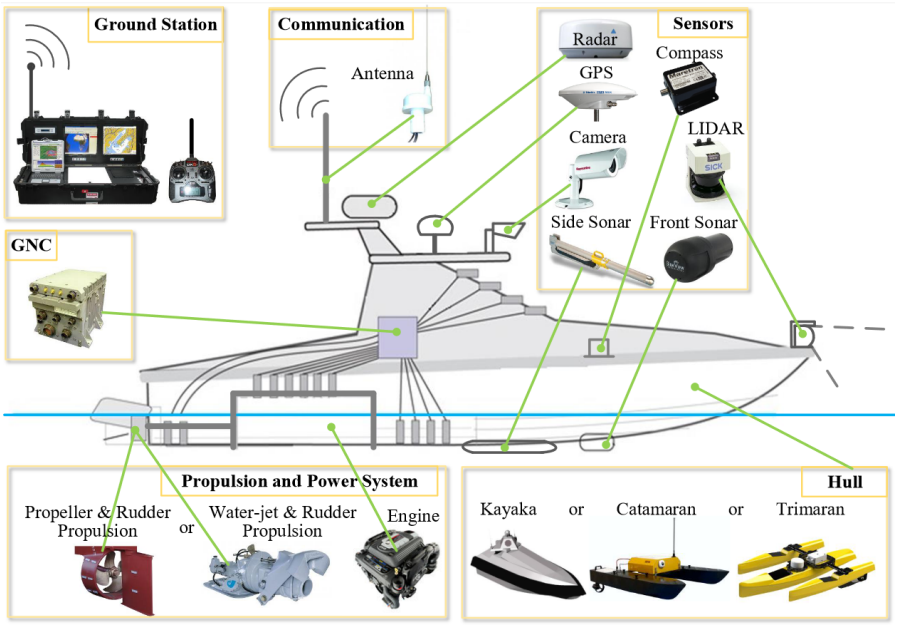

Figure 2.5: Fundamental architecture of typical USVs (Liu et al., 2016).

5. Data collection equipment. Includes not only GNC sensors like IMUs and GPS, but also other kinds of sensors specific for the application of the USV.

6. Ground station. A ground station is typically located in an onshore facility, vehicle or vessel. From these stations, missions are assigned to USVs and monitored through wireless communication.

2.4. Sailing

2.4.1. Introduction

There is substantial evidence for the argument that sailing has been ingrained in human history. Wind powered vessels have been used by humans for more than 5,000 years. The Egyptians depicted a boat under sail around 3,100 BC, which is nearly as old as the recorded history of civilisation (Kimball, 2009). The same source offers other traces that could be interpreted as sailing vessels from 5,000 to 2,000 BC in modern day Kuwait, Turkey, Syria, Greece, Bahrain and India.

Finding evidence for sailing further back in history is difficult due the the nature of unrecorded history. However, one recent historical debate springs to mind: the settlement of the Americas. Recent age estimates by Pigati et al. (2023) confirm the presence of humans in North America by 23,000 to 21,000 years ago, during the last Glacial Maximum. For decades, the prevailing theory was that humans only got to America when the glaciers began to recede by about 13,000 years ago. The ice-free route through Canada which was not present during the Glacial Maximum could not have been used by these older humans (Bennett et al., 2021). These developments have sparked speculations about the way these humans got into America. No consensus has emerged at this moment (Potter et al., 2021). Coastal migration is one of the theories, where these humans migrated on foot and by boat along the southern Beringian coast and down the Alaskan and Canadian coastline into the Americas (Davis & Madsen, 2020). You can wonder if these humans would have used a primitive version of sailing (assisted) boats to make their way halfway across the world.

For thousands of years, sailing was the main way of getting around on water. The invention of the steam engine - and later the internal combustion engine - changed this long-lived tradition. Unlike sailing ships, steamships didn't rely on winds and required less sophisticated support bases on land, allowing for faster cargo deliveries and better military capabilities. During the 1800- and 1900s, sailing vessels were pushed into narrower economic niches (Mendonça, 2013). Having left the work-connotation a long time ago, sailing has become an enjoyable pass-time of many. The establishment of the International Yacht Racing Union (now World Sailing) in 1907 formalised competitive sailing, leading to standardised rules and international competitions. The sport gained global exposure when

(a)  (b) 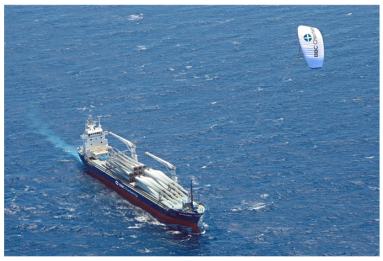 (c) 

Figure 2.6: Sail assist technologies have gained momentum since the 2000s due to sustainability concerns of cargo vessels: (a) a concept with rigid wingsails from Oceanbird (n.d.), (b) a kite from SkySails, which was successfully tested but failed commercially (Erhard & Strauch, 2018), and (c) an implementation of flettner rotors on the Enercon E-Ship 1 (Enercon, 2013).

it was included in the modern Olympic Games, starting with the Paris Games in 1900. Technological advancements in boat design, materials, and navigation have revolutionised sailing, more on that in section 2.4.4. High-profile events like the America's Cup, the (Volvo) Ocean Race, and the Vendée Globe have put sailing in the spotlight, showing off its competitive side. Sailing clubs and schools around the world have made the sport more accessible, while a growing focus on environmental responsibility has led many sailors to advocate for marine conservation.

Due to sustainability concerns, there has been a returning interest in equipping large cargo vessels with sailing technologies to curb fuel use (Hoang et al., 2022; Xing et al., 2020). This effort has gained momentum since the 2000s. Instead of fully powering these large modern vessels, the sails generate additional propulsion which allows saving fuel while sustaining the ships cruise speed (Hoang et al., 2022). The most common sailing assistance technologies are: (1) wing sail technology, (2) kite technology and (3) Flettner rotor technology (Tay & Konovessis, 2023). These are illustrated in Figure 2.6 and described below:

1. Wingsails are sails with a rigid airfoil shape, similar to the wing of an aircraft. They are typically installed on a ship's deck and can replace 15-25% of the thrust generated by a ship's propeller (Hoang et al., 2022; Xing et al., 2020). Their airfoil shape offers a better lift-to-drag ratio compared to traditional soft sails (Tay & Konovessis, 2023).

2. Kites fly at an altitude of several hundred meters to tap into the consistent prevailing winds (Tay & Konovessis, 2023). A successfully tested kite, SkySails, claimed to cut fuel consumption in half on favourable days (at Beaufort 7, depending on air and sea state) and these systems reduce consumption and emissions by on average 10 to 20% (Hoang et al., 2022; Inal et al., 2022; Tadros et al., 2023; Tay & Konovessis, 2023; Xing et al., 2020).

3. The Flettner rotor is a rotating cylindrical shaft, installed vertically on deck. Forward thrust is created by the Magnus force, when wind perpendicular to the direction of travel passes by the rotating shaft (Tay & Konovessis, 2023; Xing et al., 2020). Fuel savings account to 5 to 22.9%, depending on the size and amount or rotors (Inal et al., 2022; Tadros et al., 2023; Tay & Konovessis, 2023; Xing et al., 2020).

The commercialisation and implementation of wind-assisted propulsion systems still face significant barriers due to high initial costs, operational complexities, and reliance on unpredictable wind resources. Additionally, low fuel prices and a sluggish shipping market have dampened investment and innovation in these technologies, despite some promising early results in the shipping industry (Hoang et al., 2022; Xing et al., 2020).

2.4.2. Sailing basics

This section introduces the reader to some basic sailing know-how.

2.4.2.1. Terminology

Sailboats can be complex vessels with numerous components. Figure 2.7 shows a sailboat in its most basic form and its terminology. Table 2.1 explains these terms further.

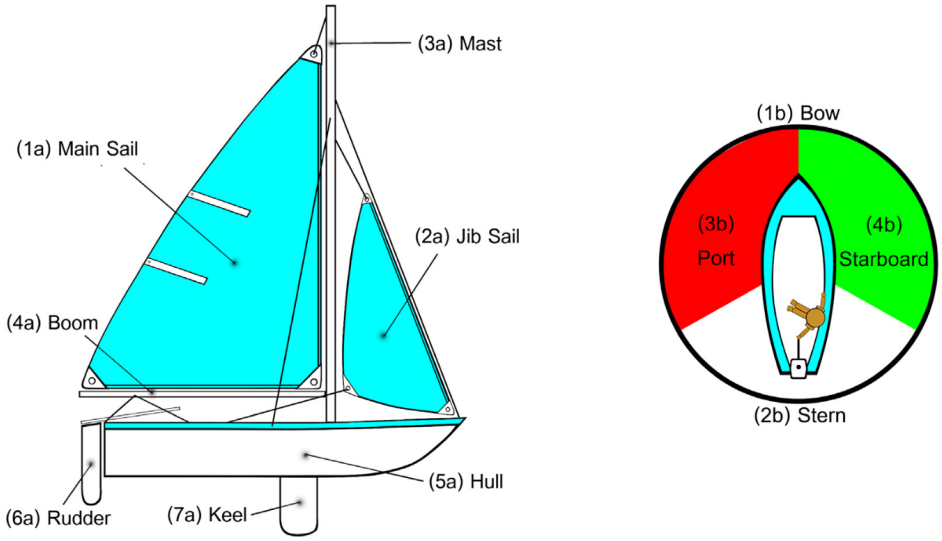

Figure 2.7: Sailing terminologies (Tipsuwan et al., 2023).

No.	Part	Description
1a	Main Sail	The main part that generates propulsion from the wind. This part can be either sailcloth or a wingsail.
2a	Jib Sail	A smaller part that works in conjunction with the main sail for propulsion when using sailcloth.
3a	Mast	The vertical pole that supports the sail.
4a	Boom	The horizontal rod that supports the sail.
5a	Hull	The main body of the boat.
6a	Rudder	The part that changes the heading direction.
7a	Keel	The part that prevents motions caused by the side force.
1b	Bow	The front part of the boat.
2b	Stern	The back part of the boat.
3b	Port	The left side of the boat.
4b	Starboard	The right side of the boat.

Table 2.1: Sailing terminologies (Tipsuwan et al., 2023).

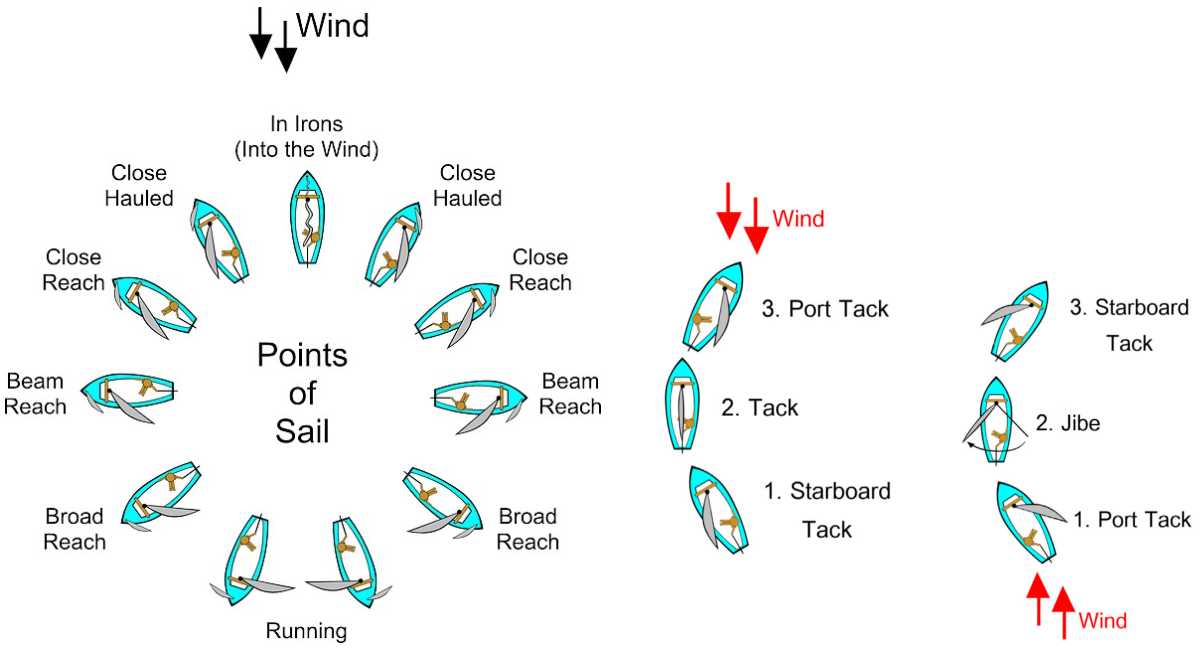

(a) Points of sail. (b) Tacking. (c) Jibing.

Figure 2.8: Points of sail and sailing manoeuvre techniques (Tipsuwan et al., 2023).

2.4.2.2. Points of sail and manoeuvres

Since a sailboat's primary means of propulsion is wind, its possible sailing directions are constrained. The "point of sail" refers to the direction a sailboat heads relative to the incoming direction of the true wind, illustrated by figure 2.8a. Sailing directly upwind is generally impossible for a sailboat, as no propulsive force is generated. However, sailors can reach their upwind destination based on a zigzag course. The manoeuvre to to sail towards the wind by turning the bow towards the wind from the port to the starboard or vice versa is called tacking. Figure 2.8b illustrates this manoeuvre. When sailing downwind, the sailboat's speed cannot exceed the wind speed, as all propulsive force is caused by drag. With increasing boat speeds, the apparent wind speed decreases and reaches zero. Similarly to sailing upwind, sailors can sail a zigzag course to achieve lift in their sails and overcome the speed limitations. The manoeuvre that turns the stern is called jibing. Figure 2.8c illustrates this manoeuvre.

2.4.3. Physics

As Fossati (2009) articulates, "sailing boats operate at the interface between two very different fluids: air and water. They obtain propulsion from the former and support from the latter." To fully understand a yacht's performance, one must examine not only how sails generate thrust but also how the underwater ship acts in the water and how the dynamics above and below the waterline interact with each other.

One of the fundamental aspects of sailing physics is hydrostatics, which governs how a boat floats and remains stable. This include the stability of a yacht, which determines how resistant the boat is to heeling or capsizing, and buoyancy, the force that keeps the boat afloat. Trim refers to the fore-and-aft balance of the boat.

Considering the hydrodynamics is an important piece of the puzzle in determining how efficiently a yacht moves through the water. Resistance to motion comes from both frictional drag, which result from the water flowing along the hull surface, and wave-making resistance, which is a result of the boat's displacement of water. Additionally, underwater appendages such as keels and rudders contribute to hydrodynamic performance, providing lift to counteract leeway (sideways drift) and improving directional stability.

The shape of the hull and keel influences both resistance and lift. Different hull designs balance speed, stability, and manoeuvrability differently. A keel is essential for counteracting the heeling moments generated by the sails, as it helps lower the vessel's centre of gravity. Keel shapes vary widely, ranging from deep fins with a heavy bulb that provide a low centre of gravity to more integrated keels

that blend into the shape of the hull and extend less deeply.

Above the waterline, the aerodynamics of the sail governs how effectively the wind's energy is converted into forward motion. Sails generate lift, similar to an aircraft wing, but also experience drag, which must be minimised to maximise performance. The geometry of the sails, their interaction with each other, and the apparent wind - the wind direction an speed experienced by the moving boat - all influence the propulsive force. Wind speed increases with height due to wind shear near the water surface. As a result, the apparent wind a boat experienced varies in both direction and speed, as illustrated by Figure 2.9.

Finally, the overall dynamics of the yacht involve complex interactions. Velocity prediction programs can be used to estimate performance under different conditions.

2.4.4. Advances in sailing technology

The last few decades have been turbulent for the sailing community due to massive amounts of change in boat designs, mostly driven by technological advances. This section covers the most striking developments.

2.4.4.1. Rigid wingsails

Sailors have used conventional cloth sails for thousands of years. Only quite recently in sailing history have rigid wingsails been introduced (Kimball, 2009). Still, fabric sails have some advantages that are responsible for their widespread use, especially when under the control of a human sailor (Neal et al., 2009). Table 2.2 lists their advantages and disadvantages.

Compared to traditional fabric sails, table 2.3 compiles the advantages and disadvantages of wingsails. One interesting note that Elkaim (2001) makes, is that a rigid wing, while technically not being able of reefing, can point straight into the wind with very little drag. This serves the same purpose as reefing a fabric sail for the purposes of decreasing drag in high wind situations. Reducing sail area is generally impossible for wingsails - in certain exotic (inflated wingsail) designs it is possible - reducing lift and drag forces is generally the goal of reefing. This is easily achieved by (continuously) pivoting the wing into the wind. Lift will reach zero and drag is minimised. Figure 2.10 demonstrates the equivalent drag in a sectioned wing and mast.

2.4.4.2. Composite technology

The use of composites in the context of sailing began in the middle of the 20th century, when yacht hulls first were constructed with glass fibres (Baley et al., 2024). Further development in sailing yachts have gone hand-in-hand with the extensive use of composite materials (Le Duigou et al., 2014). Especially racing yachts have made tremendous performance gains due to weight reduction and design optimisations made possible by composite materials (Baley et al., 2024). Some examples of developments are light, stiff hulls, hydrofoils, and wingsails.

However, Baley et al. (2024) states that the industry is starting to yearn for alternative materials, as the race for performance at any cost reveals to have a high environmental impact. A life cycle assessment from 11th Hour Racing Team (2021) on their 18m, 8600kg, IMOCA-class yacht reveals their amount of CO2 equivalent emissions during construction to be 553 tonnes. Their use of materials - which were mostly carbon composites - contributed more than 50% to that total. Ten years earlier, their previous IMOCA yacht produced 343 tonnes. According to Baley et al. (2024), this increase results from technological improvements and the use (production) of hydrofoils. 11th Hour Racing Team (2021) hypothesise the construction of the yacht to be only 25% of the total emissions of the sailing team over 5 years. Their total emissions would account to 375 years of emissions of an average French citizen, which is a very high impact for a boat using wind to navigate (Baley et al., 2024). While this is an example of one racing yacht, the extensive use of composites seem to have started a debate across the whole sailing world. Le Duigou et al. (2014) mentioned that in 2015 around 20.000 French boats reached their end of life, from which 95% were manufactured from glass fibre reinforced composites.

Biocomposites can play a role in reducing the harmful environmental aspects of traditional composite materials. Synthetic fibres (carbon, glass, aramid) and petroleum-based polymers could be substituted by natural fibres and biopolymers (Das et al., 2022; Le Duigou et al., 2014), provided that the biodegradability of these materials is proven and considered in the design phase (Baley et al., 2024). Advantages of natural (plant) fibres are their low environmental impact, availability and renewability,

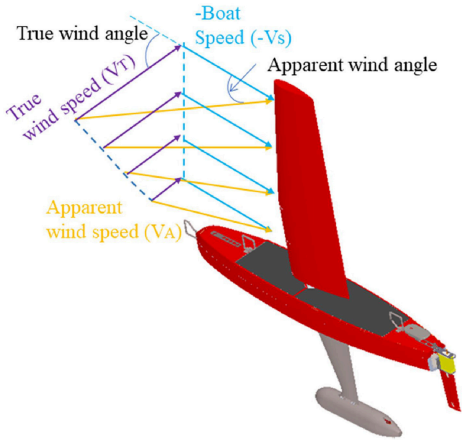

(a) The apparent wind results from the vector addition of true wind speed and the boat's speed. Due to wind shear near the water surface, the true wind speed decreases closer to the surface, affecting apparent wind magnitude and direction experienced by the boat. Image from Z. Sun, Yu, et al. (2025).

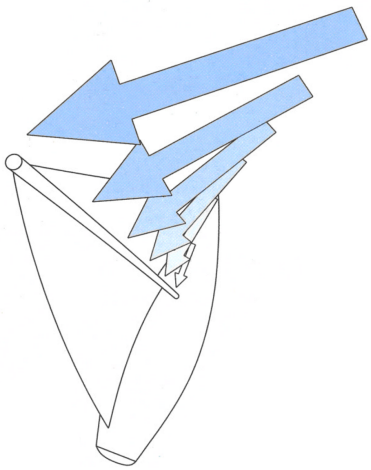

(b) Over the height of the sail, varying angles of attack are experienced. Soft sails can adopt to these variations due to twist in the fabric, whereas wingsails, due to their rigid structure, have little to no ability to adjust. Image from Fossati (2009).

Figure 2.9: Explanation of the composition and effects of apparent wind.

Table 2.2: Advantages and disadvantages of fabric sails. Compiled from Elkaim (2001), Neal et al. (2009), Sauzé and Neal (2006), and Silva et al. (2019).

Advantages of fabric sails	**Disadvantages of fabric sails**
They can be conveniently lowered and stowed when in harbour.	They are prone to wearing and tearing when incorrectly set.
They can be reduced in area relatively easily by either conventional "reefing" or by exchanging sails.	Cloth sails must be furled when not in use in order to prevent destructive flogging.
They can be relatively easily repaired and modified.	They are typically controlled through ropes (known as sheets and halliards), which frequently break or jam (particularly when swollen by salt water) and require regular attention from the crew. Performing such tasks autonomously would, even if it was conceivable, incur significant overheads resulting in excessive power usage, weight and financial cost.
Their shape and camber can be altered by tensioning and releasing control lines.	They lose their shape when not kept with a sufficient angle of attack, leading to "luffing", which reduces sailing efficiency when close-hauled and eventually leads to "flogging" and potentially complete loss of manoeuvrability.
Can compensate for different apparent wind angles over the height of the sail by being able to twist the sail. (Figure 2.9b.)	They require rigid structural spars and (often) wire rigging to maintain their shape: these introduce aerodynamic drag weight high above the waterline.
	They tend to twist, leading to different angles of attack at different points on the sail, which can reduce sailing efficiency. However, controlling the twist can also have a positive effect on efficiency, due to the different apparent wind angle higher up the sail.
	Perfectly trimmed sloop rigs (jib and main sail) have a maximum lift coefficient of $CL_{max} \approx 0.8$.

Table 2.3: Advantages and disadvantages of wingsails. Compiled from Elkaim (2001, 2008), Neal et al. (2009), Silva et al. (2019), and Tretow (2017).

Advantages of wingsails	**Disadvantages of wingsails**
Modern airfoil design allows for an increased lift vs. drag ratio of 30 to 100 times over a conventional fabric sail, providing increased thrust while reducing the overturning moment, while the lift-to-drag ratio for conventional sails is about 3 to 5.	It is difficult to design a wingsail that can simultaneously be reefed reliably;
For navigating downwind, rigid sails are more efficient than cloth sails on any standard rig because at this point of sailing, cloth sails produce thrust entirely by drag, which clearly depends on the magnitude of the apparent wind. On the other hand, when sailing downwind using wing sails, thrust can also be obtained from lift.	constructed to be stiff and lightweight, and;
They can easily be designed such that they do not suffer from problems with chafing.	constructed at a reasonable cost.
They are generally more reliable and avoid the problems of sail luffing or flapping even when the control system fails to maintain the correct angle of attack.	They can generally not compensate for the different apparent wind angles over the height of the sail.
They maintain efficiency even when sailing close to the wind.	
They do not necessarily require any additional structural elements, e.g., shrouds or stays, to support them.	
They can be oriented directly to the wind in a way so that it experiences a minimal aerodynamic force.	
Most rigid wingsails are balanced and it is known that a balanced rig design offers great potential in saving power. A balanced rig is designed in such a way that its center of pressure (CoP) lies as the rotation axis of the rig such that the lift- and drag forces do not result in a moment on the axis of rotation. This allows the sail to be trimmed with relative ease. Comparatively, a cloth sail is fixed to the mast - which is its rotation axis - and trimmed from the boom. Its center of pressure lies between those elements, which results in a trim force that must overcome a portion of the lift- and drag forces of the sail.	

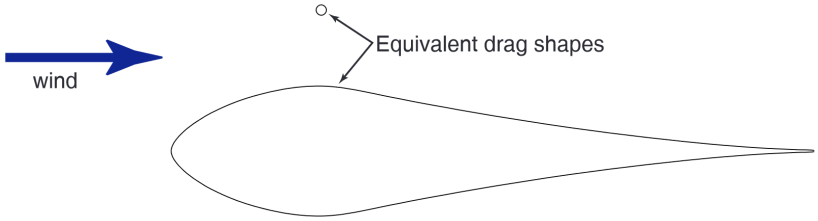

Figure 2.10: The small cylinder and the airfoil section exhibit the same total drag. This demonstrates that a rigid wing does not need to be capable of reefing (or reducing its total area) in order to protect the boat, when allowed to pivot freely. Image from (Elkaim, 2001).

biodegradability, and low cost of raw fibres (Das et al., 2022). The same author also describes their limitations, namely their lower mechanical properties and moisture sensitivity.

Multiple yachts have successfully been built with natural fibres, with flax being the most used (Crupi et al., 2023; El Hawary et al., 2023). These yachts tend to use a matrix of conventional petroleum based thermosets (epoxy or polyester) or thermoplastics (Baley et al., 2024). While emissions caused by material use and during manufacturing can be significantly decreased by using natural fibres, the same end of life concerns are still present by using conventional polymers. In case of a thermoplastic matrix, the (bio)composite can be considered recyclable according to Baley et al. (2024). While Bourmaud and Baley (2009) and Gourier et al. (2017) describe the stability of material properties after multiple recycling cycles, these studies are probably not reflective of real-world use as extensive end-of-life waste streams would have to be in place to recycle these materials.

From an environmental point of view, a bio-sourced ánd biodegradable polymer would be a good matrix material candidate for structures that could be lost at sea. Unfortunately, biodegradation of biopolymers in a marine environment has not been studied sufficiently (Haider et al., 2019). Furthermore, there is no widely-accepted method to verify bio-degradation in a marine environment (Baley et al., 2024). According to Lott et al. (2021), biosourced- and degradable plastics such as Polyhydroxyalkanoates (PHAs) and Polycaprolactone (PCL) seem promising. A designer would have to balance the expected lifetime of the structure with the degrading nature of biodegradable materials. Polymers like Polylactic acid (PLA) are regularly stated as alternatives to commodity plastics, but PLA is only degradable under specific conditions and is basically non-degradable in seawater. (Haider et al., 2019).

One note about the use of wood (100% biobased and biodegradable) as an environmental friendly alternative to composites, is that it necessary to use adhesives and paints to assemble and protect the structure. This has the effect of not being able to fully biodegrade (Baley et al., 2024).

2.5. Autonomous sailing

2.5.1. Introduction and history

Driven by the demand for long-term surface data acquisition platforms, significant progress has been made over the past 25 years into autonomous sailboats (ASBs) (An et al., 2021). Both academic and commercial organisations have developed dozens of autonomous sailboats. An et al. (2021), Silva et al. (2019), Stelzer and Jafarmadar (2011), Q. Sun et al. (2022), and Z. Sun, Feng, et al. (2025) have listed and reviewed existing designs, with Silva et al. (2019) focusing on rigid wing sailboats, and An et al. (2021) critically reflecting performance. Table 2.4 was compiled to document the configurations of previous designs, making it the most comprehensive overview of ASBs to date.

A couple of competitions, set-up between 2005 and 2010, have sparked interest from academia and accelerated development in this field:

- The Microtransat Challenge. Conceived in 2005, the goal of the Challenge is to complete a transatlantic voyage with an autonomous sailing boat, originally no longer than 4 m and since 2017 limited to 2.4 m. At present, 27 autonomous boats have attempted the challenge but none have succeeded. One unmanned sailboat has, the SB Met. In the unmanned category two-way communication is allowed, compared to the one-way communication for the fully autonomous category, where you are only allowed to receive data (“Microtransat Challenge”, n.d.). The extensive distance required for this challenge has provided valuable insights into the endurance of ASBs.

- The World Robotic Sailing Championship. (WRSC) Started in 2008 as a spinoff from the Microtransat, the WRSC is a competition open to fully autonomous and unmanned sailing boats up to 4m in length. Unlike the Microtransat, the WRSC has short distance races and different challenges. Besides a fleet race, the WRSC included a station keeping, cooperative area scanning, and obstacle avoidance competition in 2018 and 2019. The competition is accompanied by the International Robotic Sailing Conference (IRSC). 2019 has been the last edition to date. (“Robotic Sailing: Home”, n.d.).

- The International Robotic Sailing Regatta. (SailBot) A North American competition where university, college, and high school teams design and build unmanned sailboats to navigate various challenges. The event began in 2006, and is still being held yearly. The competition mainly features SailBot Class boats up to 2 meters in length, though there is also an Open Class for larger boats. Teams often start with the MaxiMOOP platform due to its manageable size and capabilities (“SailBot | International Robotic Sailing Regatta”, n.d.).

Insights into the long-term durability of ASBs have been gained through these competitions, particularly from the Atlantic crossings attempted in the Microtransat Challenge, where nearly all boats ultimately fail. Where known, endurance data has been included in Table 2.4. However, because failures often occur mid-ocean, the specific causes are rarely identifiable. An et al. (2021) reported on the known failures, the majority of which were mechanical issues with the sail, followed by less common failures of the hull, sail actuation, keel, and rudder.

Reference	Country	Year	Platform name	Team/University	Company	Hull	Length (m)	Beam (m)	Draft (m)	Displ (kg)	Speed (kn)	Sail Type	Sail Design	Sail Area (m2)	Endurance (days)	LDR	L/B	SA/D	B/D(%)
Abril et al. (1997)	Spain	1997		Universitat de les Illes Balears		Mono	1.03	0.25		4.5		Soft Sail		0.37		6.12	4.2	13.4	
(Elkaim, 2001, 2006)	US	2001	Atlantis	Stanford University UCSC		Catamaran	7.2	3		147	4	Wing Sail	Self-trimming	7.65			2.4	27.5	50
(Neal, 2006; Sauze et al., 2006)	UK	2004	AROO	Aberystwyth University		Mono	1.5			12		Wing Sail		0.24	2	5.00		4.5	29
Stelzer and Jafarmadar (2012)	Austria	2006	ASV Roboat	INNOC		Mono	3.7			300	4.5	Soft Sail	Balanced rig	4.5		2.31		12.0	20
Stelzer and Jafarmadar (2012)	Austria	2006	ASV Roboat I	INNOC		Mono	1.38	0.34	0.24	17.5		Soft Sail	Four sails	0.855		4.29	4.1	12.0	20
	UK	2007	Beagle-B	Aberystwyth University		Mono	3.5					Wing Sail		2.55	1				
	US	2007	HWT-X1	UCSC		Catamaran	9.1					Wing Sail	Self-trimming						
Stelzer et al. (2007)	US/Austria	2007	Robbe Atlantis	De Montfort University / Austrian Association for Innovative Computer Science		Mono	1.38	0.34	0.24	17.5		Soft Sail		0.86		4.29	4.1	12.7	63
(Alves et al. 2008; Alves and Cruz, 2008)	Portugal	2008	FASt	University of Porto		Mono	2.5	0.67	1.25	70		Soft Sail		3.7		3.29	3.7	27.3	40
	US	2008	First Time	United States Naval Academy		Mono	2	0.36	1.5	26.7		Soft Sail		3.1		4.22	5.6	34.7	
Briere (2008)	France	2008	IBOAT	Universite de Toulouse, ISAE		Mono	2.4	0.4		35	3	Soft Sail	Balanced rig	1.5		4.09	6.0	14.0	40
Neal et al. (2009)	UK	2008	MOOP	Aberystwyth University		Mono	0.74		0.125	4	0.51	Wing Sail		0.02	3	5.70		0.3	
	UK	2008	Pinta	Aberystwyth University		Mono	2.95	1.2		450		Soft Sail		5.39	18	1.87	2.5	9.2	
(Rynne and Ellenrieder, 2010; Rynne and Von Ellenrieder, 2008; Rynne, 2008)	US	2008	WASP	Florida Atlantic University		Mono	4.2	0.8	1	275		Wing Sail		4.48		2.48	5.3	10.6	82
Klinck et al. (2009)	US/Austria	2009	AAS Endurance	Oregon State University / Austrian Society for Innovative Computer Science		Mono	3.75			300		Soft Sail	Balanced rig	4.5		2.32		10.0	20
Giger et al. (2009)	Switzerland	2009	Avalon	ETH		Mono	3.95	1.41	2	440		Soft Sail	Balanced rig	8.4		2.08	2.8	6.9	36
Leloup et al. (2011)	France	2009	Breizh Spirit1	ENSTA Bretagne		Mono	1.5	0.35	0.8	13		Soft Sail		0.86		4.87	4.3	15.5	
	US	2009	Luce Canon	United States Naval Academy		Mono	2	0.28	1.5	24		Soft Sail		3.1		4.37	7.1	37.3	
Leloup et al. (2011)	France	2010	Breizh Spirit2	ENSTA Bretagne		Mono	2.3	0.8	0.8	55		Soft Sail		2		3.47	2.9	13.8	
	US	2010	Gill the Boat	United States Naval Academy		Mono	2	0.305	1.5	29.9		Soft Sail		3.1		4.06	6.6	32.2	
Leloup et al. (2011)	France	2011	Breizh Spirit3	ENSTA Bretagne		Mono	1.7	0.45	0.8	13		Soft Sail		0.75		5.08	3.8	13.6	
Koch and Petersen (2011)	Germany	2011	FHsailbot	FH Stralsund		Mono	1.52	0.33	0.81	15		Soft Sail		0.65		4.66	4.6	10.7	
	Germany	2011	rrMM	University of Lübeck		Mono	0.53	0.18		1.03	2	Soft Sail				8.01	2.9		
Koch and Petersen (2011)	Germany	2011	Saudade	FH Stralsund		Mono	1.12	0.26	0.26	9		Soft Sail		0.52		4.99	4.3	12.0	
	France	2011	Vaimos	ENSTA IFREMER		Mono	3.65	0.86	0.65			Soft Sail	Balanced rig		1		4.2		
Microtransat Challenge	UK	2012	Snoopy Sloop 8			Mono	1.2	0.28	0.3	14		Soft Sail			1	4.41	4.3		
Miller et al. (2013)	US	2012	SOA	United States Naval Academy		Mono	2	0.33	1.5	52.2		Soft Sail	Balanced rig	1.9		3.37	6.1	13.6	
Miller et al. (2013)	US	2012	W2H	United States Naval Academy		Mono	2	0.48	1.5	44	2.4	Soft Sail	Balanced rig	1.8		3.57	4.2	14.4	
Microtransat Challenge	France	2013	Erwan 1	Ecole Navale		Mono	3.65	0.86	0.65	300	1.2	Soft Sail			4	2.30	4.2		
(Anthierens et al., 2014; Naveau et al., 2013)	France	2013	Marius	Maison des Technologies		Mono	2	0.80	0.8	100		Soft Sail		2.9		2.71	2.5	17.1	50
Miller et al. (2014)	US/UK	2014	ARRTOO Prototype	United States Naval Academy / Aberystwyth University		Mono	1.95	0.48	0.83	29.5		Soft Sail	Double Sails			4.04	4.1		
Cabrera-Gámez et al. (2014)	Spain	2014	A-Tirma	Universidad de Las Palmas de Gran Canaria		Mono	1	0.24	0.14	4.3		Soft Sail		0.61		6.15	4.1	23.1	
Miller et al. (2015a)	US	2014	Sea Quester	United States Naval Academy		Mono	1.94	0.3		25.5		Soft Sail		2.67		4.24	6.5	30.8	43
	France	2015	ASAROME	UPMC		Mono	3.6				2.5	Soft Sail			2				
Microtransat Challenge	France/Canada	2015	Breizh Tigresse	ENSTA Bretagne / Dalhousie University		Mono	1.44	0.6	0.6	28	1	Soft Sail			32	3.72	2.4		
Miller et al. (2015b)	US/UK	2015	MaxiMOOP	United States Naval Academy / Aberystwyth University		Mono	1.2	0.35	0.41	23		Soft Sail		0.24		3.74	3.4	12.4	
	China	2015	SJTU Sailboat	Shanghai Jiao Tong University		Mono	1.5	0.476	0.433			Soft Sail		1.15			3.2		
Cruz et al. (2015)	Portugal	2015	Zarco	University of Porto		Trimaran	2.5			50		Wing Sail		0.3		3.68		2.2	
Domínguez-Brito et al. (2016)	Spain	2016	A-Tirma G2	Universidad de Las Palmas de Gran Canaria		Mono	2	0.37	0.63	43		Wing Sail	Double Sails	0.47		3.60	5.4	1.9	
Microtransat Challenge	US	2016	Gortobot v2			Mono	0.79	0.32	0.46	5.4	1	Soft Sail			8	5.27	2.5		
Augenstein et al. (2017)	US	2016	Luja	Cornell University		Mono	1			5		Wing Sail	Self-trimming	0.24		5.85		8.2	5
Microtransat Challenge	Slovakia	2016	OpenTransat (2016)			Mono	2.36	0.72	1.15	45	0.8	Soft Sail			25	3.74	3.3		
	China	2016	Sail-Based ASV	Smart China Research Institute, Hong Kong CUHK-Shenzhen		Trimaran	5.02	2.9			3.5	Soft Sail		5.47			1.7		
Rathour (2016)	Japan	2016	SOTAB-II	Osaka University		Mono	2.6	0.74		150		Soft Sail		0.56		2.59	3.5	2.0	20
	UK	2016	That'll do	Epsom College		Mono	1.4	0.47		10	1.7	Soft Sail				5.19	3		
Kang et al. (2016)	China	2016		Shanghai Jiao Tong University		Mono	1.5	0.48		15		Soft Sail		1.15		4.64	3.2	18.9	
Microtransat Challenge	US	2017	Aboat Time	United States Naval Academy		Mono	1.2	0.35	0.41	18	2.2	Soft Sail			3	4.05	3.4		
(Friebe, 2019; Friebe et al., 2017; \ M aasala and others, 2018)	Finland	2017	ASPire	Aland University of applied science		Mono	4			370		Wing Sail	Self-trimming	2.06		2.21		4.0	47
	UK	2018	Black Python	University of Southampton		Mono	1	0.165	0.42	4		Soft Sail				6.30	6.1		
Microtransat Challenge	US	2018	Gortobot v3			Mono	1.81	0.51	0.69	8.1	1.8	Soft Sail			10	6.07	3.5		
Tretow (2017)	Sweden	2018	Maribot Vane	KTH		Mono	4.16	0.8	1	280		Wing Sail	Self-trimming	3		2.46	5.2	7.0	
Microtransat Challenge	Norway	2018	SailBuoy		Offshore sensing AS	Mono	2	0.5	0.5	60	1.5	Wing Sail		1.00	365	3.22	4.0	6.5	
Microtransat Challenge	Canada	2018	SeaLeon	Dalhousie University		Mono	1.8	0.5	0.4	50	1.1	Soft Sail			76	3.30	3.6		
	US	2019	Datamaran Mark 7		Marine Systems Autonomous	Catamaran	3.7	2.00	0.3	192		Wing Sail	Two-element wing	2.5	180	2.68	1.85	7.5	
	US	2019	Datamaran Mark 8		Marine Systems Autonomous	Catamaran	5	3.3	0.8	360		Wing Sail	Two-element wing	3.5	180	2.40	1.5	6.9	
Microtransat Challenge	UK	2019	EC-Crossing / Endeavour	Epsom College		Mono	1.05	0.22	0.28	10	1.5	Wing Sail		0.06	8	4.72	4.8	1.3	
Microtransat Challenge	Czech Republic	2019	OpenTransat (2019)			Mono	2	0.32	1.02	47	0.7	Wing Sail	Self-trimming	0.37	186	3.49	6.3	2.8	
Microtransat Challenge	UK	2019	Phil's Boat			Mono	0.85	0.26	0.3	7	0.8	Soft Sail			51	4.95	3.3		
Microtransat Challenge	UK	2019	Snoopy Sloop 11			Mono	1.33	0.29	0.48	14.6	2.8	Soft Sail			8	4.50	4.6		
Microtransat Challenge	US	2020	Bearly Assailable	United States Coast Guard Academy		Mono	1.2	0.36	0.48	26	1	Wing Sail			45	3.59	3.3		
	Australia	2020	BlueBottle		OCIUS	Mono	6.8	1.3	1.6	800	3	Wing Sail	Foldable			2.04	5.2		
	US	2020	Gen6/7		SubSeaSail	Mono	1.52	0.25	1.3	28		Wing Sail		0.6		3.79	6.1	6.5	
	China	2020	OceanVoy	CUHK-Shenzhen		Catamaran	3.1	1.4	0.2	75	3	Soft Sail		3.75		3.46	2.2	21.1	
(An et al., 2022)	China	2022	Seagull	Chinese Academy of Sciences		Mono	3.25	0.97		155		Wing Sail		1.19		2.76	2.9	4.1	20
	US		Saildrone Explorer		Saildrone	Mono	7	2.59	2	750	3	Wing Sail	Self-trimming	5.04	365	2.11	2.7	6.1	
	US		Saildrone Surveyor		Saildrone	Mono	22		3	12700	6	Wing Sail	Self-trimming	40.83	365	1.20		7.5	
	US		Saildrone Voyager		Saildrone	Mono	10		2		5	Wing Sail	Self-trimming		365				
Submaran (2017)	US		Submaran		Ocean Aero	Mono	4.4	0.8	1.5	350	5				90	2.33	5.5		

Table 2.4: Existing sailing robot configurations from academia and industry. Based on available literature, this appears to be the most comprehensive list of autonomous sailboats compiled to date. Data from existing vessels can be used to inform the naval design of future vessels. This list was compiled from the review articles by An et al. (2021) and Q. Sun et al. (2022), the first of which contained numerous inaccuracies in the data. This data has been verified against the original sources, corrected, and expanded. The references in this table are included for completeness and are not listed in the reference section, unless referenced elsewhere.

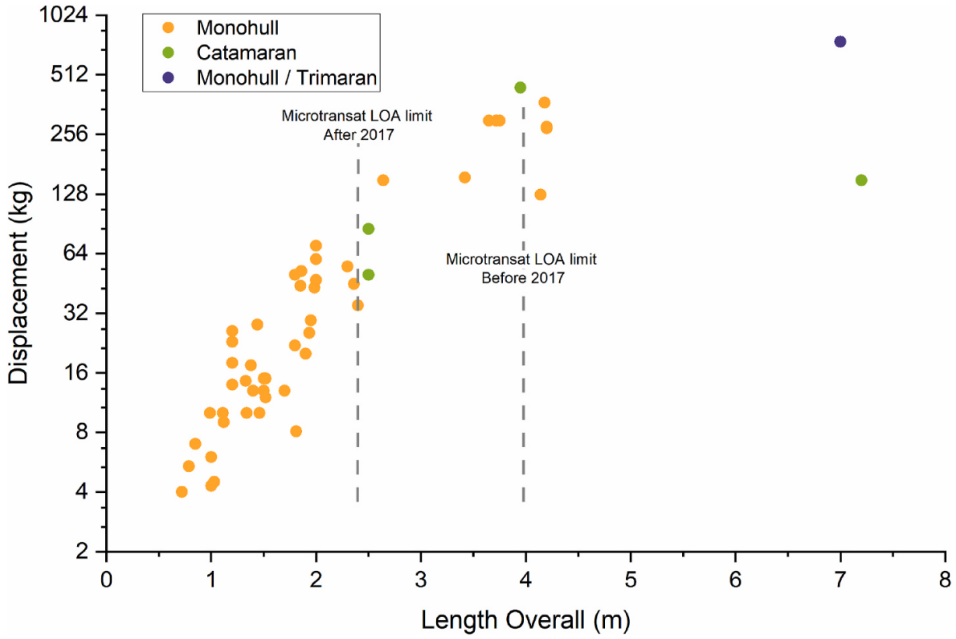

Figure 2.11: General size distribution of autonomous sailboats (An et al., 2021).

2.5.2. General naval design

Most designs opt to use monohulls, as their low inverted stability ensures righting after capsizing (An et al., 2021). While multihulls are generally more stable, they are also stable upside down. Autonomous sailboats are usually small (An et al., 2021), illustrated by figure 2.11. An et al. (2021) also note that designers often adopt existing sailboats with good stability, use longer and heavier keels to lower the centre of gravity and reduce sail area to reduce the overturning moment.

Although ASBs typically are characterised by their long endurance, sailing speed remains an important feature, as slower platforms are more likely to be captured by currents and stranded and damaged (An et al., 2021).

2.5.3. Sail design

Sailboats can be powered by traditional cloth sails, rigid wingsails, towing kites or mechanical devices such as Flettner rotors. Rigid wingsails offer greater efficiency across various conditions, require less control effort, and enhance the mechanical durability of vessels. With their airfoil-like structure, rigid wingsails achieve a significantly higher lift-to-drag ratio compared to conventional sails (Silva et al., 2019). It is therefore not surprising that the majority of autonomous sailboats use wingsails. Given their clear advantages and widespread use, the following section will focus exclusively on the properties of various wingsails.

From successful applications of wingsails and lessons learned, Silva et al. (2019) compiles a few common valuable attributes for wingsails:

- The sails should be waterproof and buoyant so that they can survive being submerged and aid in righting the boat in the event of capsize.
- They should also be light in order to simplify storage, transportation and rigging.
- If possible, cables should not run through the sail; if they do, then either slip rings should be used to allow transfer of power and signals, or the rotation of the sail must be limited, or cables should run through a fixed tube.
- The size of the sail should be kept small. When designing boats for racing it is tempting to increase sail size for increasing speed, but this is often counterproductive when sailing in winds over 15.43 m/s [30 kn] as this can lead to heeling angles of more than 45◦ most of the time, which may decrease the efficiency of the rudder if not properly designed for such situation.

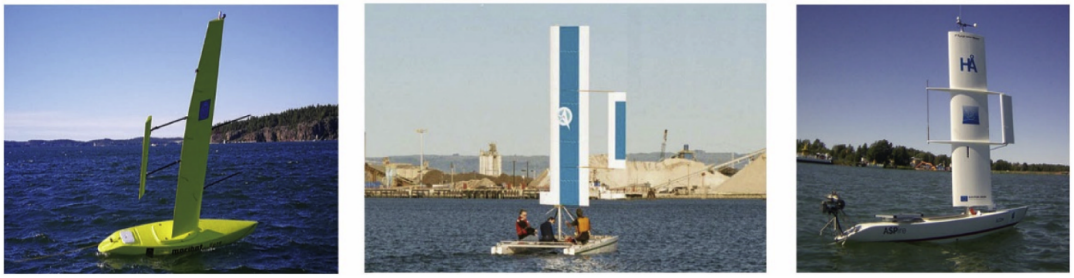

(a) (b) (c)

Figure 2.12: Self-trimming wings. (a) Maribot Vane (Tretow, 2017). (b) Atlantis (Elkaim, 2008). (c) ASPire (Friebe et al., 2017).

- Given the current lack of reliable and simple reefing mechanisms for wingsails, boats expected to encounter strong winds must be equipped with a correspondingly small sail.
- A balanced wingsail is much more efficient relating to energy consumption than any other conventional rig. Results of computer simulations showed that for a traditional sail autonomous robot a balanced rig can save about two-thirds of the power needed for the sail trim.

The actuation subsystem, which includes the trimming of the sail and rudder, is often the most significant electrical power consumer (Silva et al., 2019). Two power saving design adoptions are: (1) The use of worm screws in the actuator (Akiyama et al., 2021; Miller et al., 2013), in order not to have to expend energy to hold the sail and rudder in position, even under load; (2) Use a balanced rig design as described by Elkaim (2008) and Tretow (2017).

There are two ways of actuating the wing and controlling its angle of attack: mechanically or aerodynamically (Elkaim, 2001). Mechanical control uses an actuator that rotates the wing about the mast. According to Elkaim (2001), actuation can be quick, and due to a balanced design, forces can be kept low. However, the author states that due to the variability of the wind and the high sensitivity of the wing to the apparent wind angle - the range between zero lift and stall is about 10 degrees -, high frequency and precision actuation is necessary. Even with a balanced rig, this is a energy-consuming task (An et al., 2021).

To tackle this challenge, designers have come up with self-trimming wingsails (Newman & Fekete, 1983), which have seen considerable use in autonomous sailboats (Elkaim, 2001, 2008; Friebe et al., 2017; “Saildrone”, n.d.; Tretow, 2017). These self-trimming wings are balanced rigs which are aerodynamically controlled by an auxiliary surface to trim the wing. They exploit the main feature of a balanced rig, namely that its lift- and drag forces do not result in a moment on the mast. The auxiliary surface can be configured conventionally, as a tail behind the wing (Figure 2.13 and 2.14), in a canard setup, in front of the wing, or as a flying wing, attached to the trailing edge of the wing. In these scenarios, the actuator’s function is solely to move the trimming surface. A major advantage of this system is its ability to absorb gusts and decouple the propulsion system from the guidance system using passive stability (self-trimming). This significantly simplifies the design of the control system (Elkaim, 2008).

All boats in the review paper of Silva et al. (2019) on rigid wing sailboats use symmetrical airfoils, with the NACA00xx series being the most common ones. This comes as no surprise, as sails are required to generate lift on both sides of the wing.

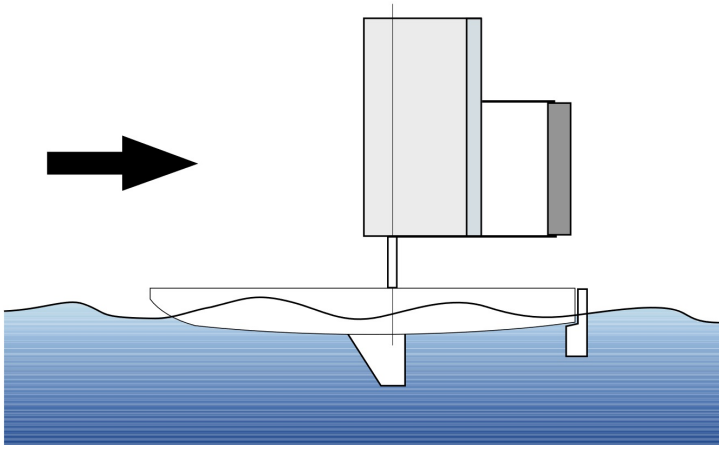

Figure 2.13: The conventional configuration of a self-trimming wingsail is by far the most used in ASBs for its stability. The conventional configuration is the equivalent of an airplane sliced in half down the length, turned sideways and mounted on the mast. This configuration has the inherent disadvantage that the design is tail heavy. This requires ballast to bring the mass centre of the wing/tail assembly in line with the mast. Image from Elkaim (2001).

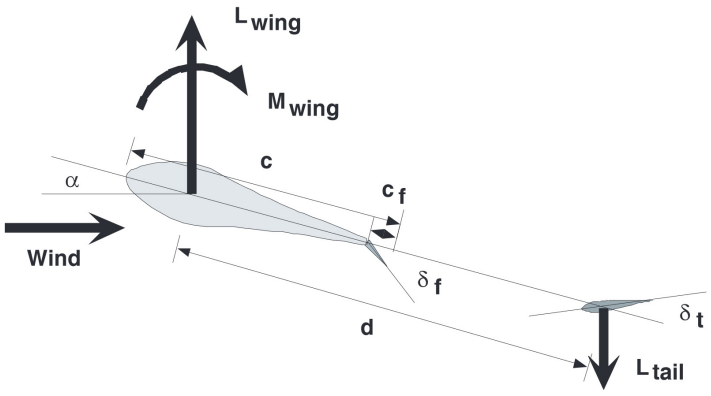

Figure 2.14: Force vectors on the conventional configuration. The forces and moments on the conventional configuration are displayed along with the relevant angles and distances. The wing is flying at an angle of attack, which in turn generates lift and a pitching moment. This pitching moment must be resisted by the lift force on the tail. Image from Elkaim (2001).

3

Design problem & scope

This chapter defines a possible application of autonomous sailboats, describes the problem based on literature and defines the scope of this thesis.

3.1. Application

In the Netherlands, large quantities of nitrogen oxides and ammonia (collectively referred to as nitrogen) are emitted, which are harmful - in those quantities - to the environment. Nitrogen can negatively affect biodiversity, soil and surface water quality, as well as human health (RIVM, n.d.). Although the issue of nitrogen pollution has been known for decades in the Netherlands, it has re-entered public debate in recent years as a result of European legislation that mandates the protection of vulnerable natural areas. As a result, stricter regulations on nitrogen emissions have been introduced.

To monitor nitrogen deposition, multiple governmental organisations conducts large-scale measurements: the RIVM (National Institute for Public Health and the Environment), Rijkswaterstaat (National Department of Water Management), and the regional water authorities. Surface waters, such as streams, ditches, canals, brackish waters, and lakes, are extensively monitored. Despite some progress over the past two decades, nitrogen concentrations often still exceed acceptable levels (CLO, 2024), as Figure 3.1 presents. Finding the right publications about monitoring and its results is a bit daunting, as these organisations and their collaborative partnerships publish separate information (Emissieregistratie, n.d.; Ministerie van Landbouw, 2023; PBL, n.d.).

The monitoring of these surface waters presents an opportunity to employ automation. While autonomous boats may be of limited use in small streams and ditches where static monitoring is sufficient, they could be beneficial for large-scale monitoring of lakes. Harmful nitrogen compounds can be measured using relatively simple, compact sensors, which could be deployed on board these vessels.

3.2. Problem

The state of the art of autonomous sailboats suggests they are still vulnerable to external factors. Considering:

1. It seems inevitable that small autonomous sailboats fail over time, according to previous research projects. While there currently are numerous design considerations to help create robust sailboats, past documented experiences show that no small autonomous vessel is invincible to natures harsh marine environments.

2. It is unreasonable to expect that I can design a more robust vessel than the state of the art within the time-frame of this graduation project.

3. In a robotic swarm, where numerous robots operate, individual failures are likely common. However, the advantage is that these swarms are resilient and can continue functioning effectively despite the loss of some agents.

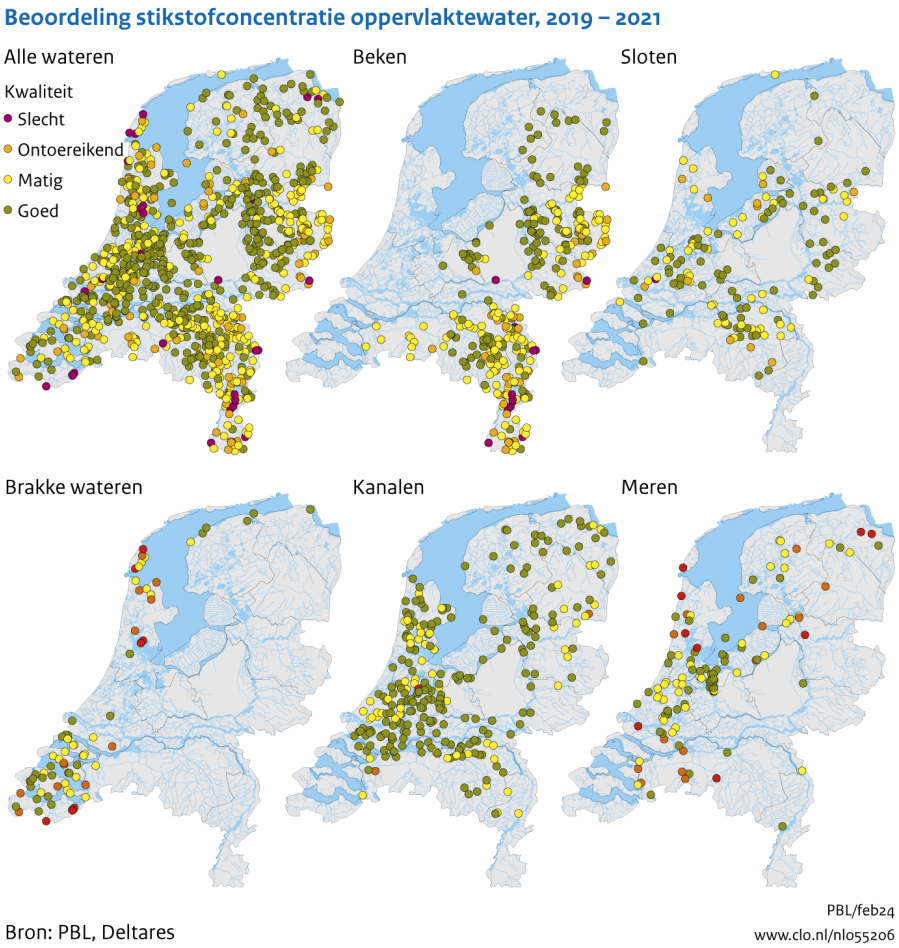

Figure 3.1: Assessment of nitrogen concentration in surface water by CLO (2024). Illustrated from left to right, top to bottom, are: all waters, streams, ditches, brackish waters, canals, lakes. Legend: bad, inadequate, moderate, good.

4. The sailing world is trying to be (a bit) more energy-conscious in terms of CO_2-eq manufacturing cost and is starting to realise the end-of-life problems with traditional petroleum based composite yachts.

An opportunity arises by embracing the failure that these boats experience over time: namely to design for the least environmental impact. Inevitable failure in a marine environment would be less of an issue if the boat is of low impact on the (overall) environment. This approach hasn't been seen in literature.

3.2.1. Research questions

Two main research questions arise:

1. Which low-impact solutions are suitable for the use in an autonomous sailboat?
2. How would the design of a low environmental impact autonomous sailboat look like?

3.3. Scope

To ensure this thesis could be completed within a reasonable timeframe, certain limitations had been placed on its scope.

Previous research on autonomous sailing for data collection has primarily focused on ocean-going vessels. The potential benefits of autonomous vessels are far more significant in open seas than in areas closer to civilisation, where static, or human-led monitoring become more practical. However, for the purposes of this work, a sea-faring vessel was deemed too ambitious, leading to a focus on inland waters. Autonomous sailboats may have limited relevance in inland waters, and the justification for using such a boat could be difficult to uphold. Nevertheless, the hope is that, if this work proves feasible, the results can either be scaled up for sea-faring vessels or applied to other fields entirely.

Autonomy is a fundamental aspect of autonomous sailboats and must be taken into account during the design process. This work does not approach it from a systems and control perspective. Instead, the focus is placed on how autonomy influences the naval design of the vessel, with the goal of developing a viable concept capable of sailing independently. The technical details of its control software will not be explored.

4

Life cycle assessment & roadmap towards net-zero

This chapter first describes the difficulties in quantifying the impact of both previous designs and marine litter, before exploring the solution space towards sustainable marine drones.

4.1. Life Cycle Assessment

The first research question asks: *Which low-impact solutions are suitable for the use in an autonomous sailboat?* Before answering this question one must first answer the follow-up question: what is the impact of current designs and where can the most progress be made? The first part of the question is addressed here through a life cycle assessment, while the second part is explored in the following section.

Life Cycle Assessment (LCA) is a tool used to evaluate the environmental impacts and resources used throughout a product's entire life cycle: from raw material extraction, to manufacturing, distribution, use, and end of life management. The environmental impact is analysed holistically through the eco-cost metric. Vogtländer (n.d.) describes the advantages of the eco-costs metric as such:

> "Despite of the fact that the carbon footprint is an excellent indicator for energy production systems and for calculations on energy consumption, it is not a good indicator for materials selection, since it does not deal with important environmental aspects like materials scarcity, the plastic soup, biodiversity, water, as well as human toxicity and eco-toxicity."

Summary

While the environmental cost of producing an ASV can be estimated when a bill of materials is provided, the available data does not allow for a life cycle analysis of previous designs. Furthermore, the total life cycle cost cannot yet be known. This is because the environmental cost of marine litter is not yet quantifiable. Thus, the impact of the degradation of an ASV at sea or lake cannot be known. This is a documented research gap (Boulay et al., 2021) that prevents this work from assessing design interventions on its absolute impacts.

4.1.1. Selection of boats

The selection process focused on identifying successful and well-designed boats from all previous designs in figure 2.4. For instance, the Sailbuoy was included as it is the only ASV to have successfully completed the Microtransat Transatlantic Challenge. Other selected boats were chosen based on clear evidence of good design or documented performance results and are presented in Figure 4.1.

A notable challenge in this process was the lack of documented bills of materials for any of the designs. Even thorough reviews of available documentation on each design and analysing any documented building processes proved insufficient to reconstruct complete material specifications.

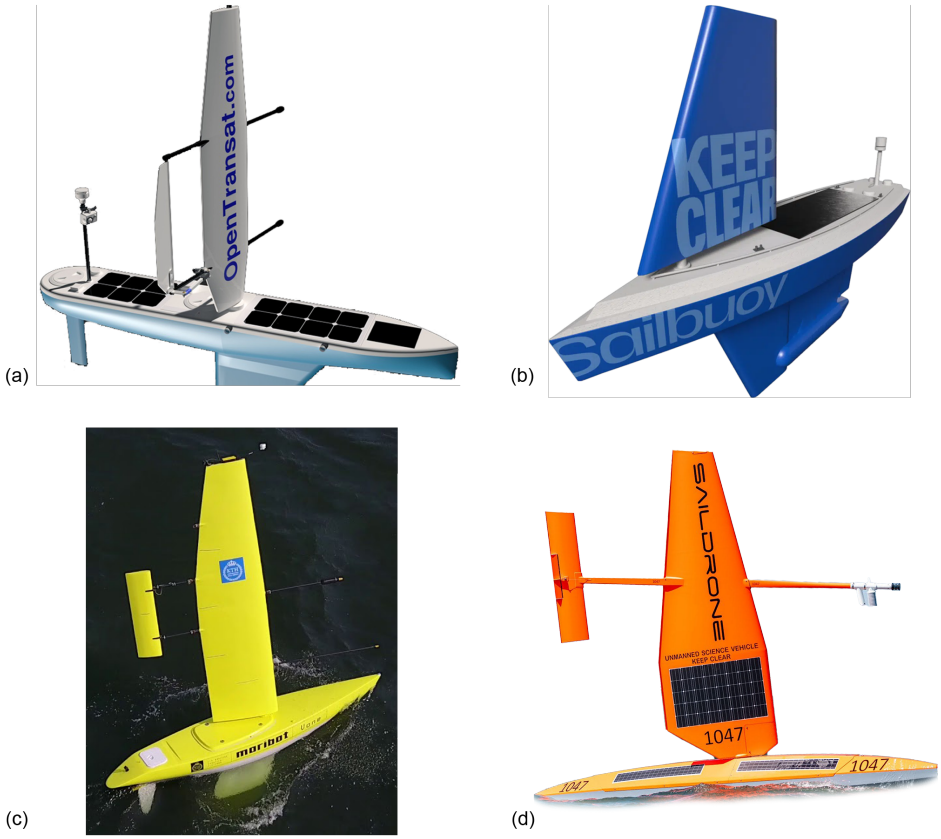

Figure 4.1: The four selected vessels. (a) OpenTransat, (b) Sailbuoy SB Met, (c) Maribot Vane, and (d) Saildrone.

Another challenge was that not all of the boats are production-ready models. Some, such as the Maribot Vane, serve as development platforms, while others, like the OpenTransat, are one-off prototypes. In contrast, the Sailbuoy and Saildrone are production boats.

4.1.2. Life cycle assessment

As a result of limited documentation, estimated material usage, and the diverse development stages, the available data is insufficient to inform a somewhat accurate life cycle assessment. Suggestions on material use can only be provided in general terms, which is provided in Section 5.2.

Research gap on marine litter

Besides not being able to perform a life cycle assessment due to the reasons stated, it is not yet possible to quantify the environmental costs of marine debris. ”To date, life-cycle studies have essentially ignored the leakage of plastic fractions to the biosphere in their inventory modelling. For instance, no major life-cycle database has yet included these emission flows in their datasets” (Boulay et al., 2021). The MarILCA project (Boulay et al., n.d.) is currently working on it, but no results have been made public. A systematic literature review comes to a similar conclusion: the search terms *quantif* AND ”marine litter*” AND (”Life cycle assessment” OR LCA)* result in only eight papers, with the only relevant ones being those by the MarILCA team, which describe the problem at hand.

4.1.3. Conclusions

No definitive results can be given. The material and manufacturing costs of previous ASBs cannot be reliably analysed, making it impossible to identify areas for improvement through LCA and directly compare new design proposals with previous alternatives.

Furthermore, these material and manufacturing costs cannot be directly compared to the impact of its end-of-life fate as marine litter, as this aspect remains unquantifiable. As a result, a complete life cycle assessment of a proposed design cannot yet be provided.

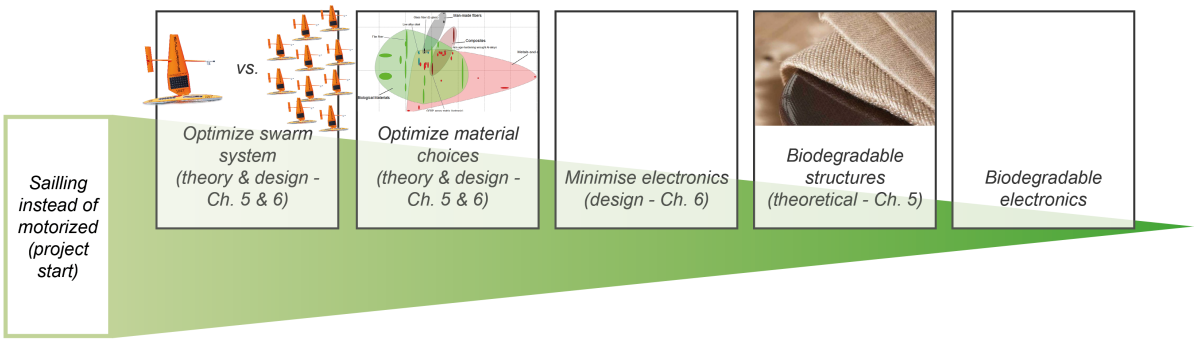

Figure 4.2: Roadmap towards environmentally friendly / net-zero marine drones in logical order of implementation.

Despite these uncertainties, it is evident that marine litter or degradation in the marine environment is inherently undesirable, making interventions that minimise material leakage a logical priority.Material leakage can be understood in two ways: first, as the loss of valuable materials and the significant energy invested in producing the vessel; and second, as the pollution of the marine environment with non-biodegradable or potentially toxic materials.

Given these limitations, rather than aiming for absolute precision in impact assessment, a more pragmatic approach is to focus on implementing design interventions that are logically better alternatives. This leads to the roadmap towards net-zero, which describes strategies for reducing environmental impact.

4.2. Roadmap towards net-zero

Figure 4.2 illustrates the roadmap towards environmentally friendly marine drone sampling. These possibilities were identified as design interventions that, logically, should significantly contribute. They are arranged in a sequence from first to last in terms of implementation priority. This ordering broadly aligns with both the anticipated impact of each intervention and the difficulty of implementation - the initial step offers the greatest effect for the least effort, except for biodegradable structures and electronics, whose impact remains uncertain due to the reasons outlined earlier regarding marine debris. Figure 4.3 further illustrates the roadmap by listing the interventions according to their scale.

The interventions are described further in this section and are worked out in detail in the next chapters. Some interventions (or parts of) are more theoretical in nature - at least for the scope of this thesis - and are therefore only described theoretically in Chapter 5. Others parts are solutions that are directly implementable in the design of the vessel in Chapter 6.

Sailing instead of motorized

Using wind instead of motor propulsion is the starting point of this thesis. It is an important point to state again, as a significant part of the progress towards sustainable marine drones will already be achieved by using wind propulsion.

Optimize swarm system

This intervention looks at the system as a whole. Swarming theoretically offers advantages, but the optimal balance between environmental costs versus performance is unknown. Section 5.1 explores this optimisation problem, focusing on the trade-off between data volume and environmental impact. Does the miniaturisation of the vessels within a swarm result in a more efficient system when optimising for environmental impact? What is the optimal size for individual vessels?

Optimize material choices

After optimizing the swarm system and selecting an approximate vessel size, the next step is to optimise the material selection to minimise environmental impact. A widely used method for selecting environmentally friendly materials is performing a material analysis in Granta EduPack, a comprehensive software tool that provides data on material properties, including mechanical characteristics and sustainability metrics. However, this analysis is mostly limited to conventional engineering materials included in the database. The findings, detailed in Section 5.2, inform the design process and are

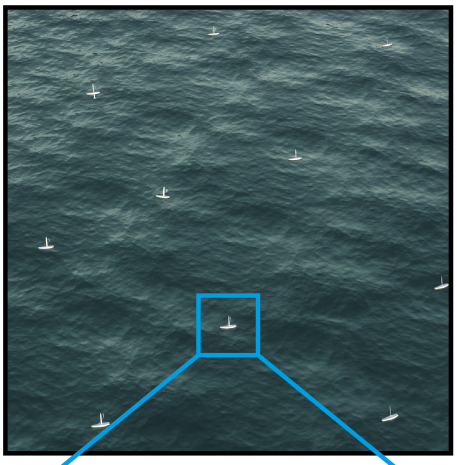

Swarm scale

Optimize swarm system
Explores the optimisation between data volume and environmental impact
► *Chapter 5.1*

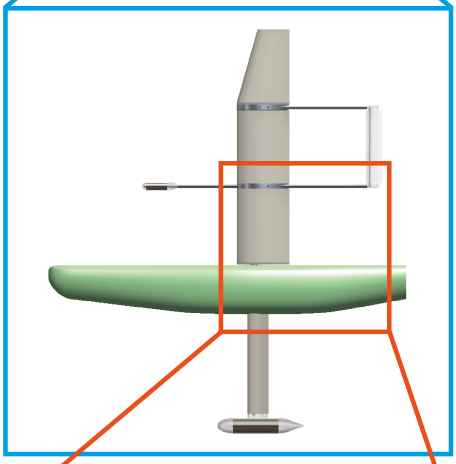

Vessel scale

Optimize material choices
Explores conventional engineering materials for alternative, more sustainable structural materials
► *Chapter 5.2, 6 & 7*

Biodegradable structures
Revisits material selection with the goal of biodegradation
► *Chapter 5.3*

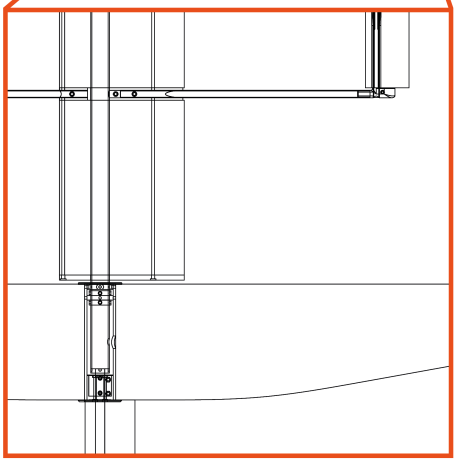

Component scale

Minimize electronics
Minimize electronic systems through smart design and engineering choices
► *Chapter 6*

Biodegradable electronics
► *not feasible*

Figure 4.3: Design interventions that improve the environmental impact of autonomous sailboats act on three different levels: the swarm scale, vessel scale, and component scale.

incorporated into the mass production design discussed in Chapter 7.1.2.

Minimize electronics
Going a step further, the aim is to minimise electronic systems through smart design and engineering choices, thereby reducing the need for environmentally impactful components such as batteries and PCBs. This intervention is highly feasible, with multiple examples in research. For example, passive aerodynamic sail control can replace electrically actuated systems, as seen in ASB with balanced self-trimming sails, which maintain position without consuming energy, significantly reducing overall power requirements (Silva et al., 2020). Since this challenge is primarily a design problem, existing solutions can be integrated into the concept design and it is therefore addressed in Chapter 6.

Biodegradable materials
This intervention revisits the material selection from the second intervention but goes a step further by aiming to develop a predominantly biodegradable vessel, likely further decreasing the environmental impact. It exists in a grey area between feasibility and infeasibility, as structural biodegradable materials do exist but are not yet widely adopted. This intervention is worked out theoretically in Section 5.3.

Biodegradable electronics
This last intervention builds upon the minimisation of electronics by replacing the necessary electronic components with into biodegradable alternatives. However, while there has been some academic progress in the field of biodegradable electronics, direct one-to-one replacement for implementation in a product remains unfeasible. As Song (2024) states:

> ”Under arguably the most intense investigation is the search for biodegradable semiconducting materials, which are necessary to replace conventional integrated circuits. However, meeting performance standards set by non-degradable electronics, which is an implicit goal of most research in green electronics, is immensely difficult. Novel materials that have been developed thus far require highly specialized processes conducted under tightly controlled laboratory conditions and with specially designed, expensive equipment.”

Achieving this step would result in an (almost) fully biodegradable vessel, making it an important long-term objective within the roadmap. However, given current technological limitations, it is not yet viable for practical implementation and will not be addressed further in this thesis.

5

Optimisation & Materialisation

This chapter expands on the design interventions outlined in the previous chapter. It first details the optimisation of the swarm system, followed by material selection, and finally explores the potential transition to suitable biodegradable materials. Conclusions will be drawn regarding the parameters relevant to reducing the environmental impact of ASBs, namely the size of an individual ASB (determined by the optimisation of the swarm system) and the materials used.

5.1. Optimize swarm system

Swarming theoretically offers advantages as different quantities relating to the swarms performance and the individual vessel size do not scale linearly. To analyse this situation, a dimensional analysis is carried out that studies the relationships between different physical quantities based on their fundamental dimensions.

The optimisation problem considers the relationship between data output volume and environmental impact in an ASB swarm system. For this analysis, (effective) data volume is assumed to be proportional to the vessel's speed. Speed is a critical factor, as the vessels must cover sufficient distances while enduring marine conditions such as strong winds and challenging sea states. Unlike a single large vessel, individual swarm vessels do not need to traverse the entire data collection area; however, they must still reach their deployment locations, which may be far away. Vessel speed is not explicitly known, but can be estimated as a function of vessel length by the Froude number equation and supported by long-term averaged speed data (collected over days to months) from ocean crossings of previous ASB designs (Table 2.4).

Additionally, it is assumed that the total displacement serves as a reasonable predictor for environmental impact, as larger vessels primarily require a greater amount of the same materials. Furthermore, it is assumed that (miniaturised) sensors can be integrated to achieve a data collection output comparable to that of a larger vessel. Finally, any cost-related aspects are deemed out of scope.

Summary

Small ASBs travel more slowly, but collectively in a swarm, they achieve higher data collection for the same total material cost as a single large vessel - or a smaller swarm with bigger vessels. A challenge is that below a certain size threshold, ASBs are more likely to fail during deployment, increasing their environmental footprint. Additionally, vessels that are too small may be incapable of operating effectively in marine conditions. These factors are difficult to quantify theoretically and need testing. In conclusion, the most environmentally beneficial approach is to minimise vessel size while ensuring sufficient operational capability and reducing failure risks associated with smaller dimensions.

5.1.1. Dimensional analysis - the argument for miniaturization

The relationship between speed (equivalent to data volume) and displacement (equivalent to environmental impact) can be expressed through proportionality, as both parameters are linked to vessel

length. The total displacement is used as the functional unit and is constant in this analysis. After accounting for swarm effects, the swarm size and area coverage are described for a similar total displacement. There, the advantages of a larger swarm composed of smaller vessels become noticeable.

Speed and displacement

Speed (v) scales with the square root of length (L_{wl}). This is governed by the hull speed equation $v \approx 1.34{L_{wl}}^{0.5}$, which is in turn based on the Froude number equation $Fn = \frac{u}{\sqrt{gL}}$[1], and supported by real-world data from Table 2.4. The trendline derived from this data follows $v = 1.21{L_{wl}}^{0.55}$, showing a close correlation. To illustrate: a vessel that is four times shorter travels at roughly half the speed.

$$v \sim {L_{wl}}^{0.5} \tag{5.1}$$

Displacement (Δ) scales with the cube of length (L_{wl}). A vessel that is four times shorter has $1/64$th the displacement, very significantly reducing the material use and environmental cost. Analysis of previous ASB designs shows a correlation close to $L^{2.5}$. While a theoretical correlation with L^3 is more intuitive, the definitive relationship remains uncertain, so the theoretical correlation is used here, based on the assumption that length, breadth, and depth (x, y, z) scale similarly.

$$\Delta \sim {L_{wl}}^{3} \tag{5.2}$$

Thus, speed (v) scales with the sixth root of the displacement (Δ). Increasing the displacement results in only a marginal increase in speed. Conversely, doubling the speed would need a 64 fold increase in displacement.

$$v^6 \sim {L_{wl}}^{3} \sim \Delta \tag{5.3}$$

Taking into account swarm effects

If each vessel covers less distance due to lower speed, the total coverage can still be maintained by increasing the number of vessels. Replacing one large vessel with two vessels that are four times shorter results in each small vessel having half the speed of the large one, a combined coverage that matches the large vessel's over time, since two vessels operate in parallel, and only $2 * 1/64 = 1/32$ of its initial environmental footprint.

Their reduced environmental impact allows for more vessels to be deployed within the same material and manufacturing budget. Replacing one large vessel with environmental cost equivalent four times shorter vessels results in 64 smaller vessels and a coverage of 32 times the collection area.

These situations can be described with the following scale equations. Figures 5.1 and 5.2 illustrate the ability of a more numerous and smaller swarm to effectively cover more area for the same total displacement.

Speed scaling

$$v' = S^{0.5} v \tag{5.4}$$

Displacement scaling

$$\Delta' = S^3 \Delta \tag{5.5}$$

Number of vessels for similar displacement

$$N = S^{-3} \tag{5.6}$$

Total area coverage

$$A = S^{-5/2} v \tag{5.7}$$

where:

- S: scale factor

[1] the Froude number equation $Fn = \frac{u}{\sqrt{gL}}$ is a dimensionless value that relates the flow velocity u (can be interpreted as boat speed v) to its length L, with g as gravitational acceleration. It is used to compare the wave-making resistance of hulls of different sizes. The number determines how many waves fit along the hull: at $Fr = 0.4$ one wave, while at $Fr = 0.28$ there are two, and so on. For displacement hulls, speeds around $Fr = 0.4 - 0.5$ typically mark the practical speed limit before wave drag increases sharply (Larsson et al., 2022).

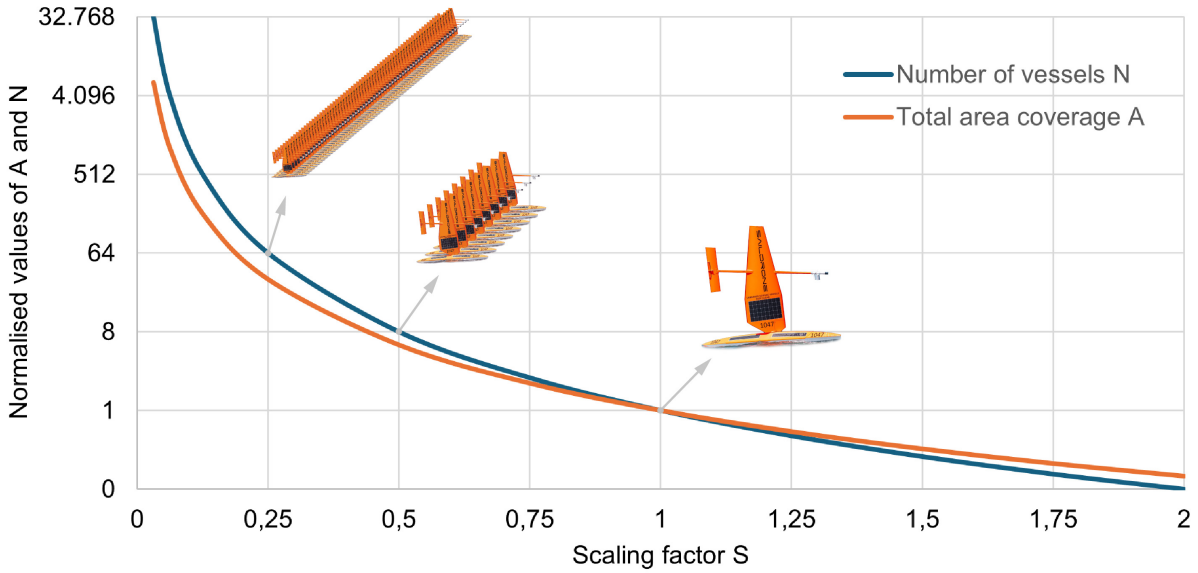

Figure 5.1: The variation in the number of vessels (N) and total area coverage (A) as a function of the scaling factor, while maintaining a constant total swarm displacement. This shows the efficiency gains of a marine swarm with smaller and more numerous vessels compared to larger and fewer vessels.

- v: speed of original vessel
- v': speed of scaled vessel
- Δ: displacement of original vessel
- Δ': displacement of scaled vessel
- N: number of vessels
- A: area covered by the vessels

5.1.2. Lifespan and operating considerations

The miniaturization argument outlined above disregards two critical factors: the reduced lifespan of smaller vessels and their ability to operate effectively in marine environments. These aspects cannot be reliably quantified through analytically methods alone and must be empirically tested.

From an ideal dataset containing endurance records for a wide range of vessels, it would be possible to derive a function relating vessel lifespan to scale. This function could then be incorporated into the scaling analysis to identify an optimal theoretical size. Specifically, the need to replace smaller vessels more frequently must be accounted for by factoring these additional replacements into the overall effective displacement. However, since existing designs vary significantly in quality, it would be a stretch to argue that the endurance data, as it stands, would be a valuable addition to this analysis. Moreover, the endurance is quite dependent on specific design choices, making the development of a generalised function unreliable.

Secondly, ignoring minimum operating requirements would lead to the unrealistic conclusion that vessels should be reduced to infinitesimal size. In reality, vessel size is constrained by several factors, including a minimum speed required for effective navigation, sufficient internal volume to accommodate sensors, and the physical dimensions of certain components such as mechanical couplings, electronics or antennae.

5.1.3. Conclusion

Figure 5.1 presents a clear theoretical advantage of smaller swarms in terms of data collection volume for the same total swarm displacement. Here, it is assumed that total displacement serves as a reasonable predictor for environmental impact. While vessel lifespan has not been accounted for, the trend

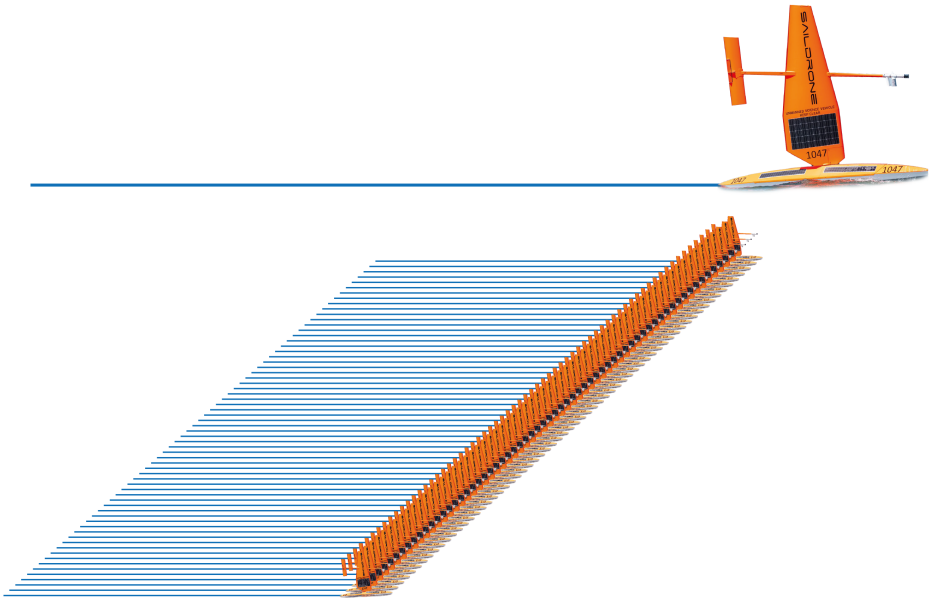

Figure 5.2: Illustration of scaling with similar total displacement. The smaller vessels are four times shorter, sail two times slower, have a displacement of $\frac{1}{64}$th, and together, can cover 32 times the area.

suggests a very significant benefit to smaller vessels. If a sufficiently healthy lifespan can be achieved in a small vessel, it is reasonable to conclude that a swarm consisting of smaller vessels would be more environmentally favourable. Therefore, designing at the minimum operating requirements would likely yield the best results. However, the effectiveness of the operation of a small(er) vessel would need to be empirically tested.

5.2. Optimize material choice

The second design intervention at vessel scale focuses on optimizing the materials used in an ASB based on material impacts. This step excludes the end-of-life scenario, as its impact is non-quantifiable, as discussed in section 4.1. The analysis further focuses on structural materials, as they constitute the largest percentage of an ASBs mass and thus present a significant opportunity for improvement.

Material analysis is conducted using Granta EDUpack by comparing the specific strength and stiffness of materials to their embodied energy. While EDUpack does not provide a comprehensive environmental impact metric like eco-cost, it does offer data on embodied energy, which represents the energy required to produce one kilogram of material. The energy consumption is closely linked to CO_2 emissions (its carbon footprint). However, it is important to note that additional energy is consumed during manufacturing. This analysis only accounts for the energy needed for raw material extraction and refinement.

Summary

Taking into account the environmental impacts of material production by looking at the embodied energy versus its specific strength and stiffness characteristics, the preferred choices are: for composites, glass fibre over flax fibre, followed by carbon fibre. The difference between glass and flax is minimal, while the production energy difference between glass and carbon is almost an order of magnitude. For metals, steel is preferred over aluminium, with steel requiring an order of magnitude less energy.

Preferred materials

This section discusses figures 5.3 and 5.4 and identifies preferred materials.

Carbon fibre composites should be avoided due to their significantly higher embodied energy, which is nearly an order of magnitude greater than that of glass fibre composites. While carbon fibre offers superior mechanical properties, the extreme stiffness it provides is not a strict necessity for ASVs, and glass fibre can be used effectively instead.

Steel should be preferred over aluminium, as it offers comparable specific properties while requiring an order of magnitude less energy for production.

It is important to distinguish between bare glass fibre and glass fibre reinforced polymer (GFRP). GFRP consists of approximately 50% glass fibre and 50% epoxy, resulting in mechanical and embodied energy properties that fall between those of pure glass fibre and epoxy. Furthermore, comparisons with natural fibres should be made against bare man-made fibres rather than composites, as the EDUpack database does not include natural fibre polymer composites. Keeping this in mind, in terms of specific stiffness, flax fibre is comparable to glass fibre, but falls significantly short in specific strength. Nonetheless, its lower embodied energy presents an advantage for the loose fibres. Ultimately though, it is the composite material that is used, rather than the fibre alone. A significant portion of the impact comes from the resin, which closes the gap between both fibres. This is particularly relevant as flax fibre needs a lower fibre-to-resin ratio of about 33/66 compared to 50/50 for a glass fibre composite.

Duflou et al. (2014) notes that the comparison between flax and glass fibre becomes even less straightforward when considering additional environmental factors:

> "...compared to glass fibres the low mechanical strength of flax fibres obstructs a replacement strategy for structural components. Targeting equal strength equivalence in such cases typically results in increased environmental impact. Where stiffness is the main design criterion, flax FRPs can offer a valid substitute on condition that sufficiently high volume fractions of flax fibres are used and that the component lifetime is not significantly shorter than for the GFRP equivalent. For compression moulded parts under bending load a robust margin could be observed making flax FRPs a clearly preferable choice from environmental perspective. It should, however, be noted that for impact categories linked to agricultural activities, such as land use and freshwater ecotoxicity, the impact of flax FRPs is typically higher in all cases."

Considering the importance of mechanical robustness in the ASV, the lower environmental impact of glass fibre when optimising for strength makes it the preferred choice.

As mentioned earlier, this analysis considers only the production of the material itself, not the manufacturing process. Selecting low-impact materials would be ineffective if paired with a high-impact manufacturing method. Therefore, the environmental impact of the manufacturing process must also be considered. Panagiotopoulou et al. (2022) identifies electrical energy consumption as the primary contributor to the environmental impact of manufacturing. A sensible design approach would be to minimise complexity, thereby reducing machine time and overall energy use.

To conclude, the suggested materials for minimising impact are all feasible for implementation in a design, as this optimisation considered only conventional engineering materials.

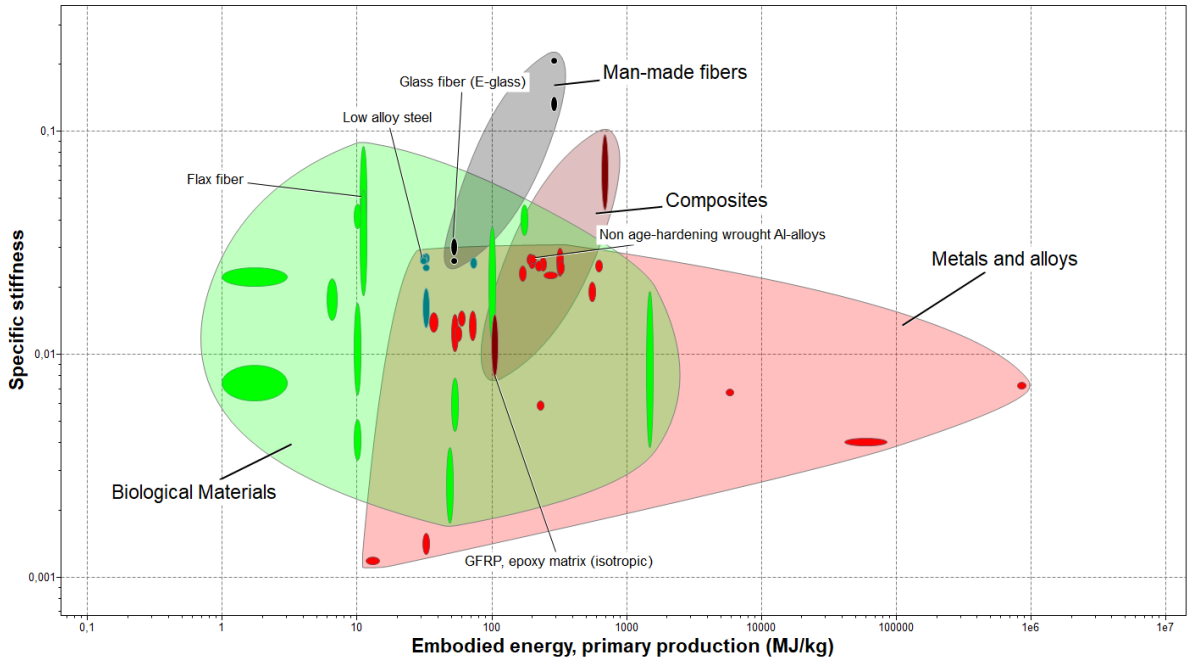

Figure 5.3: Comparison between specific stiffness and embodied energy of metals, man-made fibres and natural fibres. Composites are added as reference, as loose fibres are never used on its own. There are however no natural fibre composites in the EDUpack database.

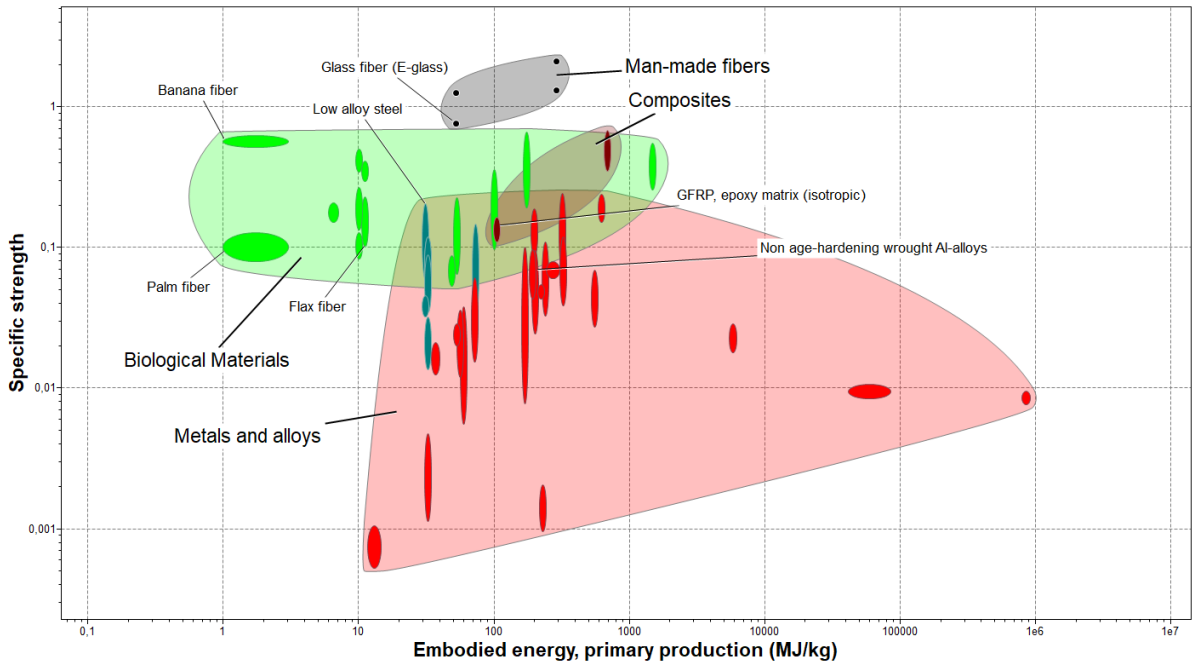

Figure 5.4: Comparison between specific strength and embodied energy of metals, man-made fibres and natural fibres. Composites are added as reference, as loose fibres are never used on its own. There are however no natural fibre composites in the EDUpack database.

5.3. Design with biodegradable materials

The second step of the roadmap at the vessel scale is the extensive use of biodegradable materials. With this design intervention, the vessel would be designed to disintegrate on its own after its operational lifetime, or be broken down by natural processes in the marine environment, eventually leaving no trace.

This step in the roadmap is particularly relevant in scenarios where minimising marine litter from broken vessels is the highest priority, for instance, if it is found that littering has a significantly greater environmental impact than production. However, as the difference in impact between production and littering remains unknown (Boulay et al., 2021), the extent to which this intervention would be beneficial is still uncertain.

An essential requirement is that both the materials and their degradation products must not have toxic or harmful effects on biological systems, as such an outcome would contradict the very goal of biodegradability.

A few distinctions are important to clarify. Strictly speaking, the conventional definition of biodegradation - degradation by biological processes - is too narrow: degradation by other natural processes is also acceptable. This work uses degradation and biodegradation interchangeably to refer to this process. Additionally, the materials origin is less relevant than its ability to break down in the environment within a reasonable time-frame while minimizing harm to the marine ecosystem. This means that the material does not necessarily have to be bio-based. Figure 5.5 illustrates the differences between conventional, bio-based, and biodegradable plastics.

Structural components offer the best opportunity for a redesign with degradable materials, as in most scenarios the vessels structure accounts for most of its mass. In this context, structural components refer to the hull, (wing) sails, mast, internal frames, and keel.

Summary

Degradable continuous fibre-reinforced polymers have been identified as an alternative to conventional engineering materials for structural components. **Flax fibre** presents a straightforward natural fibre option, offering mechanical properties roughly comparable to glass fibre. However, the use of a degradable polymer resin poses greater challenges.
One option for a relatively long-lasting resin is the thermosetting polyester polymer **polyglycerol citrate**, which gradually degrades through hydrolysis into harmless glycerol and citric acid. However, this resin requires processing and curing at elevated temperatures, and as a polyester, the by-product water must be removed during curing.
A rapidly degrading alternative is the thermoplastic **polyvinyl alcohol (PVA)**, which is water-soluble and non-toxic. However, as a thermoplastic, it must also be processed at high temperatures, above its melting temperature, to enable infusion. Due to its high solubility, components made with this resin would require a protective coating to delay degradation.
Unfortunately, testing the mechanical and degradation properties of both flax-reinforced polymers was unsuccessful due to challenges in material fabrication.
This solution focuses on reducing the impact when the ASB degrades during deployment. However, it remains unclear whether the increased production difficulties are justified, as the impact of marine litter is still unknown.

The argument for fibre reinforced polymers

Considering the complex curved shapes of hulls and sails, along with the requirement for materials to degrade, moulded composite materials were identified as a suitable solution. The sailboat will need to withstand reasonable forces during use, leading to the selection of continuous or semi-continuous fibre composites. Metals do not degrade within the desired timespan of months to years, and degradable plastics without reinforcement are unlikely to meet the necessary strength and stiffness requirements on its own.

A continuous fibre composite material is composed of a reinforcement (its structural fibres), and a polymer matrix (often called resin). Both can be selected for biodegradability, which is presented in section 5.3.1 and 5.3.2.

Degradation of a composite material can be achieved in two main ways:

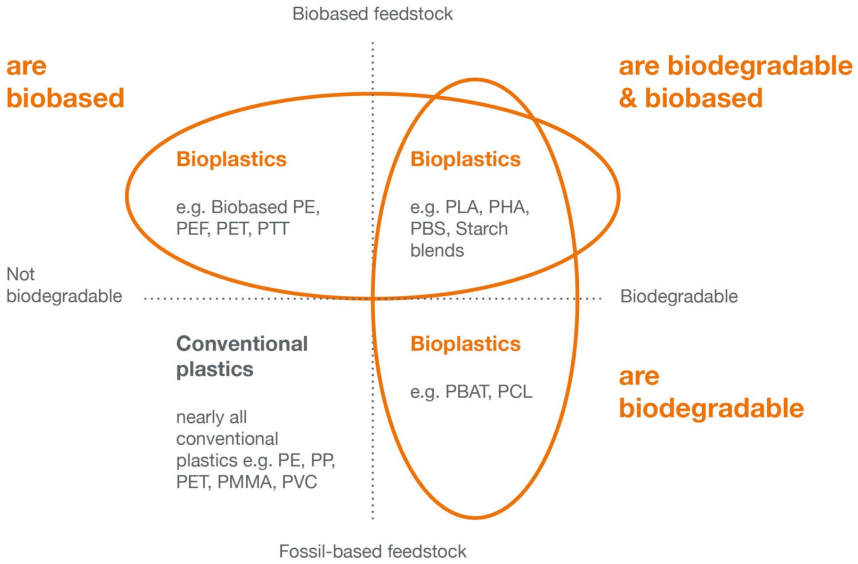

Figure 5.5: Distinctions between conventional, bio-based, and biodegradable plastics. (European Bioplastics, n.d.)

- A composite material where the matrix slowly dissolves over time. A disadvantage, as noted by professor Kaspar Jansen, is that although the design lifetime might be 6 months, the total degradation period could extend to around 10 years.
- A composite material where the matrix dissolves quickly. In this case, the composite parts would have be coated with a protective layer that degrades only after the intended design lifetime, allowing the composite to break down more rapidly afterward.

Options for both slowly and quickly degrading matrices are presented in section 5.3.2.

5.3.1. Reinforcement

Flax fibre is the most suitable natural alternative to conventional fibres and has been successfully used in numerous applications. Its mechanical properties are roughly comparable to those of glass fibre, and most importantly, it is biodegradable. Figure 5.7 illustrate various applications of flax fibre in products.

Conventional fibres as glass, carbon and aramid, are not able to degrade naturally (De et al., 2024). However, natural fibres are (De et al., 2024). For the use in continuous fibre reinforced composites, these natural fibres are quite well documented (Crupi et al., 2023; Dicker et al., 2014; El Hawary et al., 2023; Oliveira et al., 2022; Pil et al., 2016). While the degradation of fibres alone in a marine environment has not been documented, it is assumed to be equivalent to the natural decomposition of plant material in water.

The primary choice when considering natural fibres is flax fibre due to its superior mechanical properties compared with other natural fibres and is often seen as an alternative to glass fibre (Khandai et al., 2019; Le Duigou et al., 2011; Oliveira et al., 2022; Pil et al., 2016).

However, natural fibres like flax are more susceptible to environmental effects, such as moisture uptake (Dicker et al., 2014; Pil et al., 2016). Flax fibre is roughly comparable to glass fibre in strength and stiffness, particularity when compensating for its lower density. Figure 5.6 demonstrates this, and plots a wide selection of materials. Natural fibres are also cost-competitive with glass fibres; however, their lower fibre volume ratio — resulting from poorer wetting due to slight chemical incompatibility with the matrix — can lead to glass fibre composites achieving superior mechanical performance overall, especially in strength (Dicker et al., 2014; Duflou et al., 2014).

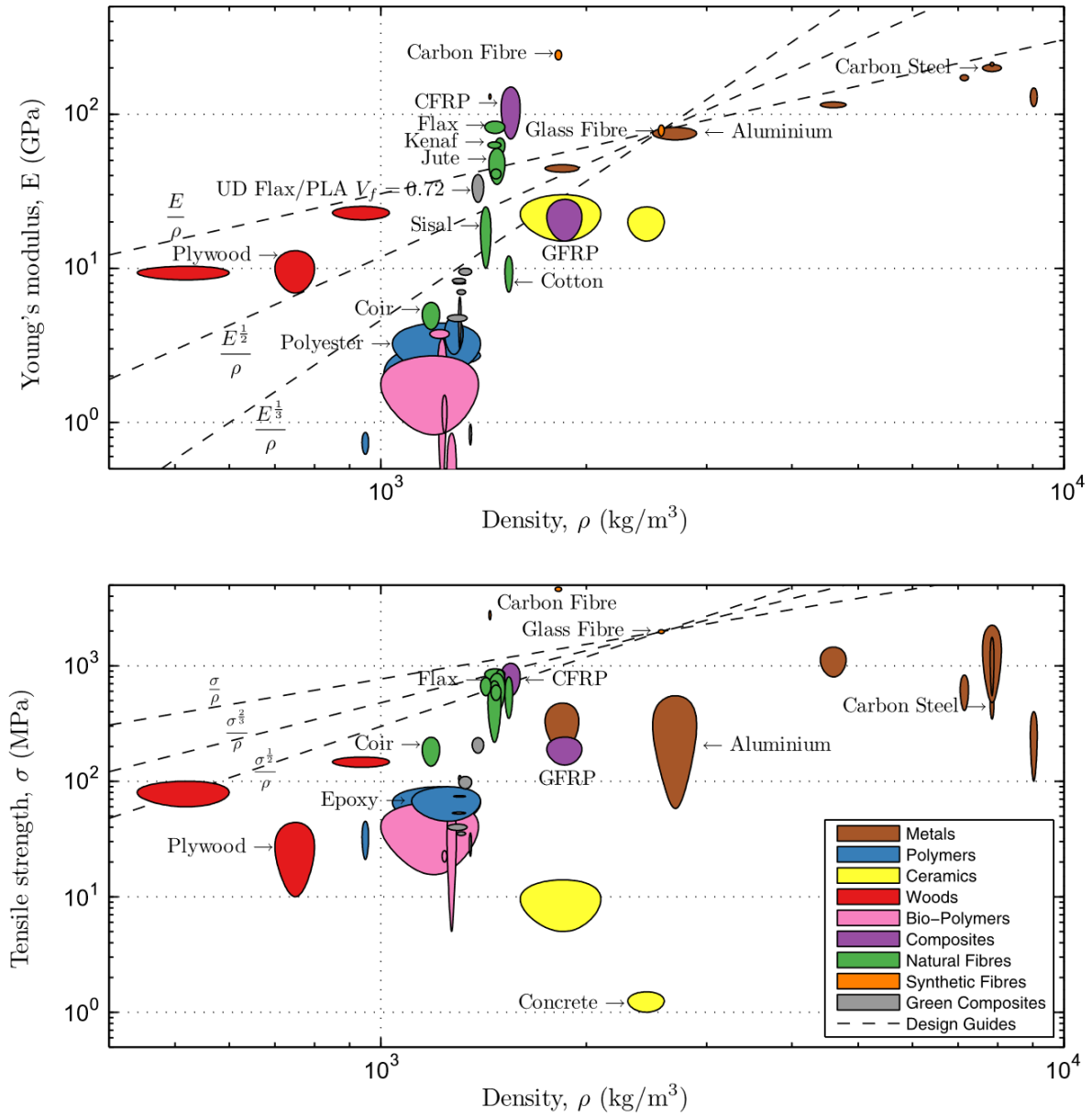

Figure 5.6: Density specific mechanical properties from Dicker et al. (2014). Conventional engineering materials are plotted together with a selection of natural fibres. Glass fibre is taken as comparison material onto which engineering ratios are drawn: Stiffness and strength to weight ratio E/ρ and σ/ρ, bending stiffness and strength to weight ratio $E^{\frac{1}{2}}/\rho$ and $\sigma^{\frac{2}{3}}/\rho$, and finally buckling stiffness and strength to weight ratio $E^{\frac{1}{3}}/\rho$ and $\sigma^{\frac{1}{2}}/\rho$. Flax fibre is one of the stronger and stiffer natural fibres and roughly comparable with glass fibre.

Figure 5.7: Various applications of flax fibre composites. Original images from Pil et al. (2016). (a) Notox surfboard, (b) Caperlan fishing rod, (c) Le Ventoux bamboo-flax bike by INBO, (d) Artengo tennis racket, (e) ArcWin Archery, (f) Kang flax ski poles, (g) BioMobile, (h) i-car Racing and (i) IGIDE bicycle helmet.

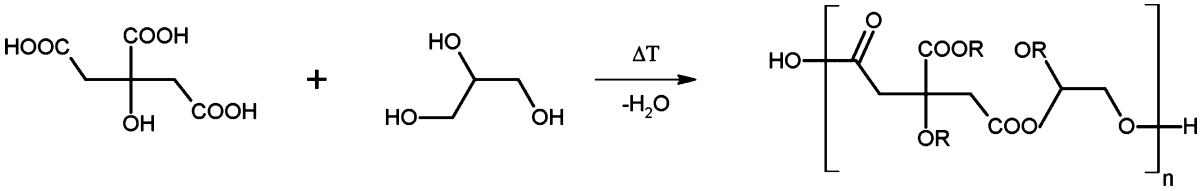

Figure 5.8: Polyvinyl alcohol. The polycondensation of citric acid with glycerol occurs under the influence of heat, with water being released. Note that the polymerisation is reversible through hydrolysis. Image from Wrzecionek et al. (2021).

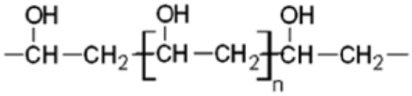

Figure 5.9: Polyvinyl alcohol. Polymerisation occurs under the influence of heat. Image from Jain et al. (2018).

5.3.2. Polymer matrix

This section discusses both slowly and quickly degrading polymers and proposes two materials, the thermosetting polymer **polyglycerol citrate** and the thermoplastic polymer **polyvinyl alcohol**. The quickly degrading polyvinyl alcohol requires a protective coating, but the specifics of this coating is deemed out of scope for this work. Figures 5.8 and 5.9 show the molecular structure of both monomers and polymers.

5.3.2.1. A slowly degrading thermoset

This paragraph breaks down the search towards viable degradable thermosets and the argumentation to the choice of polyglycerol citrate. Figure 5.10 illustrates the arguments to the choices.

Conventionally, one would argue that thermoset polymers are not degradable as a result from their irreversible cross-linked network. Thermosets, once cured, are generally chemically stable and do not degrade. This results in thermosets having superior mechanical and thermal properties and it is no surprise then that thermosets are the most frequently used matrix material in FRPs, around 90% of all resins ar thermoset polymers (De et al., 2024). By selecting for thermosets that are able to undergo hydrolysis, it is possible to create a degrading thermoset polymer (Gubbels et al., 2018).

Requirements

The (co)polymer must meet the following requirements to be used as a matrix in a composite material designed to degrade in a marine environment within a time-frame of a few months to a year.

1. Can degrade/dissolve in a marine environment.
2. Is composed of more than one monomer to become a cross-linked thermoset copolymer, for easier handle-ability during composite production. (Production is imagined as liquid composite moulding (LCM) like resin transfer moulding (RTM). Prepreg fabrics with this specific polymer won't be available.)
3. Has an acceptably low viscosity for easy fibre impregnation.
4. Monomers are (almost) liquid at room temperature (ease of production and the possibility to prototype).
5. Cures at a temperature lower than the denaturation temp of natural fibres (which is about 200 °C).
6. Monomers and polymer are non-toxic, preferably bio-based.

Condensation polymers

Condensation polymers are a type of polymer formed through a polymerisation process that involves a condensation reaction, where a small molecule, such as water or methanol, is released as a by-product. The polymers formed by releasing water are of great interest to this project, as their polymerisation is

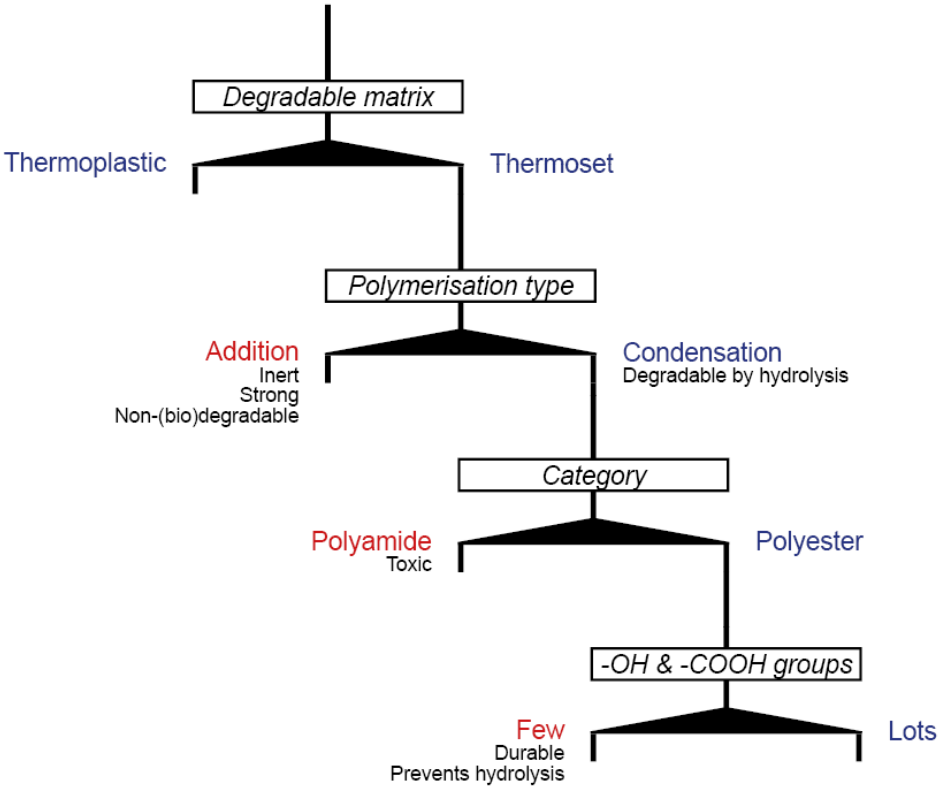

Figure 5.10: Decision tree for the thermoset degradable polymer.

reversible by hydrolysis - meaning that water can break them down into its monomers. However, efficient removal of the condensate (water) is essential to achieve a high degree of cure. Most of the water is removed in an initial reaction, resulting in a large amount of oligomers - short polymer chains consisting of a small amount of monomers, while keeping the viscosity acceptable for impregnation. After impregnation, a full cure can be achieved by applying reduced pressure (under vacuum in composite manufacturing) and increasing the temperature, while allowing the residual water to distil from the system (Gubbels et al., 2018).

Polyesters

Condensation polymers include polyesters and polyamides. Polyesters are formed through the reaction of a carboxylic acid and an alcohol, with water released as a by-product. Similarly, polyamides are synthesized by reacting a carboxylic acid with an amine, also producing water as a by-product (Gubbels et al., 2018). Unfortunately, amines are inflammable, explosive with air, odorous, and highly irritating or corrosive (Roose et al., 2015). This leaves only polyesters as an option.

The ability to undergo hydrolysis varies significantly from one polyester to the other. Petroleum-based polyester monomers contain a low amount of oxygen atoms. The resulting polyesters are hydrophobic since their low amount of hydroxyl (-OH) and carboxyl (-COOH) groups all reacted. This creates very durable materials, but prevents the hydrolysis back into its monomers (Alberts & Rothenberg, 2017).

On the contrary, monomers with more hydroxyl and carboxyl groups form polymers that are more hydrophilic, as not all of these groups react to form the polymer chain. In a humid environment, the polymer more readily absorbs water and undergoes a slow hydrolysis back into its monomers (Alberts & Rothenberg, 2017). An unfortunate side effect of monomers with more hydroxyl and carboxyl groups is their typically higher viscosity due to larger molecules. Combined with the elevated melting temperature of these larger molecules, it becomes clear that the requirement for hydrolysis, along with low viscosity and a low melting point, are contradictory. Further add to that the toxicity, or harmful nature of some carboxylic acids and alcohols, this search appears to become increasingly difficult.

(a)  (b) 

Figure 5.11: Examples of the materialisation of polyglycerol citrate. (a) Image from the original paper of Alberts and Rothenberg (2017) to show the different materialisations of polyglycerol. The transparent non-porous 'wheel' is created by slow controlled polymerisation of polyglycerol citrate during 100 hours at 90 °C, resulting in a plastic sheet with a density of 800 mg/cm^{-3}. The foam is created by fast polymerisation during only one hour at 180 °C, resulting in a open-cell foam with a density of 100-200 mg/cm^{-3} (b) Plantics (n.d.) uses the polyglycerol citrate resin in a commercial product: a set of hemp-reinforced polyglycerol citrate composite chairs.

Polyglycerol citrate

Alberts and Rothenberg (2017) nevertheless identify a polymer composed of glycerol, the simplest trialcohol, and citric acid, the simplest abundantly available triacid, as a highly promising biodegradable material that largely meets the requirements of this work. As a trialcohol and a triacid, glycerol and citric acid each contain three hydroxyl or carboxyl groups, some of which remain unreacted after polymerization. This results in a hydrophilic polyester that facilitates hydrolysis, while being completely non-toxic, cheap and even bio-based.

Another advantage of the hydrophilic nature of polyglycerol citrate its strong adhesion to other hydrophilic materials, such as natural fibres, making it particularly compatible with flax.

Processing time however suffers due to both monomers are not as reactive and the need for water to evaporate. Curing time to reach a solid material instead of a foam is in the neighbourhood of days, and at elevated temperatures of up to 150 °C, depending on pressure regiments (Alberts & Rothenberg, 2017; Alberts & Rothenberg, 2019). It is essential that the reaction is carried out above the boiling point of water, that is, above the point where the vapour pressure of the liquid equals the environmental pressure surrounding the liquid. At atmospheric pressure, it is therefore preferred to be carried out above 100 °C. At reduced pressures, the reaction can be carried out at lower temperatures (Alberts & Rothenberg, 2019). While at near-vacuum, water would already boil off at room temperature, however, such a low cure temperature would decrease the already slow reaction rate.

The rate of hydrolysis is influenced on both the density and degree of polymerisation. Alberts and Rothenberg (2017) report that samples with more than 95% polymerisation remained stable in water for months, whereas those with less than 80% polymerisation degraded after a few weeks. The authors also commented on the impact of density: a sample with a density of 0.6 g/cm^3 degraded over the course of a year, while a sample with a density of 0.16 g/cm^3 disintegrated within just a few days.

Figure 5.11 presents the different materialisations of polyglycerol citrate depending on the polymerisation speed and a commercial application of the resin.

5.3.2.2. A quickly degrading thermoplast

Thermoplastics are known to be recyclable by melting. Furthermore, most degradable (bio)plastics tend to be thermoplastics. However, the high melt viscosity and high processing temperature of thermoplastics result in challenges during production, namely poor fibre impregnation which needs to be overcome by heated and pressurised moulding (Compression- or Injection moulding), or by using Automated Fibre Placement (De et al., 2024). It is questionable if the investment costs are worth it for even mass production of multiple parts. Polyvinyl alcohol (PVA) is the choice for a quickly degrading, thermoplastic, water soluble polymer. PVA has been identified as a promising material by Jain et al. (2018), Oun et al. (2022), and Tan et al. (2015) due to a combination of its biodegradability, mechanical, thermal, adhesion and non-toxicity properties.

Figure 5.12: Manufacturing of the four sample pieces. Two are cured under vacuum, two under normal atmospheric conditions with periodic heating with a heat gun.

5.3.3. The reality of material testing

Specific data on strength and stiffness of the matrix is only discussed in general terms in literature, as is the amount and duration of degradation in water. An extensive test of material qualities would be of great help to get to know the precise technical possibilities.

The aim was to analyse the mechanical properties of the two composite materials that should be able to degrade in a marine environment: a flax-reinforced polyglycerol citrate plastic and a flax-reinforced polyvinyl alcohol plastic. Once the material samples were manufactured, they would be submerged in water. Tensile and bending tests would be conducted every two weeks over a six-week period, with four testing sessions in total.

Before proceeding with the substantial manufacturing effort, the feasibility of producing samples of these materials was first validated. Unfortunately, samples of sufficient quality could not be produced. The primary challenge stemmed from the need for both matrix materials to be handled under elevated temperatures.

5.3.3.1. Flax-reinforced polyglycerol citrate plastic

Glycerol and citric acid have to be mixed thoroughly before it can be treated as a resin. While glycerol is liquid at room temperature, the melting point of citric acid is 156 °C and mixing has therefore be performed at or around that temperature. During the layup and curing process, the whole system should also be held under elevated temperatures. Both of these process temperatures are described in the relevant patent from Alberts and Rothenberg (2014). While these requirements are very much possible to reach in a factory or specific composites laboratory setting, some necessary equipment was not available. Another method should be theoretically possible, which is described next.

By dissolving citric acid in water - citric acid is highly soluble, 60/100 w/w at 20 °C - the resin can be mixed and processed at room temperature. When the infused composite is under vacuum, the water will be boiled off. This however did not work due to three reasons. Firstly, the resulting resin is highly viscous and has a tendency to get pulled out of the reinforcement. Secondly, the amount of water (100g water for 60g citric acid) is too much. At a - for flax - conventional fibre to resin ratio of 33/66, the reinforcement is quite literally drenched in resin and cannot be handled like in a conventional vacuum bag process. Finally, the amount of water that has to boil off creates problems for the vacuum pump and results in not being able to pull to (close to) full vacuum.

5.3.3.2. Flax-reinforced polyvinyl alcohol plastic

Polyvinyl alcohol mostly suffers from the same problems as described with glycerol citrate. Is has to be processed above its melting point of 200 °C. Its solubility of about 20/100 w/w results in a solution of mostly water. With the knowledge of glycerol citrate, it is impossible to create material samples by boiling off the large amount of water within the dissolved PVA mixture.

5.3.4. Theoretical recommendations

With the appropriate equipment and controlled processing conditions for glycerol citrate (described in the patent from Alberts and Rothenberg (2014)) and PVA at elevated temperatures, these materials are likely to function effectively as matrix materials. Additionally, with sufficient research and development, alternative processing methods could be explored that do not require consistently high temperatures. However, within the scope of this thesis, neither approach could be pursued. As a result, specific material properties and degradation behaviour could not be studied.

It is also uncertain whether the investment in cost and time would be justified for the production of a few thousand units. Currently, polyglycerol citrate requires several days of moulding per product, making large-scale production impractical. Processing PVA presents other challenges. As a thermoplastic, it would require highly durable and expensive moulds to cope with the high pressures of thermoplastic resin injection, making it potentially viable only for a very large production. Furthermore, PVA would require a protective coating, the materialisation and feasibility of which remains unclear.

Given the unknown impact of marine litter and the difficulties described in the production of degradable materials, there remains too much uncertainty on the relevancy and manufacturing feasibility to proceed with design based on degradable materials. If at a later stage the environmental impact of ASB littering becomes quantifiable and is found to be significant, one could revisit this degradable approach and seek further development.

6

Concept design, prototyping & validation

This chapter presents the naval design of the ”SDC25” - Swarm Design Concept 2025 -, its prototype and the testing of it. In previous sections the first research question has been tackled, here an answer to the second is given: *How would the design of a low environmental impact autonomous sailboat look like?* It is designed as a high-fidelity prototype, where details and materialisation can differ from a final design for mass production, but it is able to present, test and evaluate the core principles. Recommendations for mass production are discussed in Section 7.1.2.

Design vision
This design takes some significant steps towards a more sustainable vessel by integrating the following design interventions from the roadmap, along with the insights of Chapter 5:

- The vessel is positioned at the shorter end of the ASB spectrum while trying to maintain effectiveness in harsh marine environments. This approach maximises the environmental benefits of minimising individual vessels in a swarm, as discussed in Section 5.1. However, extensive empirical testing on operational effectiveness will be required to evaluate the effectiveness of its current size.
- The vessel is designed using low-impact materials such as glass fibre composites and steel, while allowing for the substitution of most structures (particularly all the GFRP) with a biodegradable flax fibre composite, as discussed in Section 5.3.
- Electronics are minimised by incorporating mechanical and aerodynamic feedback control.

Design approach
Evans (1959) described ship design as a extremely complex problem, where an iterative process must be adopted. He modelled these iterations in the ship design spiral, which has been adopted by many engineers as the standard model of naval design. While originally applied to cargo ships, the process can be used for all ships and has been adapted for sailing yachts by Larsson et al. (2022), whose version is shown in figure 6.1.

The process of designing this concept roughly followed this spiral. The first iterations focussed on weight estimates, the design of the hull, and its hydrostatic characteristics, which are described in section 6.1.2. Once the dimensions of the hull were largely set, the dimensioning and design of the rig (sails) in section 6.1.3 could be addressed, followed by the design of the appendages - keel and rudder - in section 6.1.4, and concluded with a stability calculation and evaluation in section 6.3.

Furthermore, this thesis uses a statistical design approach to inform the proportion between, and the size of certain components. The statistical design approach is widely used in maritime engineering and involves using historical data to guide decisions in the design process. Instead of relying solely on first-principles physics or deterministic models, this approach essentially derives an average parameter set based on existing boats. For example: it can provide the displacement as a function of vessel length. The properties of existing ASB designs, which are compiled in Table 2.4, have proven to be valuable at this stage.

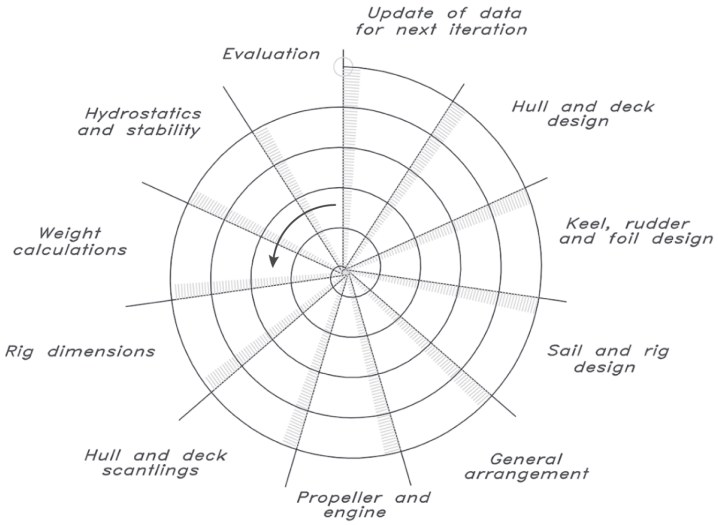

Figure 6.1: The ship design spiral, originally described by Evans (1959), adapted for sailing yachts by Larsson et al. (2022).

6.1. Concept design

6.1.1. System description & general arrangement

The SDC25 (Figure 6.2) feels like a natural progression, built upon insights gained from reviewing previous projects and their recommendations. Big inspirations were Elkaim (2001), who described his design in tremendous technical detail, Tretow (2017), who designed and built a free-rotating wingsail with aerodynamic control, and Silva et al. (2019), who compiled many learnings and best practices. Compared to previous examples however, this concept is smaller and further integrated.

The SDC25 is designed for autonomous operation on inland waters such as lakes, with the aim of collecting environmental data. Although it is not yet capable of independent sailing, its subsystems have been developed with autonomous functionality in mind. The vessel measures 1.36m in length and has a displacement of 11.2kg.

The material selection considers the likelihood of eventual failure and prioritises environmental responsibility. Steel and glass fibre composites are used to reduce the environmental impact of material production, while ensuring non-toxicity and sufficient structural integrity for long-term deployment.

The sail is designed to be aerodynamically self-stabilising, to minimise reliance on actuation (a point of mechanical or electronic failure) and reduce energy consumption and electronic complexity. It maintains a propulsion-generating orientation in response to wind direction without continuous actuation. Actuation is only required during manoeuvres such as tacking or jibing.

The design of the SDC25 is is illustrated in Figure 6.2, general specifications are listed in Table 6.1, and key dimensions are shown in Figure 6.3.

Platform name	Swarm Design Concept 2025 (SDC25)
Hull	Mono
Length (m)	1.36
Beam (m)	0.353
Draft (m)	0.516
Displacement (kg)	11.2
Sail type	Wing Sail
Sail Design	Self-trimming
Sail area (m^2)	0.168
LDR	4.95
L/B	3.9
SA/D	3.4
B/D (%)	37

Table 6.1: General specifications of the Swarm Design Concept 2025 (SDC25).

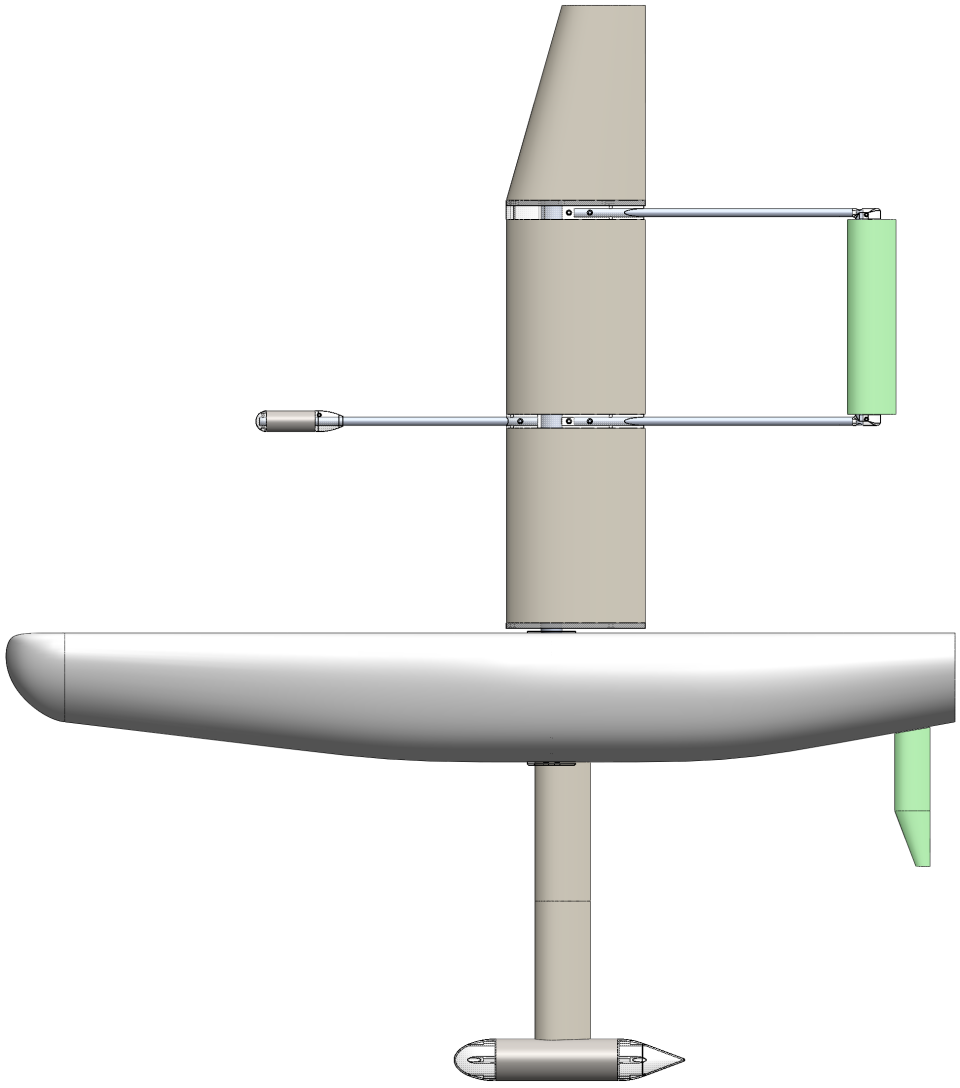

Figure 6.2: The design of SDC25.

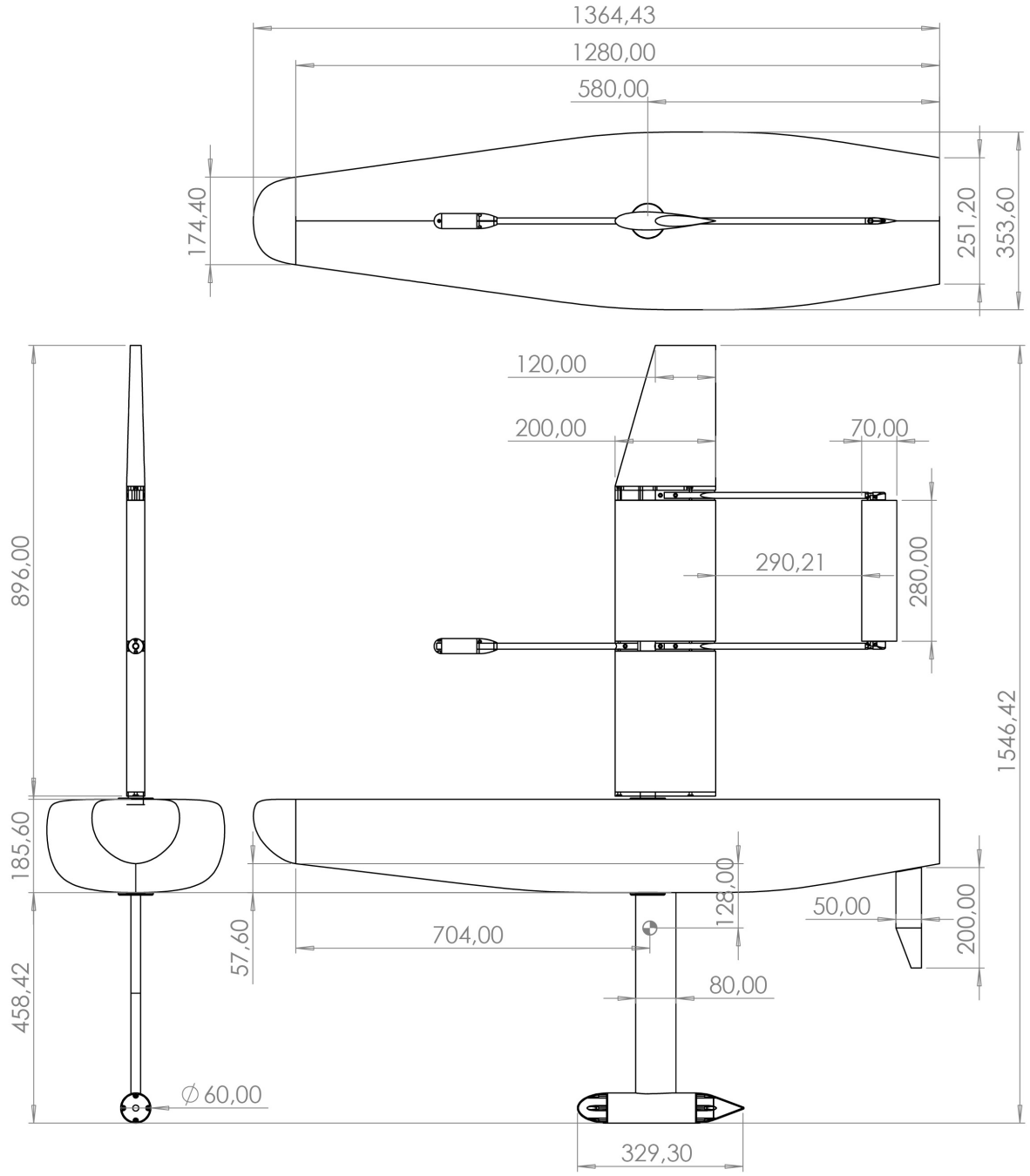

Figure 6.3: General dimensions of the SDC25.

6.1.2. Hull design

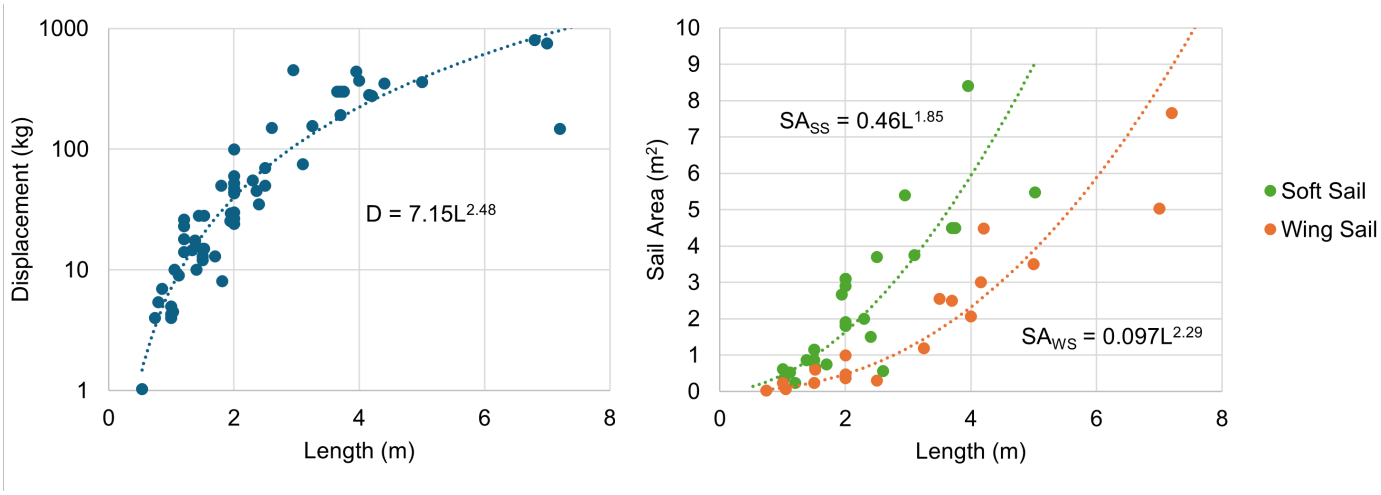

(a) The correlation between displacement and length.

(b) The correlation between sail area and length, distinguishing between soft and wing sails. Wing sails are generally more efficient but heavier, resulting in a reduced sail area for boats of a similar lengths.

Figure 6.4: Properties and correlations between naval characteristics of existing designs, based on data from Table 2.4.

A line drawing of the hull is presented in Figure 6.7. "SDC25" is designed with a waterline length (L_{wl}) of $1.28m$ and a displacement (Δ) of $11.2kg$.

The design began by roughly envisioning and selecting a reasonable size - a boat of 1 to $1.5m$ - that is on the smaller end of the existing designs. There have been many previous designs in this 'weight class' that have been proven to work, albeit not for extended periods in sea conditions. The difference is that this work will apply to a lake-going, not a sea-fearing vessel. All components envisioned for an integrated prototype for such a size were added to a table, with each part assigned an estimated mass, a longitudinal centre of gravity (LCG) position, and the corresponding moment about the LCG. After summing the masses of all components, a safety factor of 1.2 was applied, resulting in the design displacement for the hull, calculated as 11.5 kg. The initial mass estimation is attached in Appendix B.

The length-to-displacement of existing hulls was plotted in Figure 6.4a and their correlation is described as:

$$\Delta = 7.15{L_{wl}}^{2.48} \tag{6.1}$$

The corresponding waterline length for $\Delta = 11.5kg$ is $1.21m$. In a previous iteration not all existing designs had been compiled, leading to a slightly different relationship between length and displacement, resulting in a length of $1.27m$. After iterating on the hull design, a displacement of $11.2kg$ and length of $1.28m$ was settled upon. The combination of these values for displacement and length still align closely with the trend and thus serve as a reasonable and well-supported argument for the suitability of the hull design.

The following parameters were set and calculated to help shaping the hull: The Prismatic Coefficient[1] (C_p) was set to 0.55, as "*the C_p of yachts is typically* $0.45 - 0.6$" (Fossati, 2009). The beam draft ratio BDR was set to 5, similar to existing designs. Afterwards, the maximum cross sectional area[2] $AM = 0.0165m^2$, beam $B = 0.32m$ and draft $d = 0.065m$, were calculated by assuming AM to be the area of half an ellipse, as the section curve[3] of a rounded hull can be roughly approximated with an ellipse, using these equations:

$$AM = \Delta / C_p / L_{wl} \tag{6.2}$$

$$B = 2(AM * BDR/\pi)^{0.5} \tag{6.3}$$

$$d = (AM/0.25BDR * \pi)^{0.5} \tag{6.4}$$

[1] The Prismatic Coefficient (C_p) of a hull is the ratio of its actual underwater volume to the volume of an extrusion of its maximum underwater cross-sectional area (AM) over the length of the hull.

[2] The maximum (underwater) cross-sectional area (AM) is the area of its largest section, generally at the widest part of the hull.

[3] A section curve of a hull is a vertical slice taken perpendicular to the hull's centreline, showing the shape of the cross-section at a specific point along its length.

Modelling procedure in Rhino
Modelling of the hull was performed in Rhinoceros 7. The modelling procedure was as follows:

1. Create a surface with a length of the Lwl.
2. Subdivide into 6x9 control points to effectively create 9 section curves with 6 control points each over the length.
3. Transform the surface (all section curves) into the imagined midship section curve, over its whole length.
4. Shape hull with a combination of Bend and Shear commands, using it on a selection of control points.
5. Check if hydrostatics are in line with the design parameters with the Hydrostatics command. Iterate by going back to point 4.
6. Draw and loft a G3 continuous rounded bow.
7. Mirror and merge surfaces, and cap the open stern surface to create one unified surface.

During the design process, the constraints of the intended prototyping method - foam sections cut with a hot wire CNC - were considered. That meant that the prototype hull would be an assembly of multiple straight lofts. However, this limitation applies only in one dimension; the section curves, which exhibit significantly more absolute curvature than the buttock lines[4], retain full design freedom. While the intersections between straight lofts could be sanded into continuous curves, minimising this manual work is preferable. Therefore, the number of curves along the hull's length is kept to a minimum, with most sections forming straight lofts. For mass production, the hull design could incorporate more continuously curved buttock lines, though the overall impact on performance and appearance would be minor. Finally, a rounded bow was drawn and lofted. The intent behind this design choice is that a more voluminous bow allows the hull to sail over ripples rather than cut through them. This results in less pitching behaviour.

Curvature continuity analysis
Hull curvature continuity refers to the smoothness of the hull lines, with an ideal target of fully continuous (G3) curvature to minimise hydrodynamic drag. While the manufacturing constraints of the prototype have a minor impact on longitudinal continuity, all section curves are designed to be continuous.

In Rhino, the *CurvatureGraph* tool visually represents curvature variations along a curve and is a commonly used naval tool to check hull curvature. A smooth, flowing graph indicates continuity, whereas sharp spikes reveal discontinuities. This tool was used repeatedly to refine the hull sections, resulting in a relatively smooth final hull with only minor deviations due to manufacturing constraints. Figure 6.5 illustrates the sectional continuity, Figure 6.6 the longitudinal continuity.

[4] Buttock lines are vertical longitudinal slices of a hull, showing how the shape of the hull changes from the centreline outward when viewed from the side.

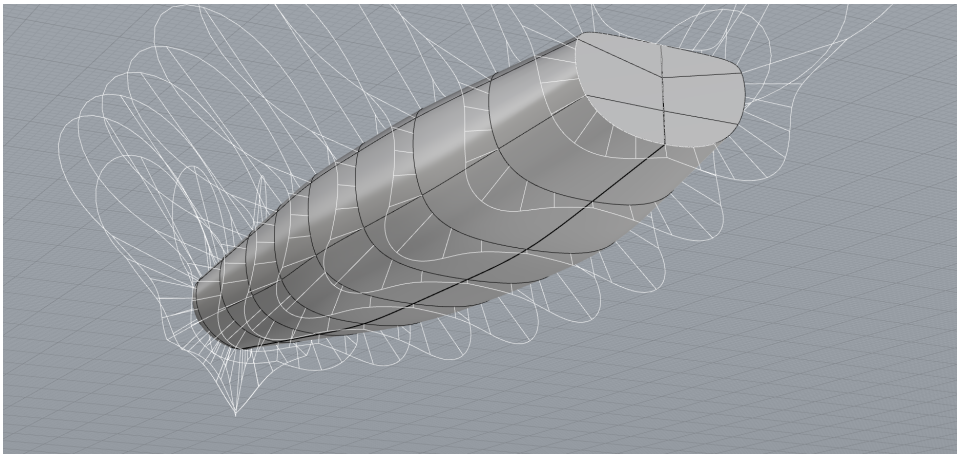

(a) Sectional continuity of the underwater ship.

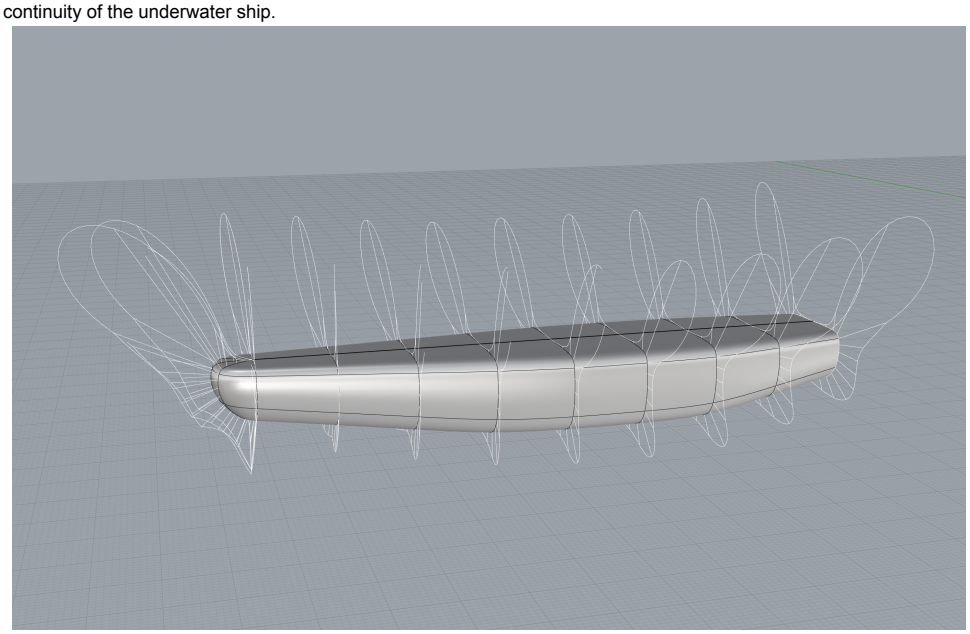

(b) Sectional continuity imaged from another angle, making the rounded bow visible.

Figure 6.5: Sectional continuity of the hull. The sections are almost fully G3 continuous. Only the interface between bow and hull could not be made fully continuous.

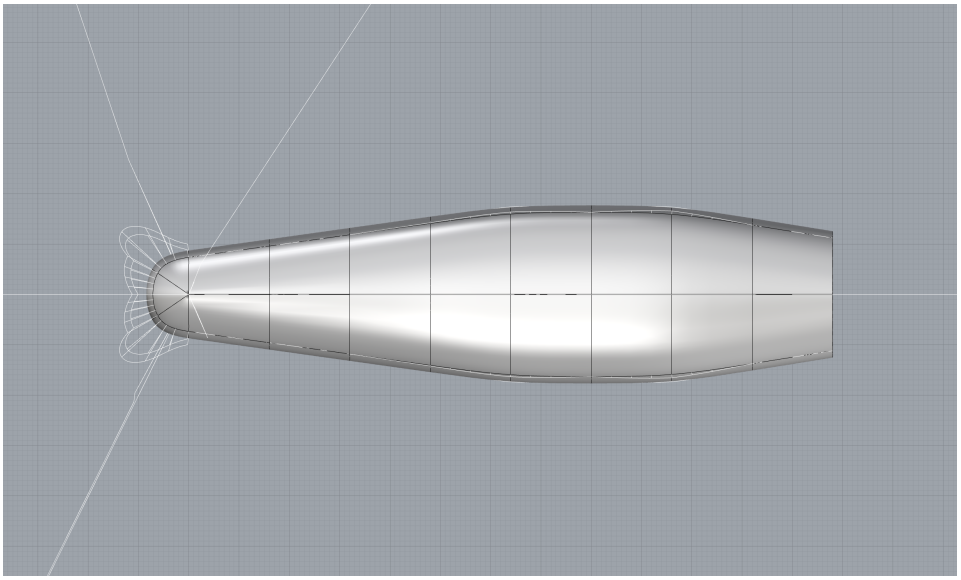

(a) Longitudinal continuity of the underwater ship, visualised from below. The scale of the *CurvatureGraph* display is on the same scale as in Figure 6.5, showing that the curvature is logically significantly lower in absolute terms than the sectional curves.

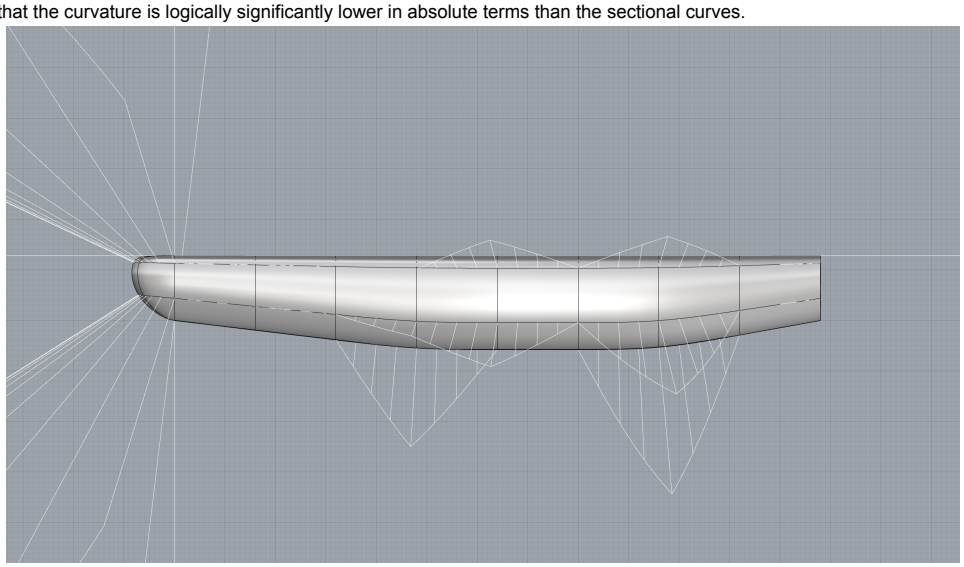

(b) Longitudinal continuity from a side view, showing only tangential (G1) and G2 continuity for the rest of the hull. The scale of the *CurvatureGraph* display is increased here for visibility reasons.

Figure 6.6: Longitudinal continuity of the hull, showing multiple areas without curvature: the impact of straight lofts that are needed for manufacturability. The spikes that fly off the illustration are a stitching fault between the bow and hull.

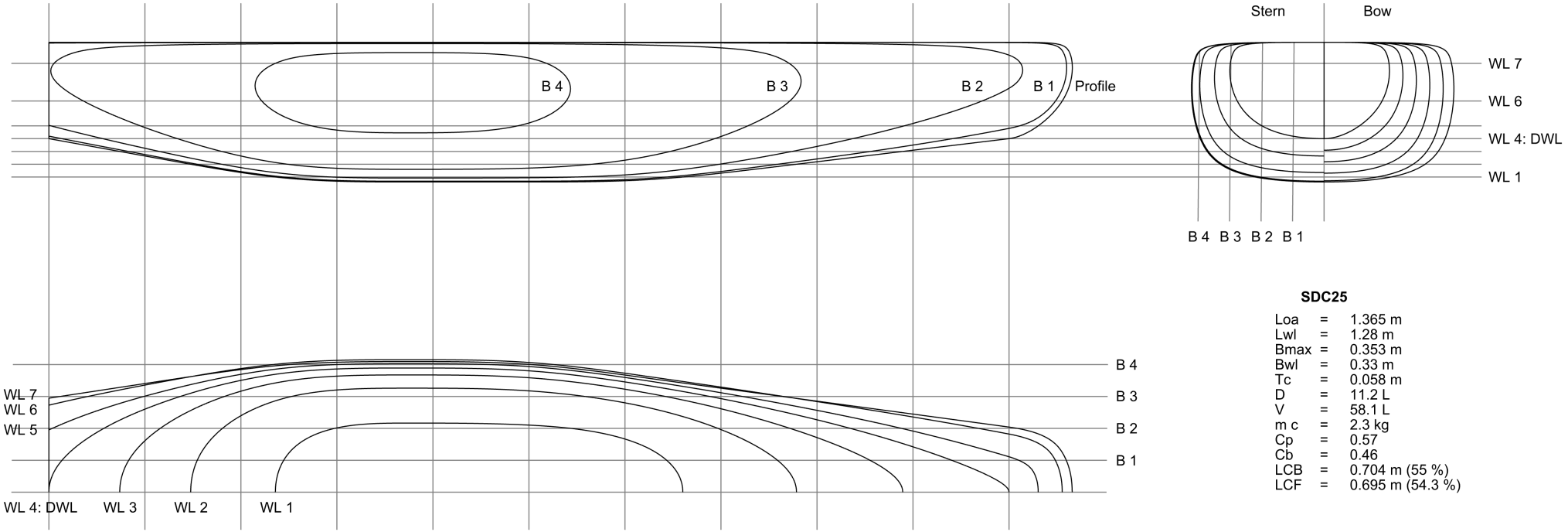

SDC25

Loa	=	1.365 m
Lwl	=	1.28 m
Bmax	=	0.353 m
Bwl	=	0.33 m
Tc	=	0.058 m
D	=	11.2 L
V	=	58.1 L
m c	=	2.3 kg
Cp	=	0.57
Cb	=	0.46
LCB	=	0.704 m (55 %)
LCF	=	0.695 m (54.3 %)

Figure 6.7: Line drawing of the hull of the SDC25.

6.1.3. Propulsion system

6.1.3.1. Design

In Chapter 2, extensive information on sails has already been compiled. Multiple sources agree that a self-trimming sail would be the ideal choice for an autonomous sailboat due to its simplicity and lack of power consumption.

The sail - specifically a wingsail - for SDC25, adjusts its angle of attack to the wind automatically through the use of a vertical stabilizer (also referred to as a trim tab or tail(wing)). This vertical stabilizer is the only lifting surface that generates a moment on the sail assembly, allowing it to rotate the whole. The main wingsail is positioned such that its centre of lift aligns with the mast, eliminating any moment acting on the mast.

Figure 6.10 describes the design evolution of the sail.

To determine the sail area, the statistical approach can once again be used. The length versus sail area of existing vessels was plotted in Figure 6.4b and the correlation of vessels with wingsails is described as:

$$SA_{WS} = 0.097{L_{wl}}^{2.29} \tag{6.5}$$

The corresponding sail area for $L_{wl} = 1.28m$ is $0.17m^2$. Silva et al. (2019) recommends keeping the sail size modest and warns against the temptation to increase sail area. An example is provided by Tretow (2017), who designed a vessel with a sail area of $3m^2$, a length of $4.16m$ and a displacement of $280kg$. Despite these parameters lying only slightly above the average SA_{WS} correlation, the vessel was reported to heel excessively under normal conditions. To be fair, while the keel length of Tretow (2017) was on the shorter side, is it reasonable to assume the correlation in Equation 6.5 should serve as an upper design limit. A short vessel does however allow for a proportionally longer keel compared to larger vessels, which can help compensate for reduced stability.

A self-trimming wingsail has a couple general design characteristics that are integrated into the design of the sail of the SDC25, which is shown in Figure 6.8:

- The mast is positioned at the centre of aerodynamic pressure (CoP) of the mainsail. The CoP is generally understood to lie at 25% of the chord of an airfoil, from the leading edge (NASA, n.d.). The wing is swept back at the top to decrease induced drag, which also slightly pushes back the overall CoP. This is also advantageous for the mechanical design, as the NACA airfoils are widest at 30% of the chord, allowing for a wider - and thus stiffer - mast to be integrated.
- The tailwing area is generally $12 - 15\%$ of the mainsail area according to Z. Sun, Feng, et al. (2025), here it is 12%.
- The only actuation in the sail system is the rotation of the tailwing. This is controlled by a linear actuator housed within the wing, protecting it from the elements. This approach has not been seen in previous ASBs, which all place the actuator externally. The placement and design of the actuator allows the tailwing to maintain a constant angle of attack without requiring continuous power consumption when not in motion, even under load. The actuator gets powered from the electronics enclosure in the hull, and should be connected through a slip ring in the mast. For the prototype however, it is simply via a conventional cable and care must be taken not to let the sail rotate continuously in one direction.
- Since the tailwing is attached far behind the mast connection point on the hull, the centre of gravity (CoG) is shifted rearward. Additionally, the CoG of the mainsail is already positioned slightly aft of the CoP. For the self-trimming mechanism to function properly, the system must be balanced, meaning the CoG should align with the CoP. To achieve this, a counterweight is added in front of the mainsail.
- The symmetrical NACA0018 airfoil section is selected, as it provides sufficient internal space to accommodate all mechanical components.

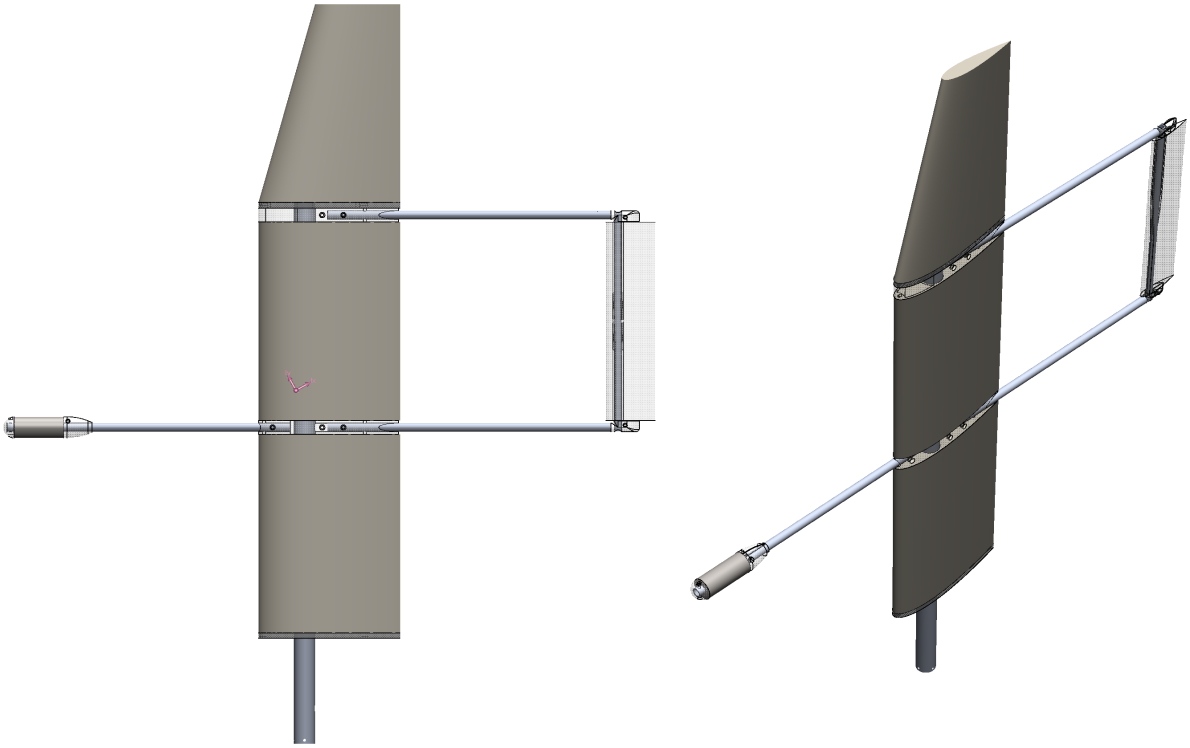

Figure 6.8: Design of the sail system. Frame connective members - those will be 3D printed - are shown translucent for clarity. Total mass is 1700g. The centre of gravity is added into the left image and it appears close to the centre of the mast. The length of the horizontal aluminium tubes can each be fine-tuned to balance the system, accounting for slight differences between the CAD model and prototype.

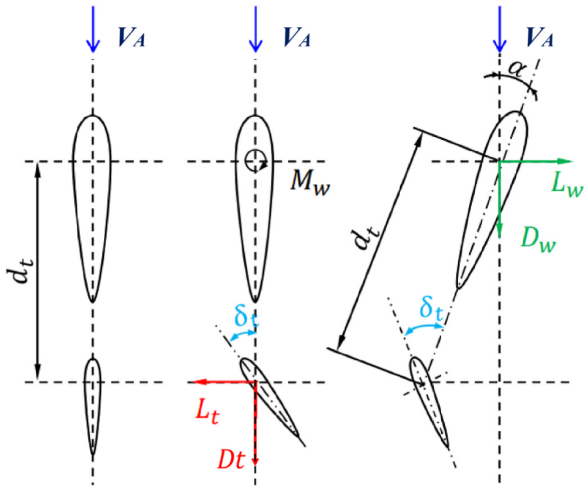

Figure 6.9: Moment balance relationship of a self-trimming wingsail (Z. Sun, Feng, et al., 2025).

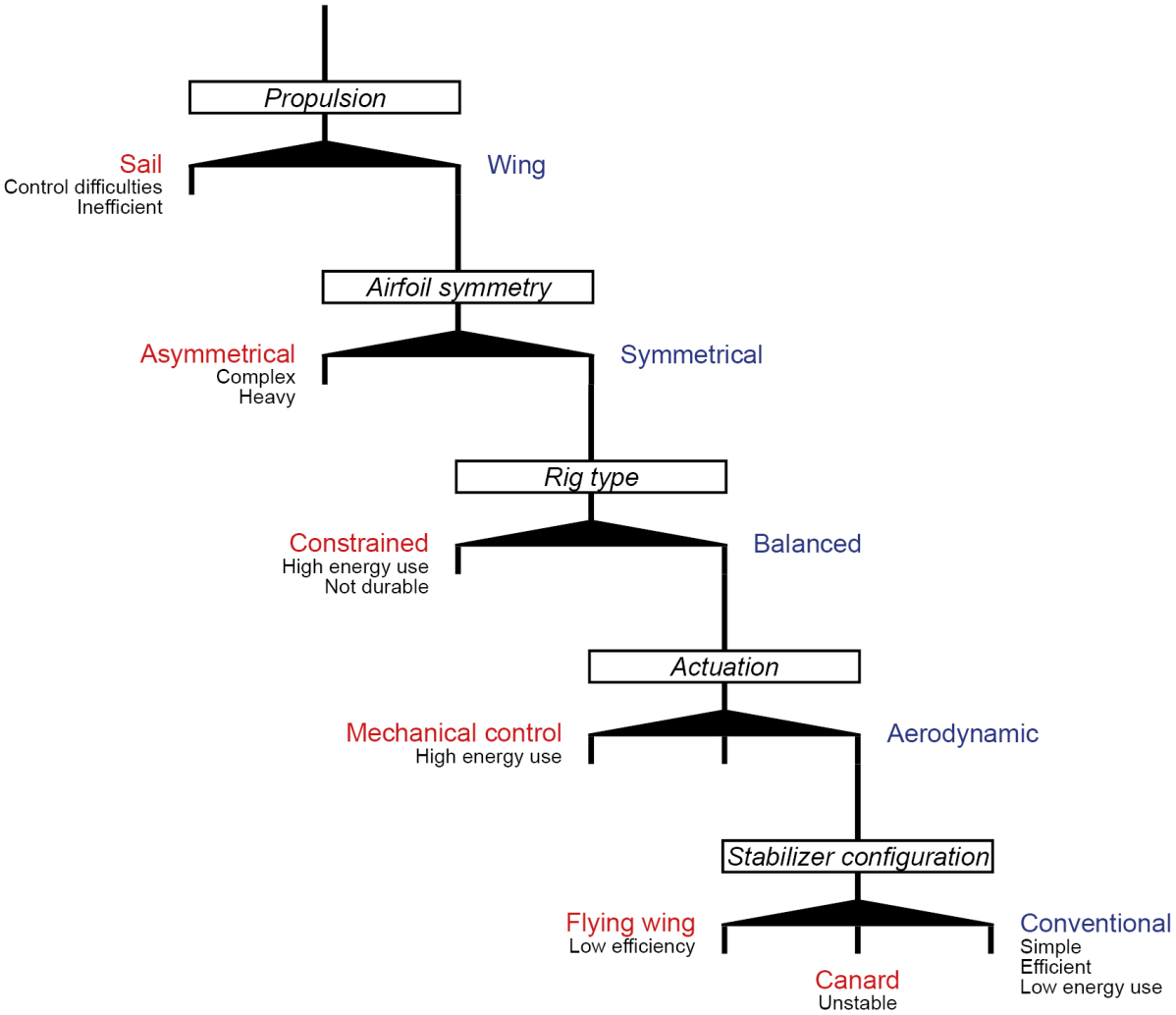

Figure 6.10: The design evolution of the propulsion system. The design problem, or design subject, is outlined. Two or three solutions are stated, of which the right solution - in blue - is the preferred one. The losing option - in red - is accompanied by its main disadvantage(s). These choices lead to a propulsion system with a rigid, symmetrical, balanced wing, which is aerodynamically controlled by a conventional stabilizer.

6.1.3.2. System dynamics

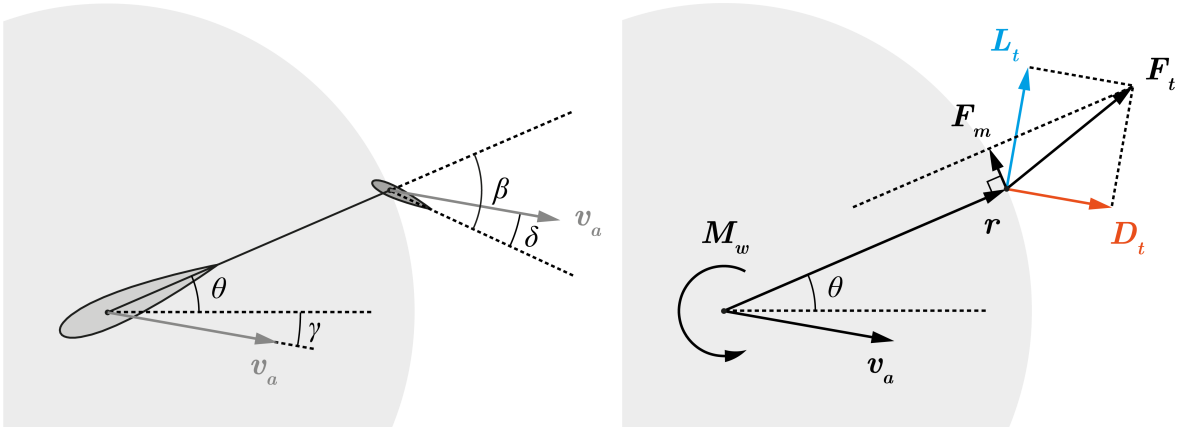

(a) Diagram showing the wingsail system with its main wing and tail wing. Four angles are defined: the position angle θ of the system, the apparent wind direction γ, the constant tail wing offset β, and the angle of attack of the tail wing δ versus the apparent wind direction. The apparent wind vector $\vec{v_a}$ is shown for clarity.

(b) Free body diagram illustrating the polar vector system of the dynamics of the sail. Lift ($\vec{L_t}$) and drag ($\vec{D_t}$) vectors are drawn for the tail wing, as are the resulting aerodynamic force vector ($\vec{F_t}$) and its orthogonal projection ($\vec{F_m}$) on the position vector ($\vec{r}$). $\vec{v_a}$ is the apparent wind vector. Aerodynamic forces of the main wing are not drawn because they do not result in angular acceleration.

Figure 6.11: Diagrams of the polar dynamics. Angles are exaggerated for clarity, and vector magnitudes are not necessarily to scale.

To understand the movement of the wingsail and the influences of certain parameters, a dynamics model was developed. This approach of modelling the dynamical system to extract design parameters quickly got out of hand and was studded on simplifications. It was later substituted with the more pragmatic statistical design approach by examining existing boats that use aerodynamic control. Diving into the dynamics however resulted in a better understanding of the system. An overview of the forces and moments acting on this polar system is illustrated in Figure 6.11. The definition of the vectors and equations of motion, python code, and results of the model is attached in Appendix E.

6.1.4. Appendages

6.1.4.1. Central construction

To decrease complexity and the strength and stiffness requirements of the hull, the sails are designed to mount to the keel with radial bearings. Instead of two rigid connections - keel-to-hull and hull-to-sails - this approach creates a direct, stiff connection between the keel and sails, with the hull clamped in between. This decision was also influenced by the potential use of biodegradable materials for the hull, which may not withstand the forces and tolerance requirements as well as traditional engineering materials. Given the likely limitations of such materials, this design helps mitigate structural concerns. However, in a final design, the clamping method should be revisited to ensure long-term reliability and durability of the connection. Figure 6.12 illustrates the design.

6.1.4.2. Rudder

The rudder features a NACA0018 profile and has an area of approximately 2% of the sail area, determined by extrapolating the recommendations from Larsson et al. (2022) for smaller vessels. It is actuated by a servo housed within the hull. The rudder and its actuation are of less importance in this concept, as greater gains can be achieved elsewhere; its primary role is to provide control authority for the prototype. In earlier ASB designs, the rudder and its actuation have proven more reliable than the sail system, which is why the focus here lies mainly on the sail. Additionally, zero-energy self-steering systems using a windvane to control the rudder have been described in the literature (Stelzer & Jafarmadar, 2011) and are commonplace on yachts. In the SDC25, the sail effectively acts as a large windvane, suggesting the potential for a future mechanical linkage between mast angle and rudder. Such a system could eliminate energy use when holding a steady angle to the wind, requiring actuation only when changing course.

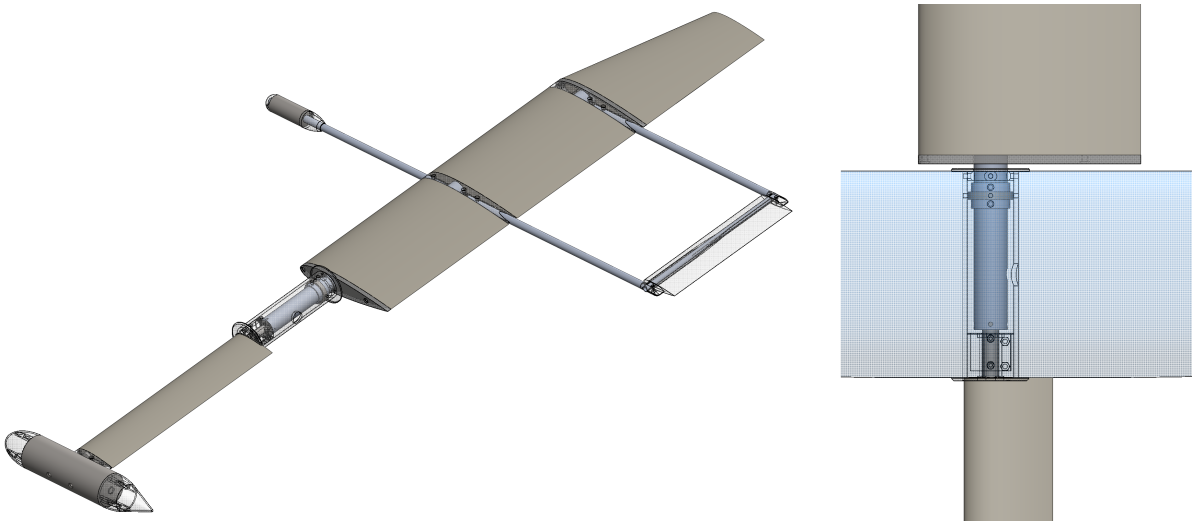

Figure 6.12: The mast rotates freely on two radial bearings, creating a direct connection between the sails and keel. This design directly couples heeling and propulsion forces, significantly reducing local strength and stiffness demands on the hull compared to conventional setups where the sail and keel are mounted separately and interact less directly.

6.1.4.3. Keel

Like yachts, many autonomous sailboats use a keel with a bulb, where the majority of the mass is concentrated to maximise the righting moment. Traditionally, lead has been the preferred ballast material due to its high density of $11.34 g/cm^3$. However, because of its toxicity, steel, with a density of approximately $7.8 g/cm^3$, is now favoured not only for structural components but also for ballast.

As with the hull and sails, the keel design is informed by statistics. The average ballast-to-displacement ratio of 37% (Table 2.4) has been applied to the SDC25, resulting in a ballast mass of 4.14kg for a total displacement of 11.2kg. Of this, 3.86kg is concentrated in a cylindrical steel bulb measuring 175mm in length and 60mm in diameter. A streamlined fairing is added to the bulb to reduce both manufacturing complexity and hydrodynamic drag. The bulb is mounted on a 400mm keel, composed of a 15mm steel shaft enclosed in a NACA0024 fairing. The design is visible in Figure 6.12. This dimension is also informed by existing designs. The draft (depth below the waterline) is described by

$$d = 0.386 L^{0.74} \tag{6.6}$$

6.1.5. Control

The control system for SDC25 is designed solely for testing purposes and does not reflect the complexities or further development required for a fully autonomous boat. Since, during testing, only naval parameters will be evaluated and further development of an autonomous control system is out of scope, a conventional radio control system is deemed sufficient. Figure 6.13 illustrates the control system and actuators in this prototype.

Actuation

A linear actuator is integrated into the tailwing for angle control. The actuator only needs to be engaged once to set the desired angle. It is housed within a slotted aluminium tube that restricts rotational motion while allowing for translation. In the rotational axis of the tailwing, an elongated helix is cut out, which interfaces with a pin through the slot and connects to the linear actuator. By designing the system such that the helix rotates 60 degrees over the full actuation range of the linear actuator, the wing can be set to an angle between -30 and +30 degrees relative to the rest of the sail assembly. Any torque on the wing during sailing will be mechanically absorbed, without the need for powering the actuator. A second actuator, a servo, controls the rudder angle with a more conventional, direct on-axis mount. The tailwing and its actuation is illustrated in Figure 6.23.

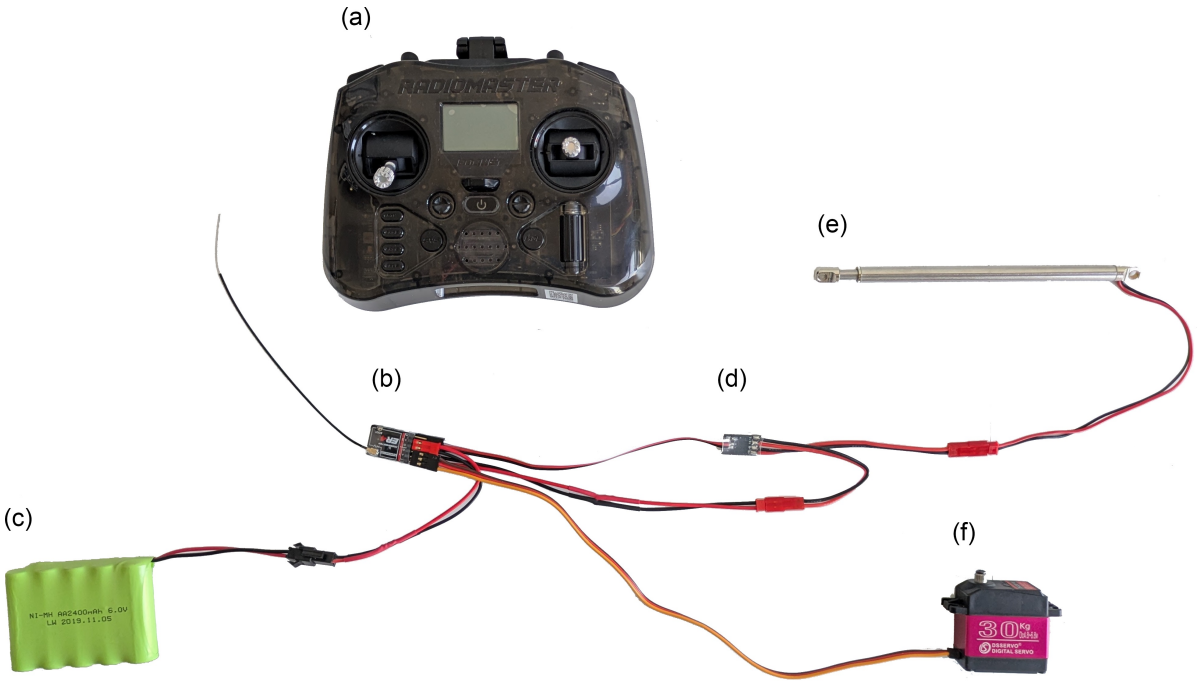

Figure 6.13: Control electronics for the SDC25. (a) Remote controller RadioMaster Pocket, (b) RadioMaster ER4 PWM receiver, (c) NiMH 2400mAh 6V battery, (d) PWM motor controller for the linear actuator, (e) Linear actuator 6V, 80mm extension, 8mm in diameter, (f) TD-8130MG Servo

6.1.6. Stability

6.1.6.1. Trim

Trim refers to the fore-and-aft balance of a vessel and is governed by the longitudinal distribution of mass. Excess weight toward the bow or stern results in bow-down or stern-down trim, respectively. Neutral trim occurs when the longitudinal centres of gravity (CoG) and buoyancy (CoB) are aligned. The mass is divided between sails, hull, and keel, and buoyancy is mainly provided by the hull. In this design, the sail system is inherently balanced around the mast, and the keel is also configured with its CoG on the centreline. As a result, the cutout for mounting the keel and sail is positioned near the hull's CoB, located at 704mm, with the cutout placed slightly forward at 700mm. This would cause a slight bow-down pitch, if not for the additional components rudder, actuator, and electronics, located toward the stern. Although their mass is small, they shift the CoG slightly aft, helping to align it more closely with the CoB.

6.1.6.2. Transverse stability

The transverse stability is described by its righting moment RM. $\overline{GM}$ is the righting arm and is the distance between the centre of gravity G and the projection Z of the heeled centre of buoyancy in line with G. Figure 6.14 illustrates this situation. The righting moment is calculated as:

$$RM = mg\overline{GM} \tag{6.7}$$

A challenge in this process is the uncertainty regarding the positioning of the heeled boat on the water surface. The only way to overcome this is by systematically iterating the sinkage to find a position where the displacement matches the original. This process is carried out in Rhino Grasshopper for numerous angles between 0 and 180 degrees. Figure 6.15 plots the results and illustrates the righting moment of SDC25.

Workflow

The boat is analysed including its appendages, as these winged structures possess significant volume and, therefore, buoyancy. A loop was developed where the centre of buoyancy (CoB) and the displacement of the submerged part of the boat were calculated. When the displacement was lower than

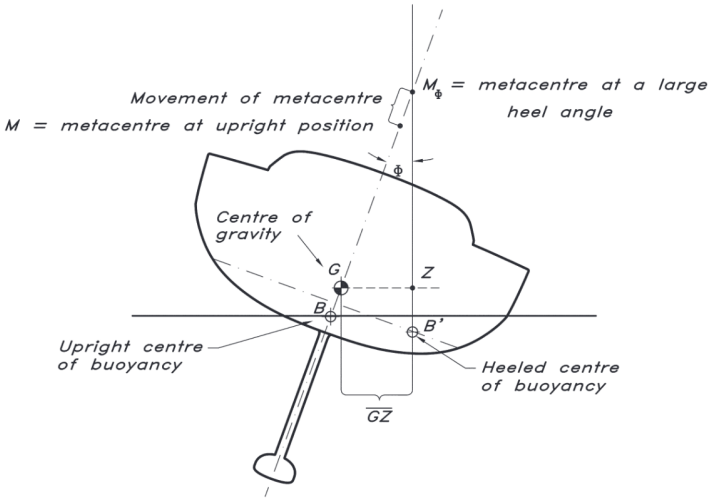

Figure 6.14: Illustration of the righting arm $\overline{GZ}$ of a general yacht. (Larsson et al., 2022)

the original value, the boat was lowered slightly until the displacement matched the original. Simultaneously, the centre of gravity (CoG) was adjusted to align with the rotation and sinkage of the boat. The distance GM was then calculated by determining the difference between the y-axis coordinates of the CoB and the CoG. Multiplying this by the mass (m) and gravitational acceleration (g) provided the righting moment for the corresponding heeling angle. This process was repeated for multiple angles to generate a figure representing the full transverse stability, as shown in figure 6.15. The full Grasshopper workflow is added in Appendix C.

Conclusion

Due to the volume in the wingsail and its distance from the hull's centre of buoyancy, a significant positive influence is exerted on the total centre of buoyancy when submerged. This results in a greater righting moment after 90°, which is unusual but ideal for this specific use case. Additionally, it ensures that the boat remains positively stable at all times. Typically, sailing yachts exhibit a small range of heel (generally between about 140° to 180°) where they are stable upside down, but this is not the case here, which fully satisfies the design criteria of designing a ship that self-rights.

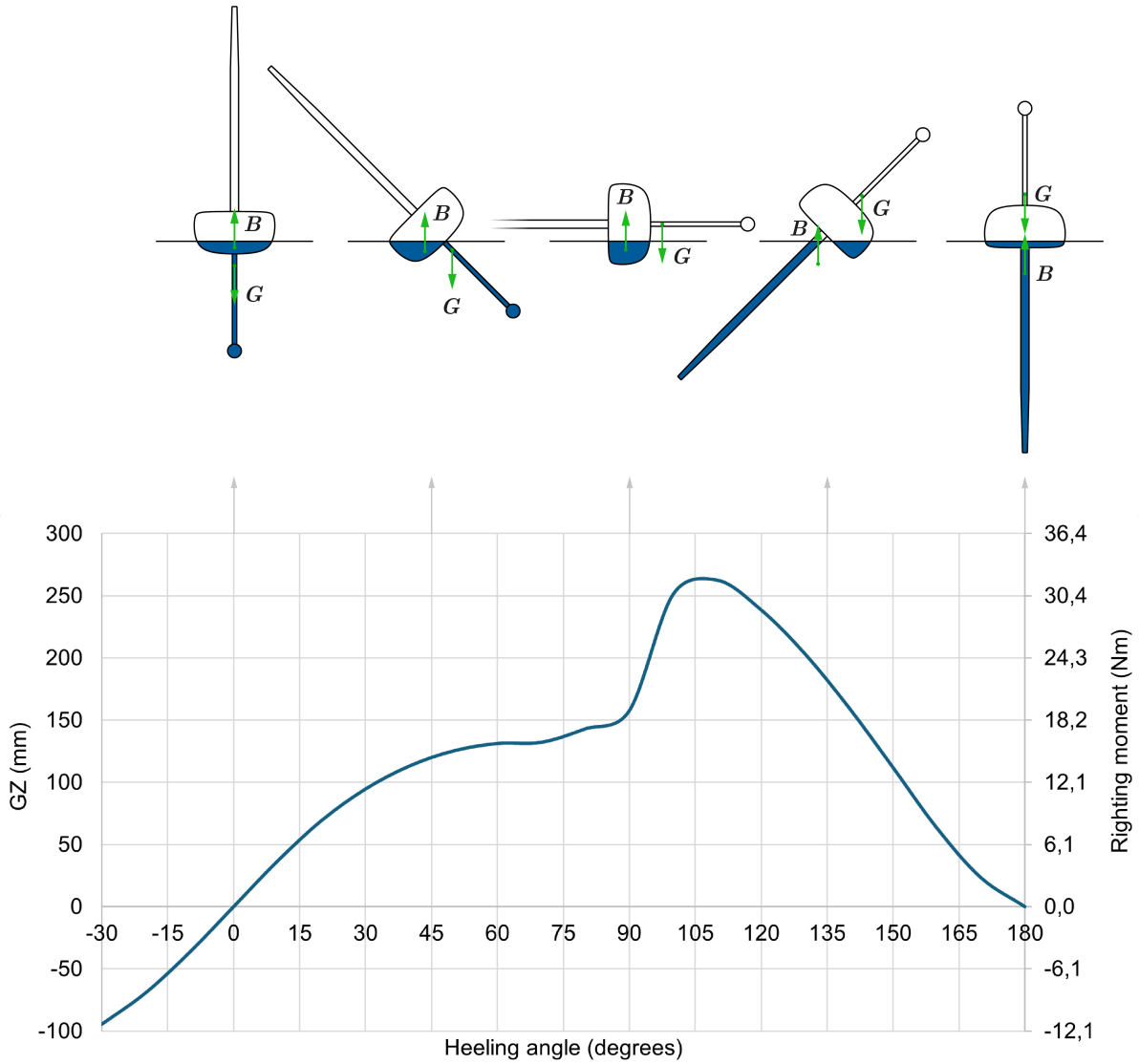

Figure 6.15: $\overline{GZ}$ and righting moment curve of the SDC25 as a result from the numerical analysis in Rhino Grasshopper, illustrated with the situation every 45° including the buoyancy force B and gravitational force G. Due to the buoyancy of the wingsail, the righting moment increases after 90° and the SDC25 is always positively stable. When inverted at 180°, the boat is in an unstable equilibrium, only the slightest disturbance will flip it back upright.

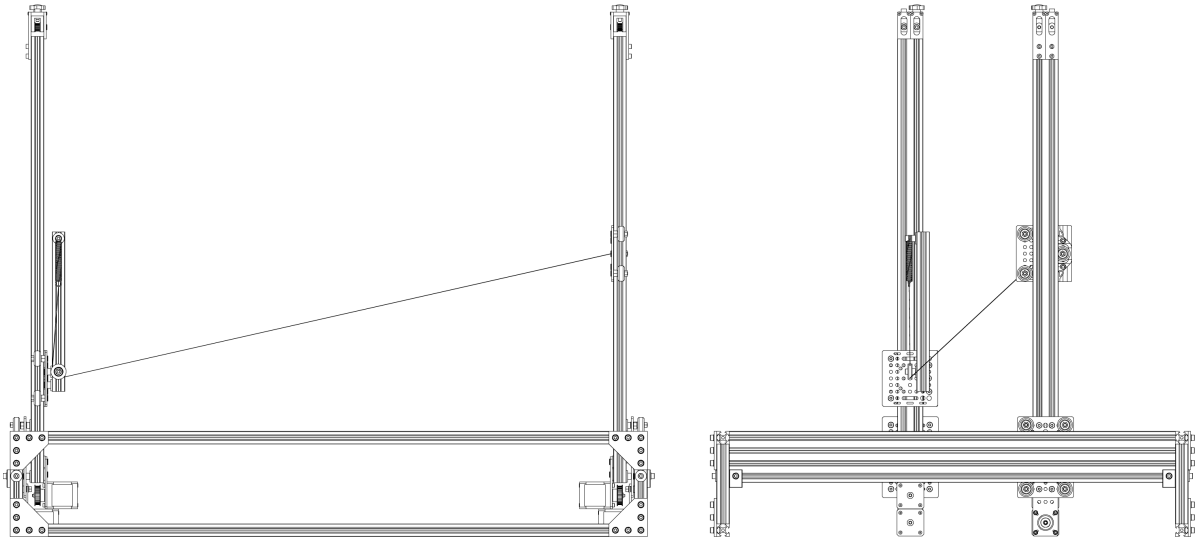

Figure 6.16: Front and side view of the hot wire CNC foam cutter.

6.2. Prototype

This section outlines the processes involved in manufacturing the prototype and provides examples of its construction. It begins by detailing the design and workflow of a hot wire CNC foam cutter, which enables the fabrication of complex, lightweight components.

6.2.1. Hot wire CNC foam cutter

The presence of parts with complex curves, such as the wingsail and hull, present challenges in their construction. Due to mass constraints, a fibreglass laminate over a foam core is the preferred choice for prototyping. Since services capable of cutting foam to specific requirements are unavailable, and driven by the desire to construct an integrated, high-fidelity prototype, a hot wire CNC foam cutter was designed and built (Figure 6.16 and 6.17). This 4-axis (2x XY) machine is capable of precisely melting through foam to carve out shapes. However, shapes are limited to straight lofts because the cutting wire spans a straight line. This limitation was kept in mind during the design phase, and more complex lofts can be constructed by carving parts in sections and joining them together.

6.2.1.1. Mechanics & actuators

The structural frame is constructed with V-slot aluminium extrusions, which also function as axes due to their ability to guide V-wheels. Gantry plates enable the mounting of the wheels and the integration of other components. The NEMA17 stepper motors are positioned close together on the 'arm' assemblies, allowing a compact arrangement and simplified cable management. Both axes are driven by GT2 belts: in this setup, the X-stepper motor moves while its belt remains static, whereas the Y-stepper motor stays stationary while its belt moves. In total, only six components are custom: all belt attachment points are custom-designed and 3D-printed - one for each Y-axis and two for each X-axis. Additionally, four extra holes were drilled into the 2080 gantry plate to provide the necessary attachment points. A Bigtreetech SKR Pico 3D printer motherboard is used as stepper controller, chosen for its built-in TMC2209 stepper motor drivers.

A nichrome wire of 0.4mm diameter is strung between the two Y-axis gantry plates, held under tension by a tension spring and guided by a V-groove bearing. Since the axes move independently and the wire stretches due to thermal expansion, the wire length changes, necessitating a system that maintains consistent tension. A solution involving a radial spring to coil the wire and maintain constant tension would be ideal, as the current setup causes the wire's tension to increase rapidly at extreme angles. For now, heating of the wire is controlled by a bench power supply, though this functionality could be integrated into the SKR Pico. The total bill of materials is added to Appendix D.

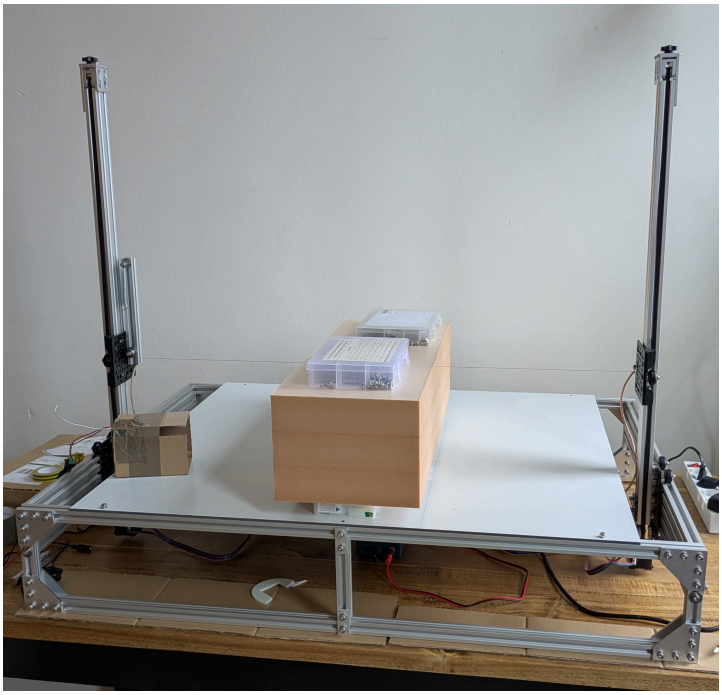

Figure 6.17: The hot wire CNC in use, squaring up a foam blank. Small weights are placed on top of the foam to keep it in position in case the wire exerts a slight pull on it.

6.2.1.2. Software

Using Grasshopper, a workflow was developed within Rhino to generate G-code directly from sections of the modelled hull or wing. Figure 6.18 illustrates this in the Rhino environment. Existing open-source or free software packages that convert 3D models or drawings to G-code were too complex, limiting, and/or time-intensive to use.

First, a loft should be created between two adjacent section curves. To ensure that the cut accurately reflects the modelled geometry, the loft should be extended beyond both ends using the ExtendSrf command in Rhino. The total length of the extended loft should match the cutting width of the CNC machine. The machine's axes will follow the curves at the edges of the extended loft, ensuring that the shape cut from the foam precisely matches the modelled version.

Generating accurate toolpaths presents a geometric challenge. If the end curves differ in curvature, naively subdividing each curve into equal-length segments results in mismatched point pairs. This causes the interpolated wire motion to deviate from the intended surface, producing twisted cuts: for example, a corner may be cut off. This mismatch arises because equal subdivision does not guarantee consistent alignment across both curves, especially when their curvature profiles vary. Consequently, the interpolated straight lines between matching points do not faithfully represent the rulings of the lofted surface.

To ensure that toolpaths follow the true geometry of the loft, sampling should occur along the loft surface itself rather than independently on each edge curve. By dividing the surface into small sections in the V direction and using the points at the edges of each loft surface sliver, the resulting point pairs are aligned according to the isoparametric structure of the surface.

From experience, what does not work in cases of mismatched curvature is simply subdividing the curves on both sides of the extended loft into equal segments and using those points as toolpath input. Another ineffective approach is projecting the original section curves directly onto the machine's XY planes and then scaling them based on the slope or relative size difference between the loft's ends. Both methods result in misaligned point pairs, leading to anything from minor mismatches between sections to more severe errors such as corners being cut off.

The resulting toolpath generation depends on several factors: the width of the part, machine dimensions, positioning of the foam blank, melt offset around the wire, and the specific geometry of the lofted surface.

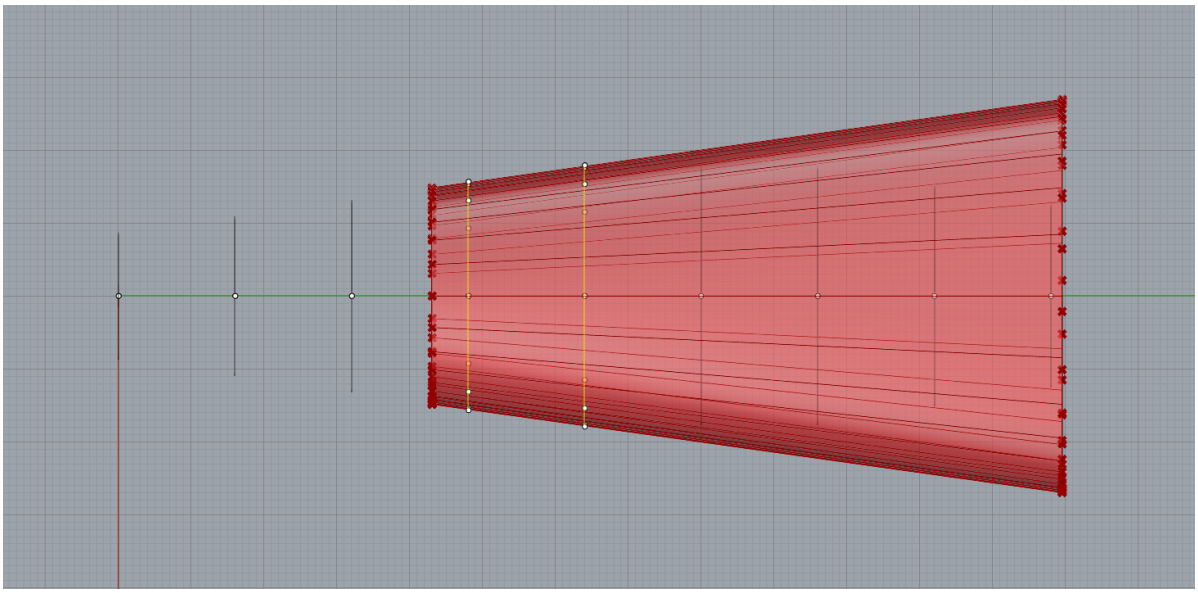

(a) Topview

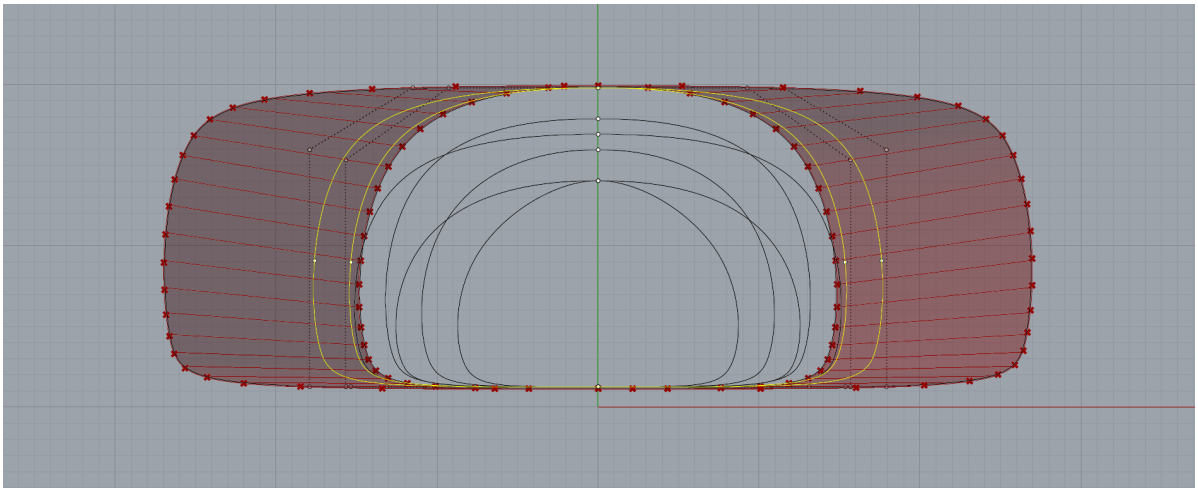

(b) Sideview

Figure 6.18: The workspace in Rhino when creating the toolpath for the CNC foam cutter. The section to be cut from a foam block is highlighted in yellow. The red surface is the extended loft from the section loft, offset by the wire melt offset, and as wide as the CNC machine, 870mm. This also illustrates that the foam block can be placed anywhere inside the machine's volume, but the placement in Rhino and placement of the foam block in the machine have to match. The red surface is divided in many slices in the V direction and only one in U, resulting in matched point pairs. For this visualisation, the slices in the V direction have been decreased. These points are used as input for the G-code.

(a) Cutting the fourth hull section.

(b) Cutting the wingsail

(c) Hull section four 'out of the mould'.

Figure 6.19: Examples of cutting parts of the hull and sails with the hot wire CNC foam cutter.

Figure 6.20: All 8 hull sections and bow, aligned from stern to bow, from top to bottom, and left to right. Holes have for the mast/keel, the electronics compartment, and cable routing have also been cut.

For CNC control, an open-source software package called GRBL is used, which has been adapted for hot wire cutters by Howlette (2022). The GRBL software processes the G-code, sends it to the CNC machine, and provides options to control parameters such as position, speed, and homing, among other settings. See Appendix D for an image of the software.

6.2.2. Manufacturing

The aluminium tubes, steel masses (bulb and sail counterweight) and the steel structural member in the keel are machined. The parts are cut to size, and holes and threads are machined by mill or drill press. Aluminium tubes - instead of the material of choice steel - are used for the prototype for its ease of machining.

The hot wire CNC foam cutter is used to cut the eight hull sections and three sail sections. Figure 6.19 shows the cutting of the hull and sail, and Figure 6.20 presents the result. The hull sections are glued together with 3M 77 spray adhesive, gaps were filled with a two-component epoxy filler, and edges are sanded to achieve a smooth transition. Figure 6.21 and 6.22 illustrate this process.

A hand layup process is used to laminate a layer of a glass fibre epoxy composite over the foam hull and sail sections for added strength and stiffness. During lamination of the hull, one glue section failed, which together with the dents left by the filler, resulted in some delamination after compressing the hull sections back together. After curing, edges were trimmed.

Connective members of the aluminium sail frame, components to clamp the sail and keel assembly around the hull, the rounded bow, the tailwing, the keel fairing, and the hydrodynamic fore and aft sections of the bulb are all 3D printed.

Figure 6.21: All hull sections placed in order, before glueing.

Figure 6.22: The hull after gluing, filling, and sanding. In hindsight, using a two-component epoxy filler to close small gaps was a mistake. The heat generated during curing caused dents in the foam wherever excess filler was applied, leaving the surface in a worse condition than before. Simply sanding would have yielded a better result. The gaps themselves were due to about half of the sections being cut using an earlier version of the toolpath code which had mismatched point pairs, though these sections were still deemed usable.

(a) An overview of the parts that make up the tailwing. The linear actuator (visible in Figure 6.13) is housed in the tube. It moves a pin up and down a milled slot. This pin interfaces with an elongated helical cutout inside the green wing, which rotates by 60° over a length of 40mm.

(b) A close look at the pin and slot. The linear actuator moves the pin up or down.

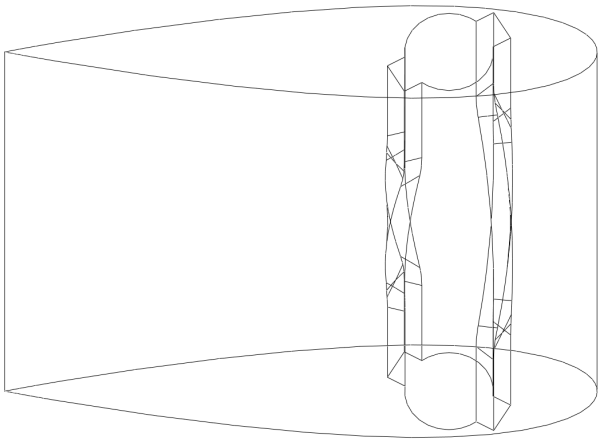

(c) A close look at the helical structure inside the wing that interfaces with the pin. Only an 80mm section of the height of the wing is shown.

Figure 6.23: The tailwing assembly. By integrating the actuator in the wing, it is more shielded to the elements than previous designs that placed the actuator externally. Furthermore, it does not need to be powered to hold position due to mechanical resistance. The wing can deflect from -30° to +30°. For a production-ready version, the coupling - slot, pin, helix - should be machined from steel to high tolerances to eliminate play and ensure durability, as the forces on this internal coupling - particularly during strong winds or when catching a wave under significant heel - are considerably greater than those acting on an externally mounted actuator.

(a) Side-view of the prototype of SDC25.

(b) SDC25 imaged in a configuration that is more representative of how it would sail, when the wind comes from the left of the image.

Figure 6.24: The fabricated prototype of the SDC25. The green tailwing and rudder are the only actuated surfaces.

6.2.3. Result

The final prototype closely resembles the intended SDC25 design, as shown in Figures 6.24 and 6.25. One notable difference is the reduced distance between the sail and its counterweight. The 3D-printed tailwing, along with other sail components, turned out lighter than the CAD model predicted due to infill in the 3D print. As a result, the counterweight had to be positioned closer to the sail to maintain balance around the mast. Another deviation from the original design is the omission of the M4 threaded rods intended to run vertically through the sail sections. These rods were meant to clamp the three sections together and prevent unwanted rotation, but accurately drilling 280mm deep, 4mm diameter holes in foam proved impossible. Fortunately, the sail sections were held sufficiently in place by the 3D-printed mast parts, and the top section could be bolted to the printed part. To prevent unwanted rotation around the mast axis, the lower section was supported by tape.

Figure 6.25: A close-up of the prototype sail from the direction of the incoming airflow shows that the main wing is pitched slightly to generate lift to the right. This orientation is controlled by the tailwing, which is angled oppositely to the flow and sets the main wing's angle of attack.

Figure 6.26: The SDC25 'under sail' in calm conditions, with the help of a fan and a push.

6.3. Evaluation

6.3.1. Tests

To evaluate the prototype, (naval) parameters such as mass, centre of gravity, and trim are be assessed. An important aspect of the evaluation is to consider whether the statistical design methods used, based on the trends from existing autonomous sailboats, have resulted in a well-balanced configuration. Do these proportions hold up in practice, and can they be reliably used as design guidelines? This evaluation also examines whether aerodynamic control remains effective at the reduced scale of the SDC25. Finally, prototyping is not only a way to validate known assumptions but also a process of discovery. What insights appear that only emerge through making and testing?

6.3.2. Results

The naval parameters of the prototype align closely with those from the CAD model, indicating that the design and prototyping process have been thorough. Table 6.2 compares these parameters with the digital design. The main deviation stems from the sail being lighter than expected, which lowered the overall mass and centre of gravity of the vessel. As a result, the transverse stability of the prototype is slightly higher than that shown in Figure 6.15.

Parameter	**Design**	**Prototype**
Mass (kg)	9.58 / 11.2 (with safety margin)	9.4
Longitudinal CoG (mm)	704	698
Vertical CoG (mm) (from waterline)	-128	-153

Table 6.2: Comparison between the designed and actual prototype parameters.

During the available testing days, conditions were unfortunately almost entirely calm, with barely any wind. The occasional light puffs had little to no effect, as the sail area was optimised for stronger wind conditions. When tested under an industrial fan, however, the sail demonstrated the intended behaviour: orienting itself into the wind at a slight angle, just as designed. (Figure 6.26.) Despite the

Figure 6.27: The trim (longitudinal placement in water) of the SDC25 appears perfect by eye, but if off by 6mm after evaluation.

lack of natural wind, handling the SDC25 gave a clear impression of it being a very stable platform. The trim of the boat appeared perfect to the eye, see Figure 6.27, though the measured longitudinal centre of gravity was ever so slightly off. While definitive conclusions are limited, the overall impression is that the statistical design approach has resulted in a vessel more suited for high-wind conditions.

6.3.3. Areas of improvement

During the manufacturing and testing phases, some areas of improvement were identified:

Clamping the hull between the sail and keel assemblies proved functional but prone to slippage. When holding the keel, it was possible to rotate the hull on its mount by applying force at its extremities, suggesting that wave impacts could potentially compromise the connection. Future iterations should revisit this interface. The direct connection between the keel and sails however proved robust and effective in maintaining a stiff connection between the two.

The linear actuator used in the tailwing operates slowly, requiring 5 to 8 seconds to move through its full range of motion (−30° to +30°). While the rudder has sufficient authority to initiate manoeuvres such as tacking or jibing rapidly, the tailwing's delayed response could result in issues in these scenarios, although this could not be tested. Additionally, the tolerances and overall stiffness of the mechanism could use refinement, as already described in Figure 6.23.

Drilling accurate holes for the two vertical threaded rods through the sail sections proved unfeasible, leading to a suboptimal connection between sail sections and the mast. These small-diameter holes could not be made on the CNC wire cutter without requiring a lead-in path directed towards them, which would have compromised the structural integrity of the wing. A more reliable method could involve bonding a plastic or metal interface to both ends of each foil section to accommodate bolted connections. This issue is primarily relevant to the prototype; a production model would likely feature a sail moulded as a single piece.

7

Discussion & conclusion

7.1. Discussion

7.1.1. Uncertainties in concept design

Just like some boats, not all arguments are entirely watertight, mainly because of the uncertainties involved. The relative impact of marine litter compared to production, the exact influence of certain design interventions, the minimum feasible vessel size, whether investing in fleet management is worth the added complexity, and the vessels actual working lifetime all remain uncertain. With so many unknowns, it is difficult to draw definitive conclusions, but these are an inevitable part of the design process. In Figure 7.1, Mavris and DeLaurentis (2000) describe the relationship between the amount of knowledge acquired related to the stage of the design timeline. Since this thesis presents a conceptual design, it is unavoidable that the level of acquired knowledge remains relatively low, resulting in significant uncertainties.

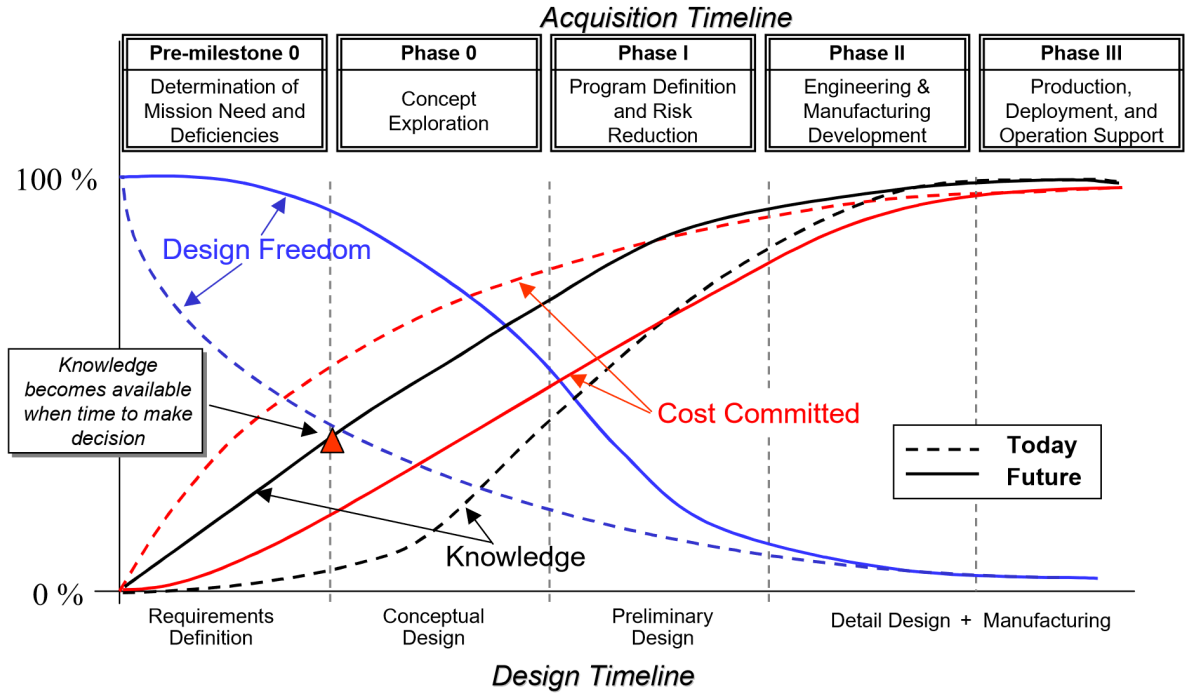

Figure 7.1: The relationship of design freedom, knowledge and cost over time described by Mavris and DeLaurentis (2000) for aircraft, is just as relevant for ship design.

7.1.2. Design recommendations for mass production

The development presented in this thesis includes the proof of concept detailed in Chapter 6, but does not end there. The following recommendations inform the potential transition from prototype to production-ready design. As discussed, there are still considerable uncertainties. However, two main approaches emerge for the sustainable design of a mass-produced ASB:

Minimise production impact

This approach prioritises low environmental impacts during production while maintaining a durable design. It does not heavily factor in the environmental impact of marine litter, as its significance remains unknown. Although the vessel is ultimately expected to become marine litter without a biodegradable design, efforts are made to minimise material leakage and toxicity. These recommendations build on the design principles of the SDC25, particularly the extensive use of steel and glass fibre composites.

- Stamped and welded steel hull: Similar to automotive body panel manufacturing, stamping panels from steel sheets is a fast, cost-effective process that also offers a high degree of design freedom. The hull would consist of a top and bottom shell, with several internal frames to provide rigidity.
- Steel keel and bulb: Similar to the prototype, the keel and bulb would be constructed from steel, but now for all parts. The keel can be bent into shape and welded along the trailing edge, removing the need for plastic fairings. The bulb can be machined into a hydrodynamic shape.
- Glass fibre polyester sails: The sail would be produced as a single piece using a mould. Standard glass fibre rods could be positioned in the mould before laminating the outer wing structure around them.
- The impact of electronic components should be minimised where possible, but not at the expense of vessel durability.

Fully biodegradable design

This approach prioritises complete degradability over time. It may be preferred when the goal is to minimise marine litter as much as possible or if it becomes evident that the environmental impact of conventional material littering is significantly greater than that of production.

- Structural components constructed primarily from flax fibre-reinforced polyglycerol citrate plastic. While this may result in a higher environmental footprint during production, it offers the key benefit of complete degradability in the marine environment.
- Strong emphasis should be placed on reducing or eliminating electronics, as biodegradable alternatives are not yet feasible.
- Stone could be used as a substitute for steel ballast to reduce the use of non-degradable materials. However, this comes at the cost of reduced performance due to the lower density of stone.

7.1.3. A perspective on scale and impact

While autonomous sailing boats are a compelling subject of study, it is important to reflect on the broader value of investing time and resources into optimising such relatively small-scale systems. This includes testing unconventional solutions and materials. In many cases, especially for small vessels, the pursuit of alternative materials like biodegradable composites may not be justified, unless the vessels are scaled up significantly in size or deployed in vast numbers.

To illustrate: even with the ambitious deployment of 5,000 ASBs - on the scale of the Argo float network - the total material use would be relatively low compared to other engineering projects. Assuming each SDC25 contains 10kg of mostly steel and glass fibre composites, the entire swarm would amount to 50 tonnes of material. In contrast, a single onshore 2MW wind turbine has a material footprint of approximately 1,538 tonnes (Guezuraga et al., 2012). In absolute terms, the environmental impact of ASB materials is marginal when compared to larger challenges. Within the maritime sector, achieving a 20% reduction in cargo ship emissions through sail-assist technology (Tadros et al., 2023) presents a far more substantial and impactful challenge worth pursuing.

Therefore, the design effort and environmental focus may be more impactful when applied to larger-scale maritime systems. That said, the insights and methodologies developed in this thesis could well be transferable to other domains. Projects such as MarILCA (Boulay et al., 2021), which evaluate the life cycle impacts of marine litter, may help identify high-impact products or materials currently contributing to environmental harm; products that could benefit from redesign using the insights developed in this thesis.

On the other hand, certain material choices recommended in this thesis are straightforward and easily adopted. Avoiding high-impact or toxic materials such as carbon fibre composites, aluminium, and lead, can be a simple yet effective way to reduce the environmental burden of ASBs, when it is known that these eventually become marine litter. Future designs could benefit from incorporating these material preferences from the outset.

Somewhere in between are the implications of the dimensional analysis. The results suggest that the smaller each individual vessel, the more effective the swarm as a whole, by a wide margin. The challenge lies in defining the lower size limit. There probably is a gradual transition from unfeasible-at-sea to long-term viable operation, making it difficult to pinpoint a universally optimal vessel size. However, this insight remains valuable: designers of swarm systems should consider the significant benefits of miniaturising individual units, even if the exact threshold for feasibility is difficult to define.

7.1.4. Future work

While research into ASBs has been ongoing since the early 2000s, actual fleet deployment remains rare. The few existing examples, such as the large vessels used by “Saildrone” (n.d.), are not true swarms in the sense of distributed, cooperative systems, and others are only deployed in very small numbers. Future research could investigate high-potential deployment scenarios and specific application domains. This would allow for more targeted design strategies that address concrete needs.

One often stated knowledge gap in this work is the lower operational limits of vessel size. Deployment trials of multiple ASB sizes in both inland and coastal/ocean waters could clarify how small an ASB can be while remaining operationally viable, and whether the statistical design method consistently yields reliable performance across different scales.

Without a concrete application, further investment of time and resources in this area may be better directed toward projects with more immediate applicability or larger potential environmental impact. Nonetheless, some of the insights may still prove valuable in adjacent fields or future applications.

An unexpected outcome of this project was the development of a custom CNC foam cutter, which became necessary during the design of the SDC25 to prototype complex curved components like the wingsail and hull sections. Currently, generating toolpaths and operating the machine remains a largely manual and labour-intensive process, with clear opportunities for refinement. Further development could significantly improve its usability and provide designers with a novel, unconventional method for manufacturing complex shapes, particularly valuable in prototyping lightweight, curved components that are otherwise difficult or expensive to produce using traditional methods.

7.2. Conclusion

This thesis set out to explore how autonomous sailboats could be designed with minimal environmental impact. On one hand, it focused on theoretical considerations such as optimal swarm and vessel size, and material selection. On the other, it involved the practical development of a more environmentally responsible ASB, building on lessons from previous projects to inform the design process. The following paragraphs present the findings in relation to the two research questions stated at the start of this thesis.

RQ1: Which low-impact solutions are suitable for the use in an autonomous sailboat?

A number of low-impact solutions have been identified that could reduce the environmental footprint of autonomous sailboats, but their suitability depends on how impact is defined, whether in terms of production, operation, or end-of-life degradation.

The environmental cost of materials can be assessed through embodied energy relative to mechanical performance. From this perspective, steel emerges as the preferred metal over aluminium due to its significantly lower energy requirement during production. Among fibre-reinforced composites, glass fibre is slightly more favourable than flax fibre, while carbon fibre should be avoided due to its very high embodied energy. While flax fibre offers the advantage of being biodegradable, its use becomes more

compelling only when the vessel's full lifecycle including degradation is taken into account.

One of the key challenges in identifying the most sustainable design choices is the lack of reliable data on the environmental cost of marine litter. As highlighted by Boulay et al. (2021), this is a documented research gap. Without this data, it is currently impossible to assess whether the additional complexity of using biodegradable materials is justified.

In the scenario that marine litter has to be minimised, offer biodegradable continuous fibre-reinforced polymers a promising alternative for structural components. Flax fibre, paired with degradable resins like polyglycerol citrate or polyvinyl alcohol, has the potential to reduce long-term pollution. However, these resins are still challenging to process, with elevated temperature requirements and difficulties in managing degradation timing (especially in the case of highly soluble resins like PVA). Testing of these materials has been unsuccessful.

A swarm of small ASBs offers better data collection per unit of material used than a few large ones. Minimising vessel size without compromising functionality is an important strategy to reduce impact. However, there are practical constraints. Below a certain size, ASBs become more prone to failure during deployment, and their ability to operate effectively in marine conditions diminishes. This trade-off between miniaturisation and robustness cannot be determined analytically and must be determined through testing.

RQ2: How would the design of a low environmental impact autonomous sailboat look like?
The design of the SDC25 demonstrates how a focus on small vessel size, thoughtful material selection, and aerodynamic sail control can be successfully integrated into a functional autonomous sailboat prototype. It uses an effective self-trimming wingsail that requires no continuous energy input, using power only during manoeuvres such as jibing and tacking. For potential mass production, two approaches were explored: a durable, relatively low-impact version using conventional materials and standardised processes, and a fully biodegradable concept for minimising long-term marine litter.

The statistical design approach was a central element throughout this project. As a starting point, an extensive collection of previous ASB designs was compiled in Table 2.4, representing the most comprehensive overview of naval parameters for autonomous sailboats to date. This dataset enabled the identification of correlations between naval design properties, of which the design of the SDC25 was informed. These correlations remain valuable for future ASB development and are worth restating as design references. Although testing time was limited, initial results suggest that the statistical method led to a remarkably stable vessel.

$$\Delta = 7.15{L_{wl}}^{2.48} \tag{7.1}$$

$$SA_{SS} = 0.46{L_{wl}}^{1.85} \tag{7.2}$$

$$SA_{WS} = 0.097{L_{wl}}^{2.29} \tag{7.3}$$

$$d = 0.386{L_{wl}}^{0.74} \tag{7.4}$$

$$\overline{B/\Delta} = 37\% \tag{7.5}$$

where:

- L_{wl}: length of the vessel at its waterline in m.
- Δ: displacement in kg.
- SA_{SS}: sail area for a soft sail in m^2.
- SA_{WS}: sail area for a wing sail in m^2.
- d: draft of the boat in m, which informs keel length.
- $\overline{B/\Delta}$: percentage of mass in ballast compared to displacement.

Bibliography

11th Hour Racing Team. (2021). Sustainable design and build report.

Akiyama, T., Bousquet, J.-F., Roncin, K., Muirhead, G., & Whidden, A. (2021). An engineering design approach for the development of an autonomous sailboat to cross the atlantic ocean. *Applied Sciences*, *11*(17), 8046. https://doi.org/10.3390/app11178046

Alberts, A. H., & Rothenberg, G. (2017). Plantics-GX: A biodegradable and cost-effective thermoset plastic that is 100% plant-based. *Faraday Discussions*, *202*, 111–120. https://doi.org/10.1039/C7FD00054E

Alberts, A. H., & Rothenberg, G. (2014, March 20). *US-20140080973-a1* (U.S. pat. No. -20140080973-A1). Retrieved September 6, 2024, from https://ppubs.uspto.gov/dirsearch-public/patents/html/20140080973?source=US-PGPUB&requestToken=eyJzdWIiOiI4MGY2OTk5MS1iYTk4LTQ2ZTItYTdjOC0xMD

Alberts, A. H., & Rothenberg, G. (2019, June 18). *Composite material comprising bio-filler and specific polymer* (U.S. pat. No. 10323355B2). Retrieved September 6, 2024, from https://patents.google.com/patent/US10323355B2/en?inventor=Alberts+Albert+Henderikus&oq=Alberts+Albert+Henderikus

An, Y., Yu, J., & Zhang, J. (2021). Autonomous sailboat design: A review from the performance perspective. *Ocean Engineering*, *238*, 109753. https://doi.org/10.1016/j.oceaneng.2021.109753

Apium [Apium]. (n.d.). Retrieved July 16, 2024, from http://apium.com/ocean-option-2

Argo [Argo]. (n.d.). Retrieved July 17, 2024, from https://argo.ucsd.edu

Bai, X., Li, B., Xu, X., & Xiao, Y. (2022). A review of current research and advances in unmanned surface vehicles. *Journal of Marine Science and Application*, *21*(2), 47–58. https://doi.org/10.1007/s11804-022-00276-9

Baley, C., Davies, P., Troalen, W., Chamley, A., Dinham-Price, I., Marchandise, A., & Keryvin, V. (2024). Sustainable polymer composite marine structures: Developments and challenges. *Progress in Materials Science*, *145*. https://doi.org/10.1016/j.pmatsci.2024.101307

Bennett, M. R., Bustos, D., Pigati, J. S., Springer, K. B., Urban, T. M., Holliday, V. T., Reynolds, S. C., Budka, M., Honke, J. S., Hudson, A. M., Fenerty, B., Connelly, C., Martinez, P. J., Santucci, V. L., & Odess, D. (2021). Evidence of humans in north america during the last glacial maximum [Publisher: American Association for the Advancement of Science]. *Science*, *373*(6562), 1528–1531. https://doi.org/10.1126/science.abg7586

Boulay, A.-M., Vazquez, I., & Verones, F. (n.d.). *MarILCA - marine impacts in life cycle assessment* [MarILCA]. Retrieved January 27, 2025, from https://marilca.org/

Boulay, A.-M., Verones, F., & Vázquez-Rowe, I. (2021). Marine plastics in LCA: Current status and MarILCA's contributions. *The International Journal of Life Cycle Assessment*, *26*(11), 2105–2108. https://doi.org/10.1007/s11367-021-01975-1

Bourmaud, A., & Baley, C. (2009). Rigidity analysis of polypropylene/vegetal fibre composites after recycling. *Polymer Degradation and Stability*, *94*(3), 297–305. https://doi.org/10.1016/j.polymdegradstab.2008.12.010

Brambilla, M., Ferrante, E., Birattari, M., & Dorigo, M. (2013). Swarm robotics: A review from the swarm engineering perspective. *Swarm Intelligence*, *7*(1), 1–41. https://doi.org/10.1007/s11721-012-0075-2

CLO. (2024). *Vermesting van oppervlaktewater, 1990 - 2021*. Retrieved October 20, 2024, from https://www.clo.nl/indicatoren/nl055206-vermesting-van-oppervlaktewater-1990-2021

Crupi, V., Epasto, G., Napolitano, F., Palomba, G., Papa, I., & Russo, P. (2023). Green composites for maritime engineering: A review [Number: 3 Publisher: Multidisciplinary Digital Publishing Institute]. *Journal of Marine Science and Engineering*, *11*(3), 599. https://doi.org/10.3390/jmse11030599

Das, S. C., La Rosa, A. D., & Grammatikos, S. A. (2022, January 1). Chapter 19 - life cycle assessment of plant fibers and their composites. In S. Mavinkere Rangappa, J. Parameswaranpillai, S. Siengchin, T. Ozbakkaloglu, & H. Wang (Eds.), *Plant fibers, their composites, and applications* (pp. 457–484). Woodhead Publishing. https://doi.org/10.1016/B978-0-12-824528-6.00015-1

Davis, L. G., & Madsen, D. B. (2020). The coastal migration theory: Formulation and testable hypotheses. *Quaternary Science Reviews*, *249*, 106605. https://doi.org/10.1016/j.quascirev.2020.106605

De, B., Bera, M., Bhattacharjee, D., Ray, B. C., & Mukherjee, S. (2024). A comprehensive review on fiber-reinforced polymer composites: Raw materials to applications, recycling, and waste management. *Progress in Materials Science*, *146*, 101326. https://doi.org/10.1016/j.pmatsci.2024.101326

Dicker, M. P. M., Duckworth, P. F., Baker, A. B., Francois, G., Hazzard, M. K., & Weaver, P. M. (2014). Green composites: A review of material attributes and complementary applications. *Composites Part A: Applied Science and Manufacturing*, *56*, 280–289. https://doi.org/10.1016/j.compositesa.2013.10.014

Dorigo, M. (2007). Swarm intelligence - scholarpedia.

Duflou, J. R., Yelin, D., Van Acker, K., & Dewulf, W. (2014). Comparative impact assessment for flax fibre versus conventional glass fibre reinforced composites: Are bio-based reinforcement materials the way to go? *CIRP Annals*, *63*(1), 45–48. https://doi.org/10.1016/j.cirp.2014.03.061

Dunbabin, M., & Marques, L. (2012). Robots for environmental monitoring: Significant advancements and applications. *IEEE Robotics & Automation Magazine*, *19*(1), 24–39. https://doi.org/10.1109/MRA.2011.2181683

El Hawary, O., Boccarusso, L., Ansell, M. P., Durante, M., & Pinto, F. (2023). An overview of natural fiber composites for marine applications [Number: 5 Publisher: Multidisciplinary Digital Publishing Institute]. *Journal of Marine Science and Engineering*, *11*(5), 1076. https://doi.org/10.3390/jmse11051076

Elkaim, G. H. (2001). System identification for precision control of a wingsailed GPS-guided catamaran.

Elkaim, G. H. (2008). Autonomous surface vehicle free-rotating wingsail section design and configuration analysis. *Journal of Aircraft*, *45*(6), 1835–1852. https://doi.org/10.2514/1.27284

Emissieregistratie. (n.d.). *Over emissieregistratie | emissieregistratie*. Retrieved October 20, 2024, from https://www.emissieregistratie.nl/over-emissieregistratie

Enercon. (2013). Enercon e-ship 1: A wing-hybrid commercial cargo ship. Retrieved March 26, 2025, from https://www.stg-online.org/onTEAM/shipefficiency/programm/06-STG_Ship_Efficiency_2013_100913_Paper.pdf

Erhard, M., & Strauch, H. (2018, April 1). Automatic control of pumping cycles for the SkySails prototype in airborne wind energy [Journal Abbreviation: Green Energy and Technology]. In *Green energy and technology* (pp. 189–213). https://doi.org/10.1007/978-981-10-1947-0_9

European Bioplastics. (n.d.). *Bioplastics* [European bioplastics e.v.]. Retrieved February 7, 2025, from https://www.european-bioplastics.org/bioplastics/

Evans, J. H. (1959). Basic design concepts. *A. S. N. E. Journal*, 671–678.

Fossati, F. (2009). *Aero-hydrodynamics and the performance of sailing yachts: The science behind sailing yachts and their design* [Section: 354 blz. ; .. cm.]. International Marine/McGraw-Hill.

Friebe, A., Olsson, M., Le Gallic, M., Springett, J. L., Dahl, K., & Waller, M. (2017). A marine research ASV utilizing wind and solar power. *OCEANS 2017 - Aberdeen*, 1–7. https://doi.org/10.1109/OCEANSE.2017.8084648

Gourier, C., Bourmaud, A., Le Duigou, A., & Baley, C. (2017). Influence of PA11 and PP thermoplastic polymers on recycling stability of unidirectional flax fibre reinforced biocomposites. *Polymer Degradation and Stability*, *136*, 1–9. https://doi.org/10.1016/j.polymdegradstab.2016.12.003

Gubbels, E., Heitz, T., Yamamoto, M., Chilekar, V., Zarbakhsh, S., Gepraegs, M., Köpnick, H., Schmidt, M., Brügging, W., Rüter, J., & Kaminsky, W. (2018). Polyesters [ISSN: 1435-6007 _eprint: https://onlinelibrary.wiley.com/doi/pdf/10.1002/14356007.a21_227.pub2]. In *Ullmann's encyclopedia of industrial chemistry* (pp. 1–30). John Wiley & Sons, Ltd. https://doi.org/10.1002/14356007.a21_227.pub2

Guezuraga, B., Zauner, R., & Pölz, W. (2012). Life cycle assessment of two different 2 MW class wind turbines. *Renewable Energy*, *37*(1), 37–44. https://doi.org/10.1016/j.renene.2011.05.008

Haider, T. P., Völker, C., Kramm, J., Landfester, K., & Wurm, F. R. (2019). Plastics of the future? the impact of biodegradable polymers on the environment and on society. *Angewandte Chemie International Edition*, *58*(1), 50–62. https://doi.org/10.1002/anie.201805766

Hoang, A. T., Foley, A. M., Nižetić, S., Huang, Z., Ong, H. C., Ölçer, A. I., Pham, V. V., & Nguyen, X. P. (2022). Energy-related approach for reduction of CO2 emissions: A critical strategy on

the port-to-ship pathway. *Journal of Cleaner Production*, *355*, 131772. https://doi.org/10.1016/j.jclepro.2022.131772

Howlette, K. (2022, October 7). *Grbl HotWire for CNC foam cutters*. Retrieved January 23, 2025, from https://rckeith.co.uk/grbl-hotwire-for-cnc-foam-cutters/

Inal, O. B., Charpentier, J.-F., & Deniz, C. (2022). Hybrid power and propulsion systems for ships: Current status and future challenges. *Renewable and Sustainable Energy Reviews*, *156*, 111965. https://doi.org/10.1016/j.rser.2021.111965

Jain, N., Singh, V., & Chauhan, S. (2018). A review on mechanical and water absorption properties of polyvinyl alcohol based composites/films. *Journal of the Mechanical Behavior of Materials*, *26*, 213–222. https://doi.org/10.1515/jmbm-2017-0027

Khandai, S., Nayak, R., Kumar, A., Das, D., & Kumar, R. (2019). Assessment of mechanical and tribological properties of flax/kenaf/glass/carbon fiber reinforced polymer composites. *Materials Today: Proceedings*, *18*, 3835–3841. https://doi.org/10.1016/j.matpr.2019.07.322

Kimball, J. (2009, December 18). *Physics of sailing*. CRC Press. https://doi.org/10.1201/9781420073775

Larsson, L., Eliasson, R. E., & Orych, M. (2022). *Principles of yacht design* (Fifth edition). Adlard Coles.

Le Duigou, A., Bourmaud, A., Davies, P., & Baley, C. (2014). Long term immersion in natural seawater of flax/PLA biocomposite. *Ocean Engineering*, *90*, 140–148. https://doi.org/10.1016/j.oceaneng.2014.07.021

Le Duigou, A., Davies, P., & Baley, C. (2011). Environmental impact analysis of the production of flax fibres to be used as composite material reinforcement. *Journal of Biobased Materials and Bioenergy*, *5*(1), 153–165. https://doi.org/10.1166/jbmb.2011.1116

Lin, M., & Yang, C. (2020). Ocean observation technologies: A review. *Chinese Journal of Mechanical Engineering*, *33*(1), 32. https://doi.org/10.1186/s10033-020-00449-z

Liu, Z., Zhang, Y., Yu, X., & Yuan, C. (2016). Unmanned surface vehicles: An overview of developments and challenges. *Annual Reviews in Control*, *41*. https://doi.org/10.1016/j.arcontrol.2016.04.018

Lott, C., Eich, A., Makarow, D., Unger, B., van Eekert, M., Schuman, E., Reinach, M. S., Lasut, M. T., & Weber, M. (2021). Half-life of biodegradable plastics in the marine environment depends on material, habitat, and climate zone [Publisher: Frontiers]. *Frontiers in Marine Science*, *8*. https://doi.org/10.3389/fmars.2021.662074

Lyhne Christensen, A., Oliveira, S., Postolache, O., João De Oliveira, M., Sargento, S., Santana, P., Nunes, L., Velez, F., Sebastião, P., Costa, V., Duarte, M., Gomes, J., Rodrigues, T., & Silva, F. (2015). Design of communication and control for swarms of aquatic surface drones: *Proceedings of the International Conference on Agents and Artificial Intelligence*, 548–555. https://doi.org/10.5220/0005281705480555

Manfreda, S., McCabe, M. F., Miller, P. E., Lucas, R., Pajuelo Madrigal, V., Mallinis, G., Ben Dor, E., Helman, D., Estes, L., Ciraolo, G., Müllerová, J., Tauro, F., De Lima, M. I., De Lima, J. L. M. P., Maltese, A., Frances, F., Caylor, K., Kohv, M., Perks, M., … Toth, B. (2018). On the use of unmanned aerial systems for environmental monitoring [Number: 4 Publisher: Multidisciplinary Digital Publishing Institute]. *Remote Sensing*, *10*(4), 641. https://doi.org/10.3390/rs10040641

Manley, J. E. (2008). Unmanned surface vehicles, 15 years of development [ISSN: 0197-7385]. *OCEANS 2008*, 1–4. https://doi.org/10.1109/OCEANS.2008.5152052

Mavris, D. N., & DeLaurentis, D. (2000). Methodology for examining the simultaneous impact of requirements, vehicle characteristics, and technologies on military aircraft design.

Mendonça, S. (2013). The “sailing ship effect”: Reassessing history as a source of insight on technical change. *Research Policy*, *42*(10), 1724–1738. https://doi.org/10.1016/j.respol.2012.12.009

Microtransat challenge. (n.d.). Retrieved February 1, 2025, from https://www.microtransat.org/content.php?p=history&top=history

Miller, P. H., Hamlet, M., & Rossman, J. (2013). Continuous improvements to USNA SailBots for inshore racing and offshore voyaging. In C. Sauzé & J. Finnis (Eds.), *Robotic sailing 2012* (pp. 49–60). Springer. https://doi.org/10.1007/978-3-642-33084-1_5

Ministerie van Landbouw, N. e. V. (2023, July 17). *Verbeteren kwaliteit landelijke meetnet en rekenmodellen - Basis herstellen - Levend Landschap* [Last Modified: 2023-09-11T15:51 Publisher: Ministerie van Landbouw, Natuur en Voedselkwaliteit]. Retrieved October 20, 2024, from https://www.onslevendlandschap.nl/basis-herstellen/nks/verbeteren-kwaliteit-landelijke-meetnet-en-rekenmodellen

NASA. (n.d.). *Center of pressure*. Retrieved April 23, 2025, from https://www.grc.nasa.gov/www/k-12/VirtualAero/BottleRocket/airplane/cp.html

Neal, M., Sauzé, C., Thomas, B., & Alves, J. (2009). Technologies for autonomous sailing: Wings and wind sensors.

Newman, B. G., & Fekete, G. I. (1983). Analysis and preliminary design of a sailboat with self-trimming wing sail. *Marine Technology and SNAME News*, *20*(4), 370–376. https://doi.org/10.5957/mt1.1983.20.4.370

Oceanbird. (n.d.). [The oceanbird]. Retrieved March 26, 2025, from https://www.theoceanbird.com/

Oliveira, P. R., May, M., Panzera, T. H., & Hiermaier, S. (2022). Bio-based/green sandwich structures: A review. *Thin-Walled Structures*, *177*, 109426. https://doi.org/10.1016/j.tws.2022.109426

Oun, A. A., Shin, G. H., Rhim, J.-W., & Kim, J. T. (2022). Recent advances in polyvinyl alcohol-based composite films and their applications in food packaging. *Food Packaging and Shelf Life*, *34*, 100991. https://doi.org/10.1016/j.fpsl.2022.100991

Panagiotopoulou, V. C., Stavropoulos, P., & Chryssolouris, G. (2022). A critical review on the environmental impact of manufacturing: A holistic perspective. *The International Journal of Advanced Manufacturing Technology*, *118*(1), 603–625. https://doi.org/10.1007/s00170-021-07980-w

PBL. (n.d.). *Monitoring en Evaluatie Stikstofreductie en Natuurverbetering | Planbureau voor de Leefomgeving*. Retrieved October 20, 2024, from https://www.pbl.nl/mesn

Pigati, J. S., Springer, K. B., Honke, J. S., Wahl, D., Champagne, M. R., Zimmerman, S. R. H., Gray, H. J., Santucci, V. L., Odess, D., Bustos, D., & Bennett, M. R. (2023). Independent age estimates resolve the controversy of ancient human footprints at white sands [Publisher: American Association for the Advancement of Science]. *Science*, *382*(6666), 73–75. https://doi.org/10.1126/science.adh5007

Pil, L., Bensadoun, F., Pariset, J., & Verpoest, I. (2016). Why are designers fascinated by flax and hemp fibre composites? *Composites Part A: Applied Science and Manufacturing*, *83*, 193–205. https://doi.org/10.1016/j.compositesa.2015.11.004

Plantics. (n.d.). *Hemp chair collection* [Hemp chair collection]. Retrieved March 25, 2025, from https://plantics.com/hemp-chair-collection/

Potter, B., Chatters, J., Prentiss, A., Feidel, S., Haynes, G., Kelly, R., Kilby, D., Lanoe, F., Holland-Lulewicz, J., Miller, D., Morrow, J., Perri, A., Rademaker, K., Reuther, J., Ritchison, B., Sanchez, G., Sánchez-Morales, I., Spivey-Faulkner, S., Tune, J., & Haynes, C. (2021). Current understanding of the earliest human occupations in the americas: Evaluation of becerra-valdivia and higham (2020). *PaleoAmerica*, *8*, 62–76.

RIVM. (n.d.). *Stikstof*. Retrieved October 20, 2024, from https://www.rivm.nl/stikstof

Robotic sailing: Home. (n.d.). Retrieved June 24, 2024, from https://www.roboticsailing.org/

Roose, P., Eller, K., Henkes, E., Rossbacher, R., & Höke, H. (2015). Amines, aliphatic [ISSN: 1435-6007 _eprint: https://onlinelibrary.wiley.com/doi/pdf/10.1002/14356007.a02_001.pub2]. In *Ullmann's encyclopedia of industrial chemistry* (pp. 1–55). John Wiley & Sons, Ltd. https://doi.org/10.1002/14356007.a02_001.pub2

SailBot | international robotic sailing regatta. (n.d.). Retrieved July 8, 2024, from https://www.sailbot.org/

Saildrone: Defense, commercial & science data solutions. (n.d.). Retrieved July 12, 2024, from https://www.saildrone.com/

Sauzé, C., & Neal, M. (2006). An autonomous sailing robot for ocean observation.

Schill, F. S., Bahr, A., & Martinoli, A. (Eds.). (2019). Vertex: A new distributed underwater robotic platform for environmental monitoring [Meeting Name: 13th International Symposium on Distributed Autonomous Robotic Systems (DARS) Place: Cham Publisher: SPRINGER INTERNATIONAL PUBLISHING AG]. *Distributed Autonomous Robotic Systems*. https://doi.org/10.1007/978-3-319-73008-0_47

Schmickl, T., Thenius, R., Moslinger, C., Timmis, J., Tyrrell, A., Read, M., Hilder, J., Halloy, J., Campo, A., Stefanini, C., Manfredi, L., Orofino, S., Kernbach, S., Dipper, T., & Sutantyo, D. (2011). CoCoRo – the self-aware underwater swarm. *2011 Fifth IEEE Conference on Self-Adaptive and Self-Organizing Systems Workshops*, 120–126. https://doi.org/10.1109/SASOW.2011.11

Schranz, M., Di Caro, G. A., Schmickl, T., Elmenreich, W., Arvin, F., Şekercioğlu, A., & Sende, M. (2021). Swarm intelligence and cyber-physical systems: Concepts, challenges and future trends. *Swarm and Evolutionary Computation*, *60*, 100762. https://doi.org/10.1016/j.swevo.2020.100762

Schranz, M., Umlauft, M., Sende, M., & Elmenreich, W. (2020). Swarm robotic behaviors and current applications [Publisher: Frontiers]. *Frontiers in Robotics and AI*, *7*. https://doi.org/10.3389/frobt.2020.00036

Silva, M. F., Friebe, A., Malheiro, B., Guedes, P., Ferreira, P., & Waller, M. (2019). Rigid wing sailboats: A state of the art survey. *Ocean Engineering*, *187*, 106150. https://doi.org/10.1016/j.oceaneng.2019.106150

Silva, M. F., Malheiro, B., Guedes, P., & Ferreira, P. (2020). Airfoil selection and wingsail design for an autonomous sailboat [Series Title: Advances in Intelligent Systems and Computing]. In M. F. Silva, J. Luís Lima, L. P. Reis, A. Sanfeliu, & D. Tardioli (Eds.), *Robot 2019: Fourth iberian robotics conference* (pp. 305–316, Vol. 1092). Springer International Publishing. https://doi.org/10.1007/978-3-030-35990-4_25

Song, K. W. (2024). Backyard-degradable interactive electronics. https://www2.eecs.berkeley.edu/Pubs/TechRpts/2024/EECS-2024-145.pdf

Stelzer, R., & Jafarmadar, K. (2011). History and recent developments in robotic sailing. In A. Schlaefer & O. Blaurock (Eds.), *Robotic sailing* (pp. 3–23). Springer. https://doi.org/10.1007/978-3-642-22836-0_1

Sun, Q., Qi, W., Liu, H., Ji, X., & Qian, H. (2022). Toward long-term sailing robots: State of the art from energy perspectives. *Frontiers in Robotics and AI*, *8*, 787253. https://doi.org/10.3389/frobt.2021.787253

Sun, X., Wang, G., Fan, Y., Mu, D., & Qiu, B. (2018). An automatic navigation system for unmanned surface vehicles in realistic sea environments [Number: 2 Publisher: Multidisciplinary Digital Publishing Institute]. *Applied Sciences*, *8*(2), 193. https://doi.org/10.3390/app8020193

Sun, Z., Feng, A., Yu, J., Zhao, W., & Huang, Y. (2025). Development of autonomous sailboat sails and future perspectives: A review. *Renewable and Sustainable Energy Reviews*, *207*, 114918. https://doi.org/10.1016/j.rser.2024.114918

Sun, Z., Yu, J., Zhao, W., Hu, F., Wang, J., & Jin, Q. (2025). Autonomous sailboat velocity prediction program considering the sea-surface wind velocity gradient. *Applied Ocean Research*, *155*, 104442. https://doi.org/10.1016/j.apor.2025.104442

SWARMs. (n.d.). Retrieved July 16, 2024, from http://swarms.eu/index.html

Tadros, M., Ventura, M., & Soares, C. G. (2023). Review of current regulations, available technologies, and future trends in the green shipping industry. *Ocean Engineering*, *280*, 114670. https://doi.org/10.1016/j.oceaneng.2023.114670

Tan, B. K., Ching, Y. C., Poh, S. C., Abdullah, L. C., & Gan, S. N. (2015). A review of natural fiber reinforced poly(vinyl alcohol) based composites: Application and opportunity [Number: 11 Publisher: Multidisciplinary Digital Publishing Institute]. *Polymers*, *7*(11), 2205–2222. https://doi.org/10.3390/polym7111509

Tay, Z. Y., & Konovessis, D. (2023). Sustainable energy propulsion system for sea transport to achieve united nations sustainable development goals: A review. *Discover Sustainability*, *4*(1), 20. https://doi.org/10.1007/s43621-023-00132-y

Tipsuwan, Y., Sanposh, P., & Techajaroonjit, N. (2023). Overview and control strategies of autonomous sailboats—a survey. *Ocean Engineering*, *281*, 114879. https://doi.org/10.1016/j.oceaneng.2023.114879

Tretow, C. (2017). *Design of a free-rotating wing sail for an autonomous sailboat*. Retrieved June 24, 2024, from https://urn.kb.se/resolve?urn=urn:nbn:se:kth:diva-215000

Vagale, A., Oucheikh, R., Bye, R. T., Osen, O. L., & Fossen, T. I. (2021). Path planning and collision avoidance for autonomous surface vehicles i: A review. *Journal of Marine Science and Technology*, *26*(4), 1292–1306. https://doi.org/10.1007/s00773-020-00787-6

Vogtländer, J. (n.d.). *Eco-costs* [Sustainability Impact Metrics]. Retrieved February 18, 2025, from https://www.ecocostsvalue.com/eco-costs-eco-efficient-value-creation-and-fast-track-lca/

Wrzecionek, M., Matyszczak, G., Bandzerewicz, A., Ruśkowski, P., & Gadomska-Gajadhur, A. (2021). Kinetics of polycondensation of citric acid with glycerol based on a genetic algorithm. *Organic Process Research & Development*, *25*(2), 271–281. https://doi.org/10.1021/acs.oprd.0c00492

Xing, H., Spence, S., & Chen, H. (2020). A comprehensive review on countermeasures for CO2 emissions from ships. *Renewable and Sustainable Energy Reviews*, *134*, 110222. https://doi.org/10.1016/j.rser.2020.110222

Ye, J., Li, C., Wen, W., Zhou, R., & Reppa, V. (2023). Deep learning in maritime autonomous surface ships: Current development and challenges. *Journal of Marine Science and Application*, *22*(3), 584–601. https://doi.org/10.1007/s11804-023-00367-1

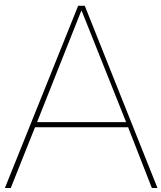

Project brief

DESIGN FOR our future

TU Delft

Personal Project Brief – IDE Master Graduation Project

Name student Daniël Korvemaker **Student number** 4,359,550

PROJECT TITLE, INTRODUCTION, PROBLEM DEFINITION and ASSIGNMENT

Complete all fields, keep information clear, specific and concise

Project title Design of an autonomous sailing vessel for environmental monitoring on inland waters

Please state the title of your graduation project (above). Keep the title compact and simple. Do not use abbreviations. The remainder of this document allows you to define and clarify your graduation project.

Introduction

Describe the context of your project here; What is the domain in which your project takes place? Who are the main stakeholders and what interests are at stake? Describe the opportunities (and limitations) in this domain to better serve the stakeholder interests. (max 250 words)

The sailing vessel will act as a replacement for static environmental sensors in inland waters. It offers great flexibility in deployment, as the vessel can travel to any location autonomously and installation is not necessary. Environmental monitoring on water means recording data on among other things, windspeed, direction, wave amplitude and frequency. This data is essential for (local) climate modelling, which is done by Rijkswaterstaat. Usecases for these models are the dimensioning and maintanance of dikes, to name two examples. The gathered data is also useful for offering realtime information about weather and water conditions for the shipping industry and recreational water users.

I will design for Lake IJssel (IJsselmeer) as there is already extensive (static) monitoring in place, which could be replaced by a sailing fleet. Datasets on wind and wave properties are also available, which can be used to design and dimension the vessel. As the vessels then are designed with data from Lake IJssel, they would be perfect to launch there, but they would also be applicable in other lakes.

Limitations in this domain considering the stakeholders, is the indepentent nature of this graduation project. I'm not working together with a client. I will have to invest some time in the first weeks of the project to thorougly research which stakeholders are relevant and which interests and requirements they have, in order to create a valid design.

→ *space available for images / figures on next page*

Figure A.1: Project brief (1/4)

introduction (continued): space for images

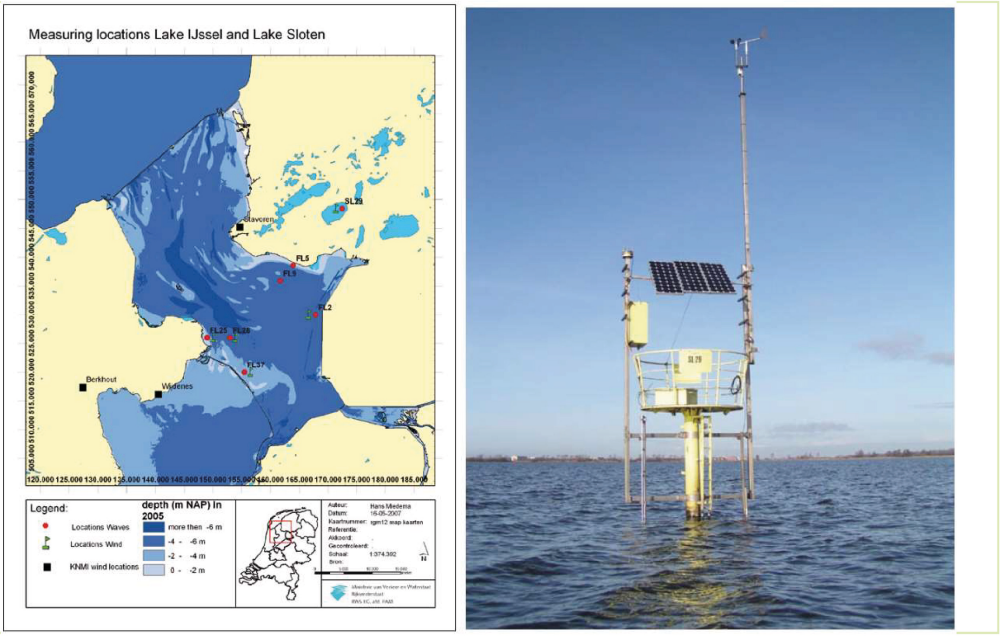

image / figure 1 Measuring locations Lake IJssel and an example of a measuring station. (Rijkswaterstaat, 2007)

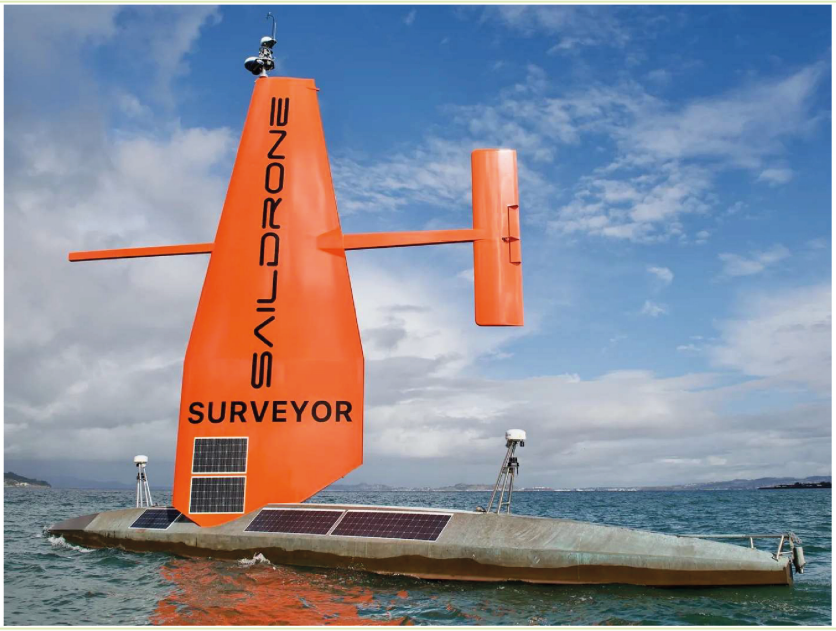

image / figure 2 An uncrewed sailling vehicle developed by Saildrone for the open oceans, length = 22m. (Saildrone, 2015)

Figure A.1: Project brief (2/4)

Problem Definition

What problem do you want to solve in the context described in the introduction, and within the available time frame of 100 working days? (= Master Graduation Project of 30 EC). What opportunities do you see to create added value for the described stakeholders? Substantiate your choice.
(max 200 words)

To keep our low-lying land safe for habitation, measuring changes in the environment is essential. In the field of climate data gathering I want to offer researchers more flexibility, coverage and value for money. The approach I take is to gather data via autonomous sailing vessels that could work in a fleet to cover a large area. The vessels would be able to autonomously travel to and return from their destination. Sailing offers an energy neutral way of transportation and these vessels can therefore be online for long periods of time. These vessels offer greater flexibility, coverage, and cost-effectiveness compared to static instruments that have to be built or placed on location. This project focusses on the Netherlands, but the sailing vessel could be deployed worldwide to monitor conditions on local inland waters.

Within the 100 working days I want to create a design of an autonomous climate monitoring sailing vessel. Furthermore, I want to manufacture, build, and test the most important subssystems to show their feasibility.

Assignment

This is the most important part of the project brief because it will give a clear direction of what you are heading for. Formulate an assignment to yourself regarding what you expect to deliver as result at the end of your project. (1 sentence) As you graduate as an industrial design engineer, your assignment will start with a verb (Design/Investigate/Validate/Create), and you may use the green text format:

Design an autonomous sailing vessel to monitor its environment for Rijkswaterstaat in inland waters like Lake IJssel.

Then explain your project approach to carrying out your graduation project and what research and design methods you plan to use to generate your design solution (max 150 words)

I imagine 5 main sections in my graduation project:
1. Research
   The first weeks. Exploring the context, stakeholders, and creating list of requirements.
2. Design
   Weeks 3-8. Dimensioning of critital sailing aspects, designing parts, 3D modeling, ending with a BOM.
3. Manufacturing
   Weeks 8+. Manufacturing of custom parts, building of the essential subsystems.
4. Testing
   Weeks 8+. Testing subsystems, and afterwards whole system tests.
5. Iteration
   Weeks 8+. Evaluating, updating parts or systems.

See the attached Gantt chart planning for a more complete version.

Figure A.1: Project brief (3/4)

Project planning and key moments

*To make visible how you plan to spend your time, you must make a planning for the full project. You are advised to use a Gantt chart format to show the different phases of your project, deliverables you have in mind, meetings and in-between deadlines. Keep in mind that all activities should fit within the given run time of 100 working days. Your planning should include a **kick-off meeting**, **mid-term evaluation meeting**, **green light meeting** and **graduation ceremony**. Please indicate periods of part-time activities and/or periods of not spending time on your graduation project, if any (for instance because of holidays or parallel course activities).*

Make sure to attach the full plan to this project brief.
The four key moment dates must be filled in below

Kick off meeting	20 juni 2024
Mid-term evaluation	11 sept 2024
Green light meeting	13 nov 2024
Graduation ceremony	16 dec 2024

In exceptional cases (part of) the Graduation Project may need to be scheduled part-time. Indicate here if such applies to your project

Part of project scheduled part-time	
For how many project weeks	
Number of project days per week	

Comments:

Motivation and personal ambitions

Explain why you wish to start this project, what competencies you want to prove or develop (e.g. competencies acquired in your MSc programme, electives, extra-curricular activities or other).

Optionally, describe whether you have some personal learning ambitions which you explicitly want to address in this project, on top of the learning objectives of the Graduation Project itself. You might think of e.g. acquiring in depth knowledge on a specific subject, broadening your competencies or experimenting with a specific tool or methodology. Personal learning ambitions are limited to a maximum number of five.
(200 words max)

The biggest motivation to start this particular project is my interest in multidiciplinary engineering. During my time at IDE, I was mostly underwhelmed by the quality and quantity of the engineering courses. Therefore, I opted to broaden my engineering skills during my minor project and electives by following courses from maritime, mechanical and aerospace engineering. Especially during my minor project at maritime engineering, and the project Advanced Embodiment Design in the IPD master, I discovered my passion for making technically ambitious ideas into reality. During this project, I want to show that I have got the competencies to tackle such an ambitious multidiciplinary engineering assignment on my own.

Figure A.1: Project brief (4/4)

B

Initial mass estimation

Part	#	Outer diameter (r	(Wall)thickness (mm)	Length (m)	Material	Density (kg/m^3)	Volume	Mass/part (kg)	LCG (bow=0, stern=1)	Moment about LCG 0,5
Hull										
Foam core					EPS	33	0,04	1,32	0,5	0
Glass fibre shell					GFRP+Epoxy	2000	0,00048	0,96	0,5	0
Total								**2,28**		**0**
Sails										
Foam core				1	EPS	33	0,006	0,198	0,52	0,00396
Glass fibre shell					GFRP+Epoxy	2000	0,00024	0,48	0,52	0,0096
Horizontal tubes	3	20	1,5	0,4	Aluminum	2700	0,0001	0,2825	0,6	0,02824606
Mast tube	1	30	2	0,4	Aluminum	2700	0,0001	0,1900	0,5	0
Linear actuator								0,05	0,8	0,015
Tail elevator assembly								0,2	0,9	0,08
Counterweight					Stone/concrete	2500		0,34	0,1	-0,136
alu stang massief						2700	0,0000	0	Sail assemly should be moment/mass balanced	
Total								**1,740464119**		**0,00080606**
Keel										
Foam core				0,3	EPS	33	0,00015	0,00495	0,5	0
Threaded rod M6	3	6	3	0,35	Steel	7800	0,0000	0,2316	0,5	0
Glass fibre shell					GFRP+Epoxy	2000	0,0001	0,2	0,5	0
								0		0
Keel					Stone/concrete/g	2750	0,00127273	3,5	0,5	0
Total								**3,936516794**		**0**
Central construction										
Main cylinder	1	50	4	0,1	Aluminum	2700	0,0001	0,1561	0,5	0
6806 bearing	2				Steel			0,05	0,5	0
Rudder tube (approx.)	1	20	2	0,4	Aluminum	2700	0,0000	0,1221	0,75	0,030536281
Connecting ring	1	42	5	0,01	Aluminum	2700	0,0000	0,0157	0,5	0
Top ring	1	70	19	0,01	Aluminum	2700	0,0000	0,0822	0,5	0
Hardware	lots				RVS			0,1	0,52	0,002
Battery								0,3	0,5	0
Electronics								0,1	0,5	0
Cables								0,2	0,7	0,04
Sensor payload								0,25	0,5	0
Total								**1,376105189**		**0,072536281**
Rudder										
Aproxx								0,25	0,95	0,1125
Total								**0,25**		**0,1125**
										should be 0:
Total								**9,583086103**		**0,18584234**

Existing designs			
LDR average (LWL 0-2m)	4,8		(Waterline length / volume of displacement)^1/3
SA/D average (LWL 0-2m)	12,7		(Sail area / volume of displacement)^2/3
BD average	36	%	ballast to displacement ratio
My displacement	11,4997	kg	
	0,0115	m^3	

Plugging those in:							
My Length	**1,271775**	**m**	L = LDRaverage^3 * displacement			**Iteration 1**	
My SA	**0,520466**	**m^2**	SA = SA/Daverage^3/2 * displacement		Length	1,27	m
					Beam	0,33	m
					Draft	0,064	m
Set Cp	0,55		Cp = displ / AM * L	Fossati: "yachts are typically 0,45-0,6"	Cp	0,55	
My AM (max cross sectional area)	0,01644	m^2	AM = displ / Cp / L			Normalised to 0-1	
2AM	0,032881				Length	1	
					Beam	0,25984252	0,12992126
					Draft	0,050393701	
Beam draft ratio	5		BDR = B/d = 2b/d	assume AM= 1/2 ellipse			
				2AM = b * d * pi			
Beam	**0,323517**	**m**	B=2(AM*BDR/pi)^0,5				
Draft	**0,064703**	**m**	d=(AM/0,25BDR*pi)^0,5				
Control displacement	11,4997	kg					

Figure B.1: The initial mass estimation, which was the start of the hull iterations.

C

Stability calculation in Grasshopper

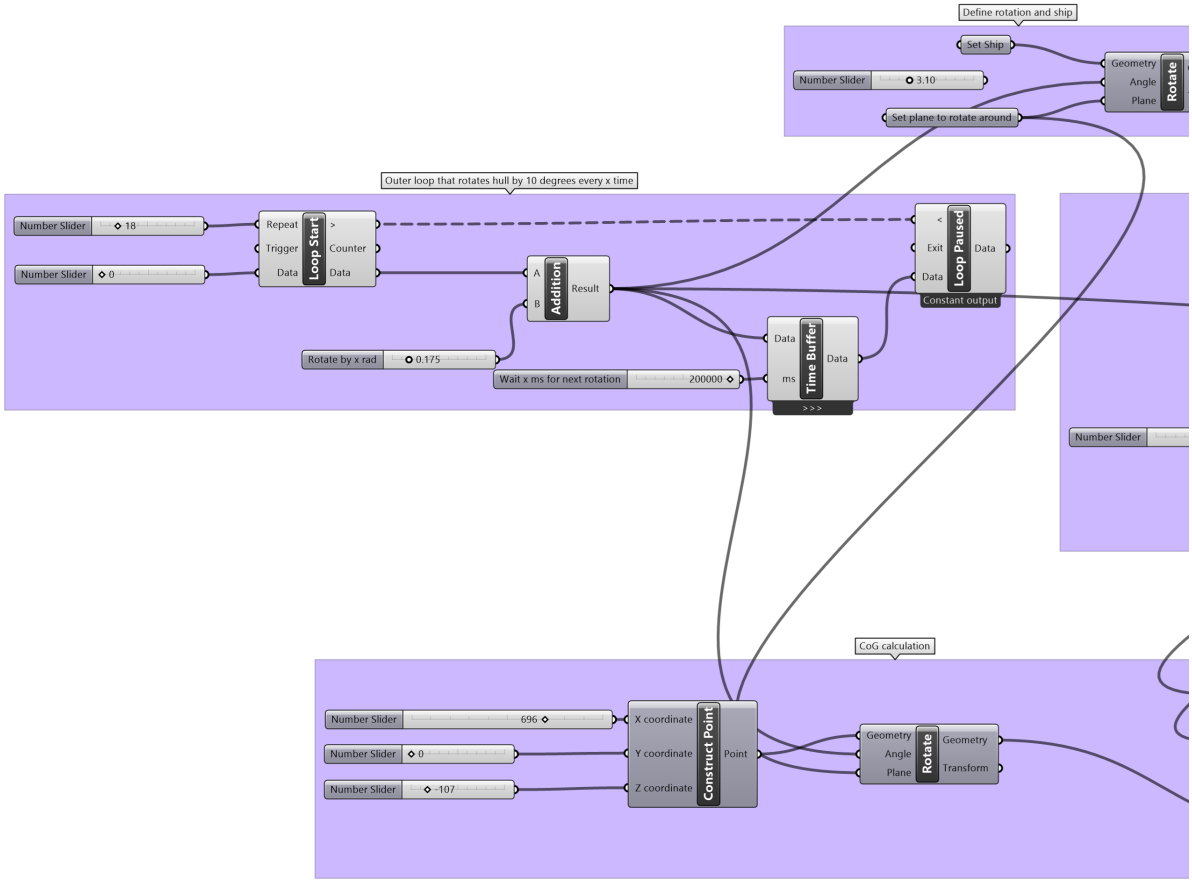

Figure C.1: Grasshopper file for the analysis of the stability. (1/5)

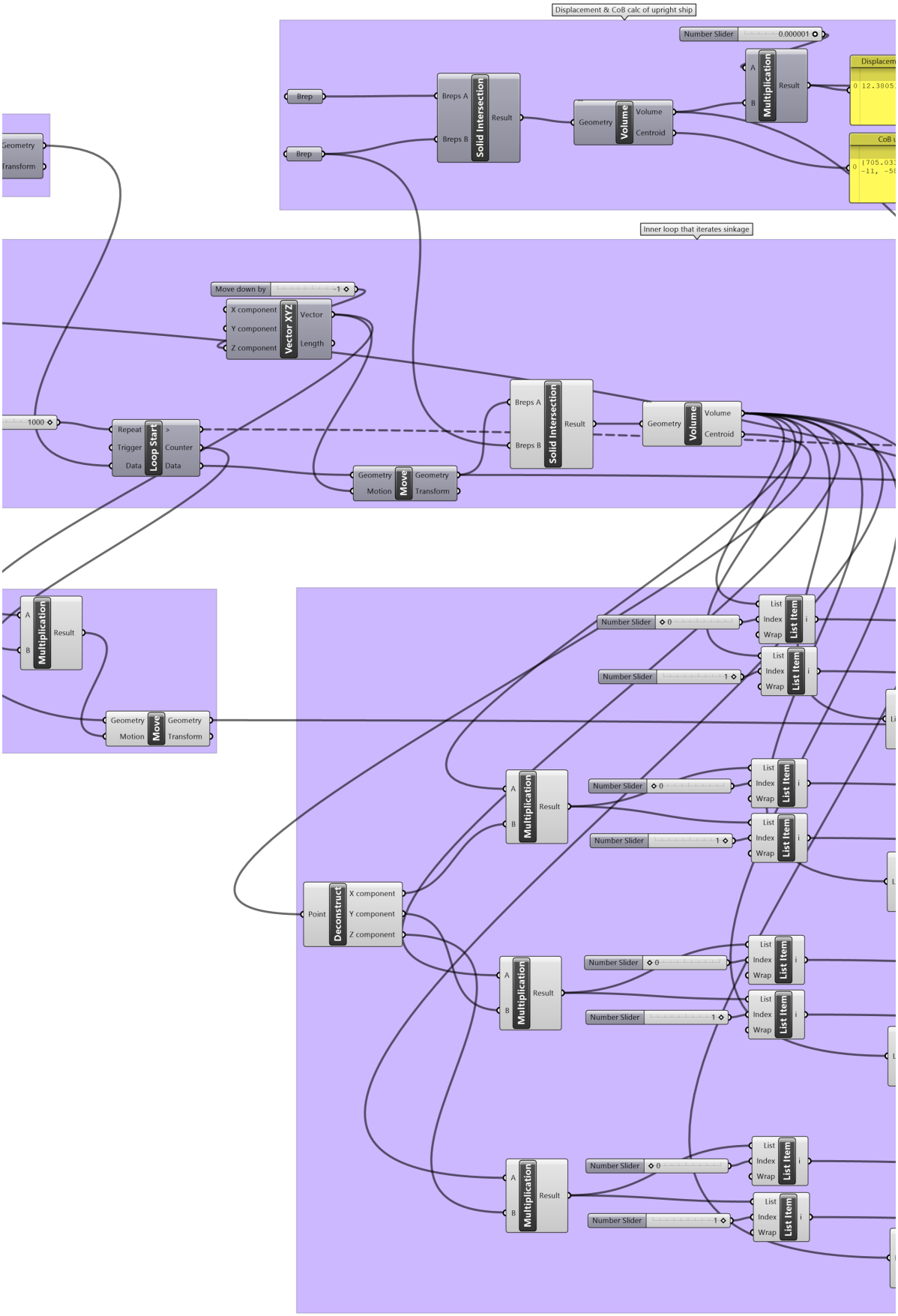

Figure C.1: Grasshopper file for the analysis of the stability. (2/5)

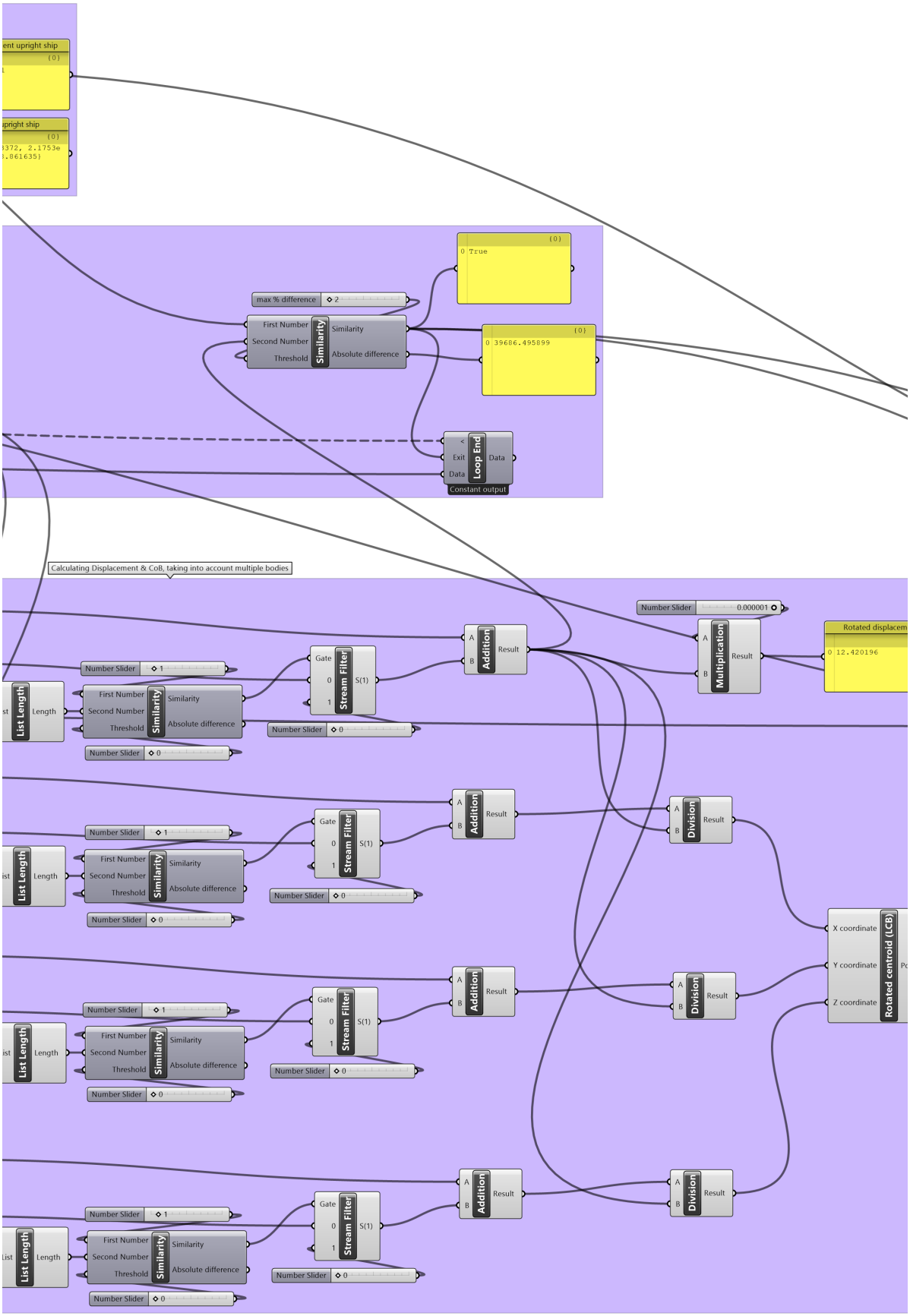

Figure C.1: Grasshopper file for the analysis of the stability. (3/5)

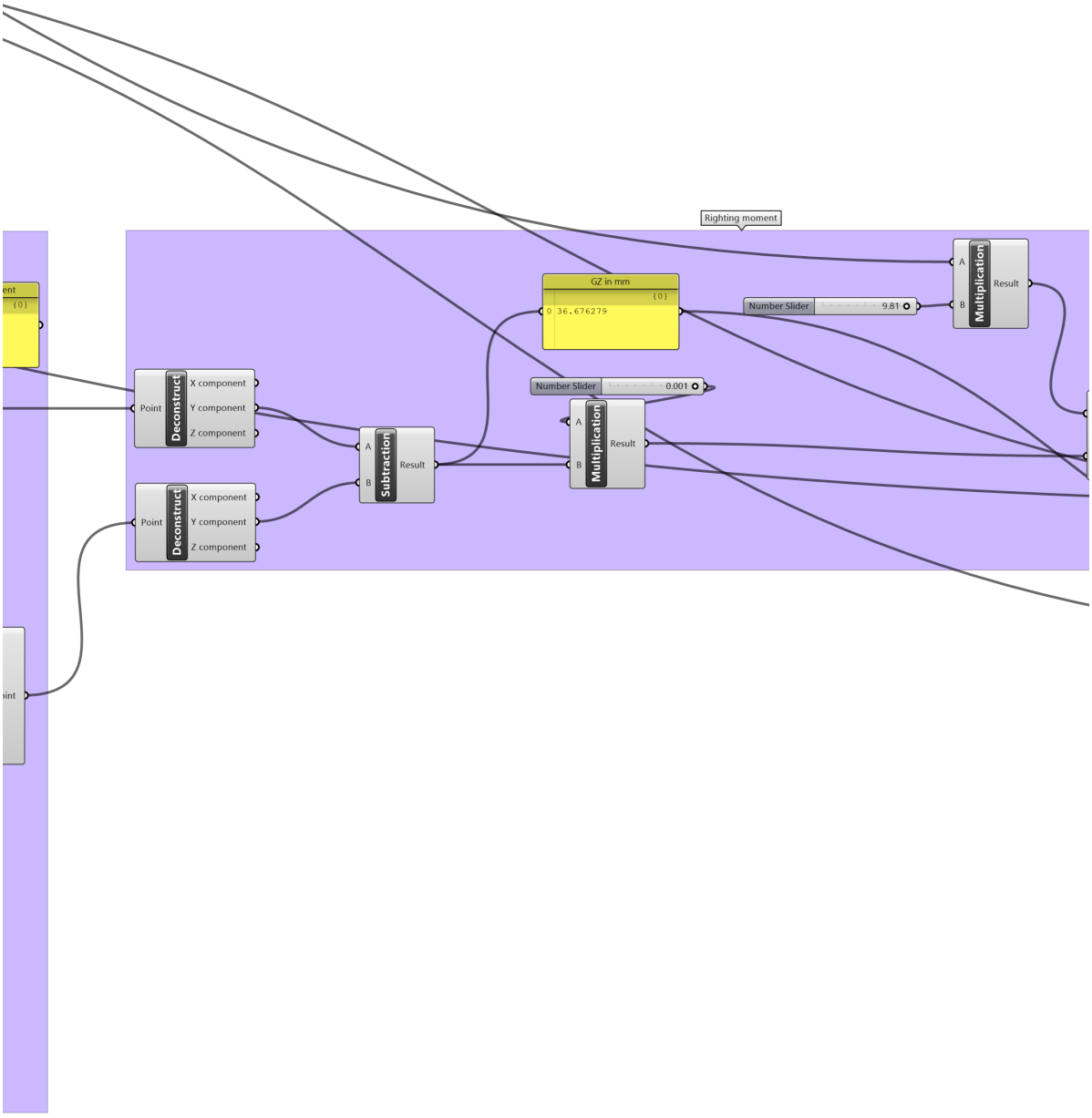

Figure C.1: Grasshopper file for the analysis of the stability. (4/5)

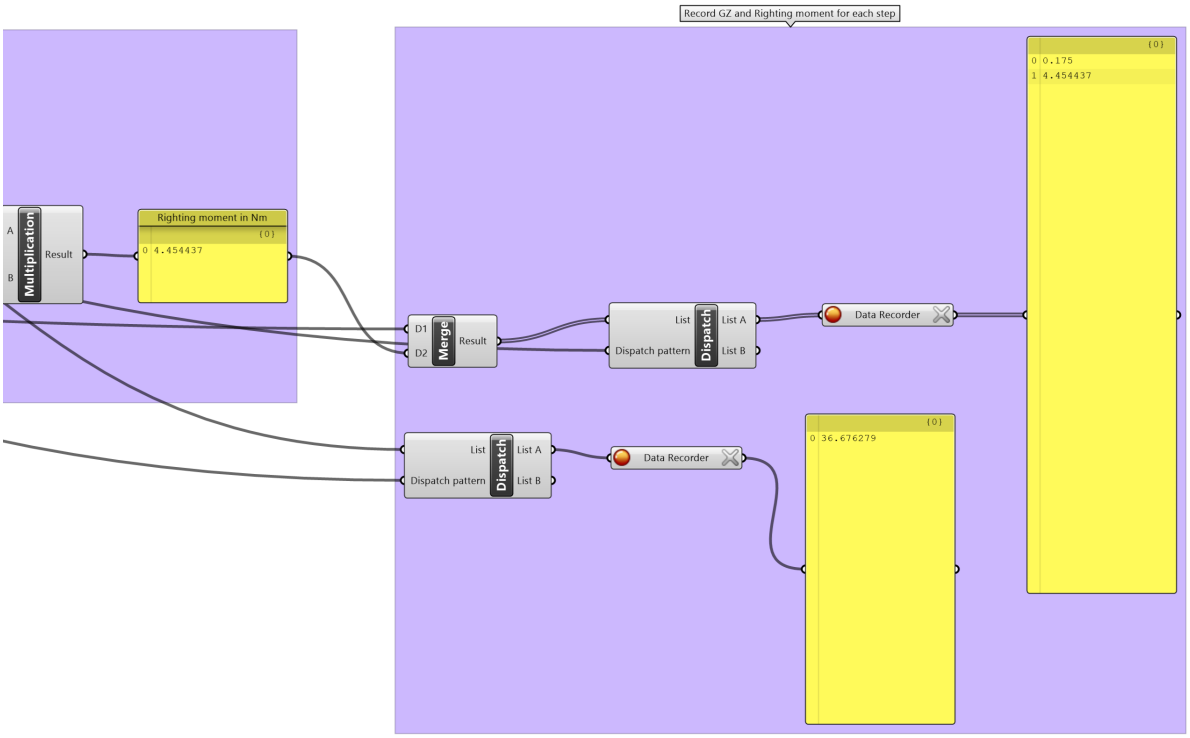

Figure C.1: Grasshopper file for the analysis of the stability. (5/5)

D

Hot wire CNC foam cutter

Table D.1 lists all materials used for the machine. The code for G-code generation in Grasshopper is imaged in Figure D.1. An example of the CNC control software during use is shown in in Figure D.2.

Table D.1: Bill of materials for the hot wire CNC foam cutter.

Item no.	Part	Description	Quantity
1	2020 Belt Tensioner assembly		4
2	2020 V-Slot 1000mm		4
3	2020 V-Slot 160mm		4
4	2020 V-Slot 250mm		1
5	2040 Gantry Plate		2
6	2040 V-Slot 700mm		2
7	2080 Gantry Plate	Drill 4 extra holes per plate	2
8	2080 V-Slot 700mm	Tap threads at both ends	2
9	24mm Groove Bearing		1
10	Aluminum Spacer 6mm		24
11	BIGTREETECH SKR Pico motherboard		1
12	Ecentric Spacer 6mm		6
13	GT2 20T pulley		2
14	GT2 48T pulley		2
15	GT2 belt ∼1.5m		2
16	GT2 belt ∼1m		2
17	GT2 belt attachment to 2040 carriage	Custom part - 3D printed	2
18	GT2 belt clamp	Custom part - 3D printed	2
19	GT2 belt clamp mirrored	Custom part - 3D printed	2
20	ISO 4032 Nut M5		22
21	ISO 4762 Bolt M3 x 10		16
22	ISO 4762 Bolt M5 x 16		80
23	L-Plate		8
24	M5 flat head bolt 10mm		12
25	M5 flat head bolt 14mm		18
26	M5 flat head bolt 25mm		14
27	Motor Mount Plate Nema 17		4
28	Nema 17 stepper motor		4
29	Nichrome wire ∼1.5m		1
30	Slider T-Nut for 2020 - M4		8
31	Slider T-Nut for 2020 - M5		53
32	Stepper motor cables		4
33	Tension spring		1
34	V Wheel		14
35	Washer ISO 7089 - M5		28
36	Washer ISO 7090 - M5		40
37	Washer ISO 7092 - M5		14
38	Washer ISO 7094 - M5		28
39	Aluminium dibond panel as platform		1

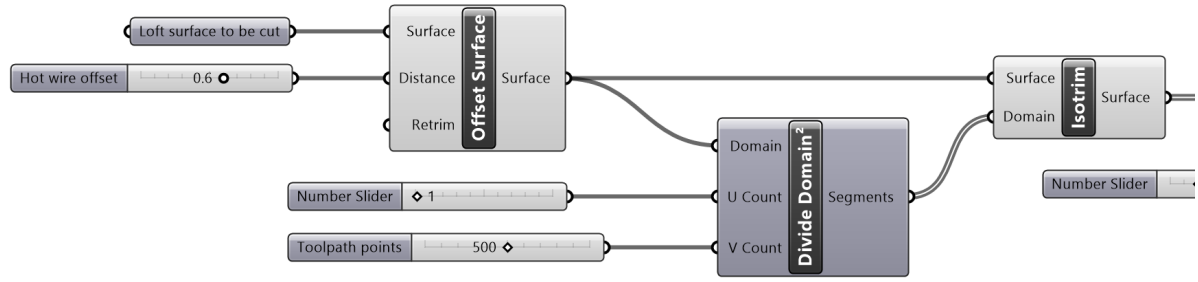

Figure D.1: Grasshopper file for the generation of G-code. (1/3)

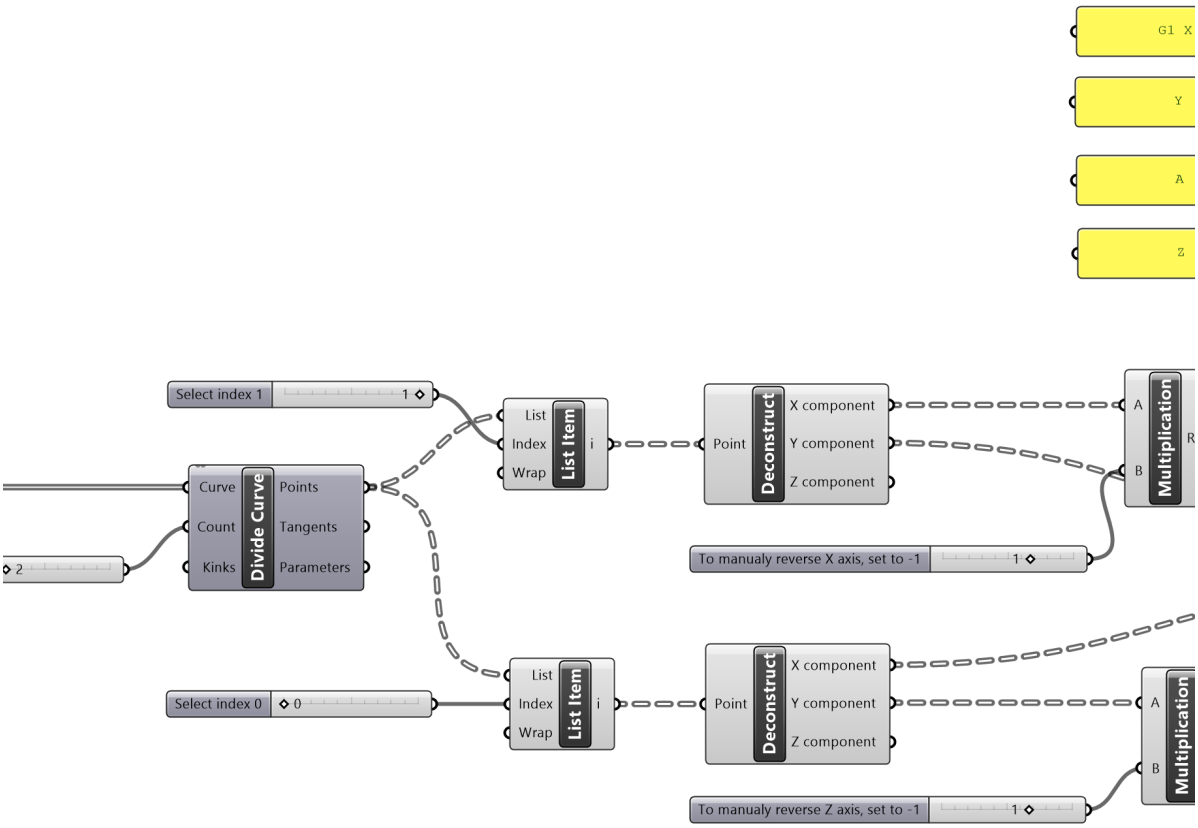

Figure D.1: Grasshopper file for the generation of G-code. (2/3)

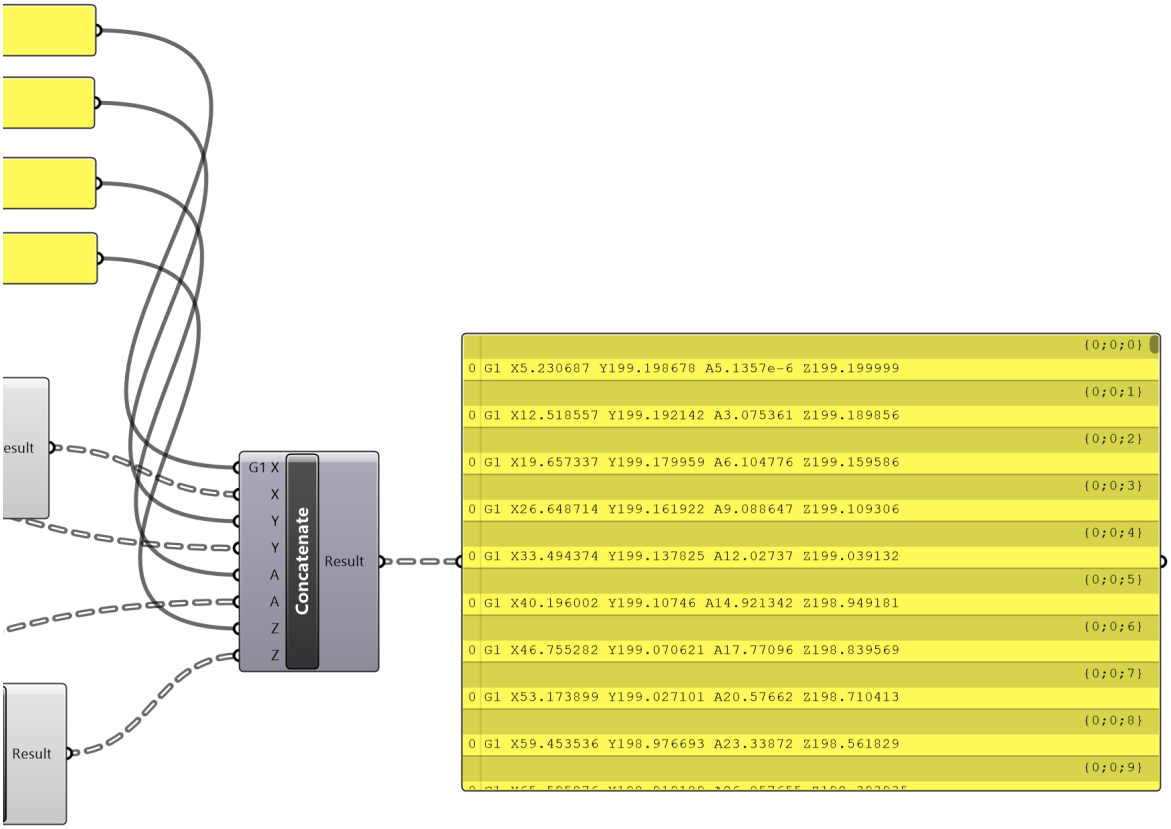

Figure D.1: Grasshopper file for the generation of G-code. (3/3)

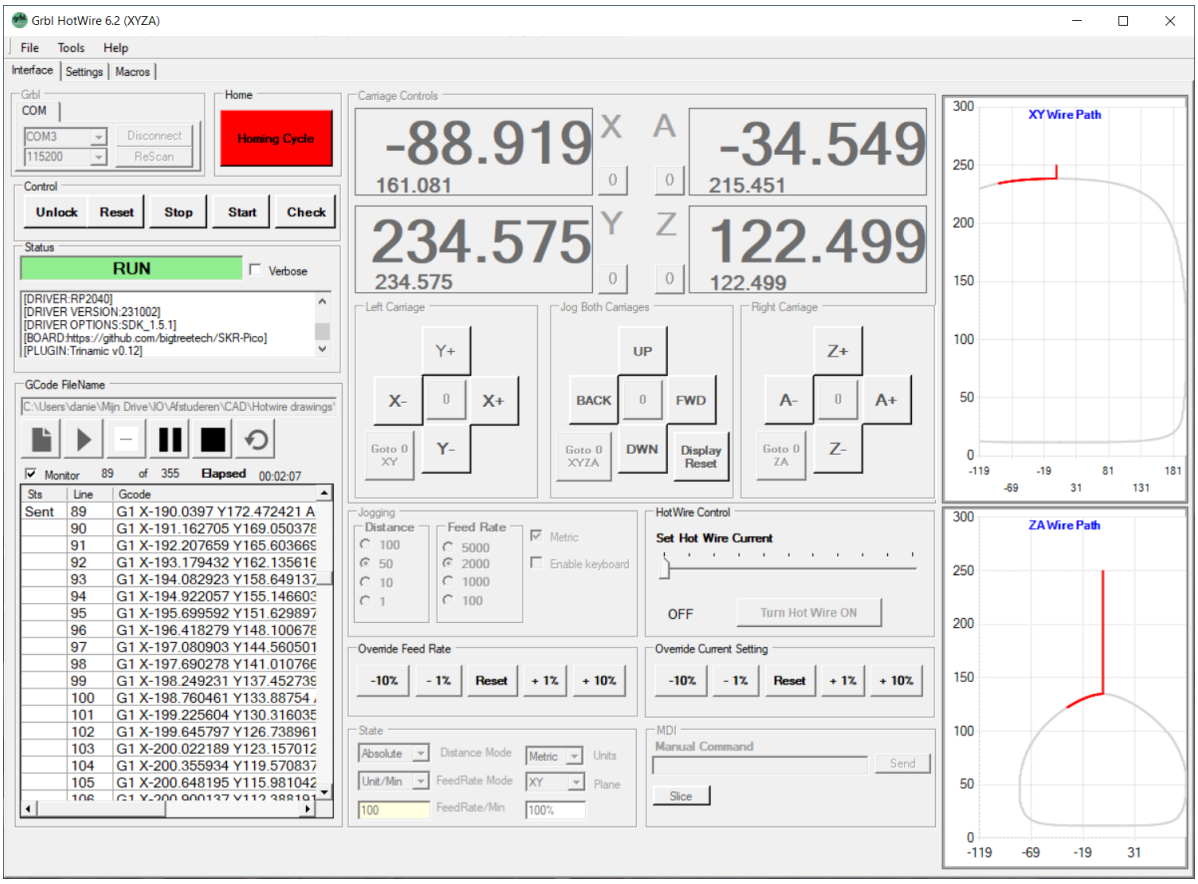

Figure D.2: GRBL HotWire by Howlette (2022) is used as CNC control software.

E

Dynamics model

To understand the movement of the wingsail and the influences of certain parameters, a dynamics model was developed. This approach of modelling the dynamical system to extract design parameters quickly got out of hand and was studded on simplifications. It was later substituted with the more pragmatic statistical design approach by examining existing boats that use aerodynamic control. The full analysis is described here.

E.1. Vector definitions and equations of motion

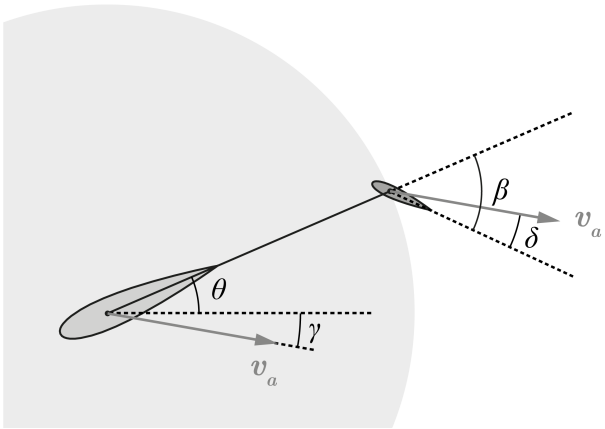

(a) Diagram showing the wingsail system with its main wing and tail wing. Four angles are defined: the position angle θ of the system, the apparent wind direction γ, the constant tail wing offset β, and the angle of attack of the tail wing δ versus the apparent wind direction. The apparent wind vector $\vec{v_a}$ is shown for clarity.

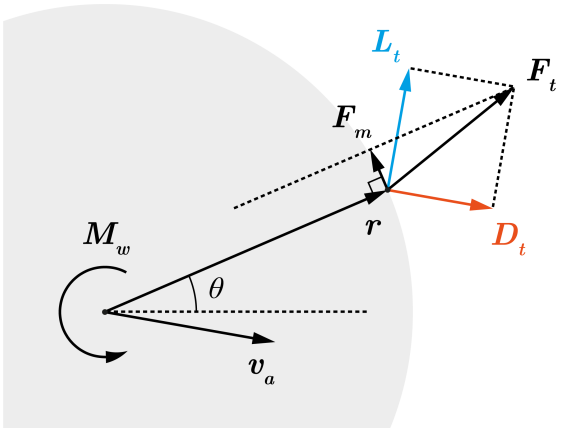

(b) Free body diagram illustrating the polar vector system of the dynamics of the sail. Lift ($\vec{L_t}$) and drag ($\vec{D_t}$) vectors are drawn for the tail wing, as are the resulting aerodynamic force vector ($\vec{F_t}$) and its orthogonal projection ($\vec{F_m}$) on the position vector ($\vec{r}$). $\vec{v_a}$ is the apparent wind vector. Aerodynamic forces of the main wing are not drawn because they do not result in angular acceleration.

Figure E.1: Diagrams of the polar dynamics. Angles are exaggerated for clarity, and vector magnitudes are not necessarily to scale.

To understand the movement of the wingsail and the influences of certain parameters, a dynamics model was developed with the following assumptions:

- Perfect alignment of the main wing on its axis, ensuring that the aerodynamic forces acting on it produce no moment arm and, therefore, no net moment on the entire system. The only moment inducing force(s) originate from the tailwing.
- No aerodynamic effect of the connective rods between the wings. The wings are looked at in isolation.
- Damping is added and is estimated.

- The C_l and C_d coefficients of a NACA0015 are used and are extrapolated manually to have coefficients outside of $15°$. These coefficients are used in a lookup table.
- The lift and drag is analysed without 3D effects.

The convention for polar vector notation is defined as follows:

$$\vec{v} = (r, \theta)$$

where r is the magnitude and θ the angle.

Position vector

$$\vec{r} = (r, \theta) \tag{E.1}$$

Wind vector

$$\vec{v_a} = (v_w, \gamma) \tag{E.2}$$

Angle of attack tail wing $\delta(t)$: the angle of attack of the tail wing versus oncoming flow γ.

$$\delta(t) = \theta(t) + \beta - \gamma(t) \tag{E.3}$$

- $\theta(t)$: Time-dependent angular position of the system.
- β: Fixed angle offset between $\theta(t)$ and the tail wing.
- $\gamma(t)$: Time-dependent wind angle. Can also be constant.

Lift vector

$$\vec{L_t} = (0.5\rho {v_w}^2 A C_l(\delta(t)), \gamma(t) + 0.5\pi) \tag{E.4}$$

- ρ: Air density (kg/m^3).
- v_w: Wind speed (m/s).
- A: Wing area (m^2).
- $C_l(\delta(t))$: Lift coefficient, which is a function of the angle of attack $\delta(t)$. Inserted from a lookup table. Dimensionless.
- $\gamma(t) + 0.5\pi$: Angle perpendicular to the wind direction, as lift is defined to act perpendicular to the wind.

Drag vector

$$\vec{D_t} = (0.5\rho {v_w}^2 A C_d(\delta(t)), \gamma(t)) \tag{E.5}$$

- ρ: Air density (kg/m^3).
- v_w: Wind speed (m/s).
- A: Wing area (m^2).
- $C_d(\delta(t))$: Drag coefficient, which is a function of the angle of attack $\delta(t)$. Inserted from a lookup table. Dimensionless.
- $\gamma(t)$: Wind angle, as drag is defined to act in the direction of the wind.

Net aerodynamic force vector

$$\vec{F_t} = \vec{L_t} + \vec{D_t} \tag{E.6}$$

Perpendicular force vector: Orthogonal projection of net aerodynamic force onto position vector, resulting in force vector F_m that can be used to calculate angular acceleration

$$\vec{F_m} = \frac{\vec{F_t} \cdot \vec{r}}{\vec{r} \cdot \vec{r}} \vec{r} \tag{E.7}$$

Angular acceleration: the moment of inertia of the system is $I = mr^2$. Using $\vec{F_m}$, the angular acceleration is

$$\alpha = \frac{\vec{F_m}}{I} - \frac{c\omega}{I} \tag{E.8}$$

- $\frac{\vec{F_m}}{I}$ is the torque-induced angular acceleration.
- $-\frac{c\omega}{I}$ represents the damping due to the damping coefficient c.

Equations of motion: The dynamics are described by these coupled first-order differential equations.

Angular velocity ω, the rate of change of the angle θ:

$$\frac{d\theta}{dt} = \omega \tag{E.9}$$

Angular acceleration α: the rate of change of angular velocity ω:

$$\frac{d\omega}{dt} = \alpha = \frac{\vec{F_m}}{I} - \frac{c\omega}{I} \tag{E.10}$$

The dynamics system was implemented in Python to generate an animation illustrating the system's behaviour over time and to visualize the forces at play.

E.2. Results

Results are plotted in Figure E.2 and E.3 with the following initial conditions. Results show that the system is expected to settle after a few seconds, when beginning at an angle offset of 60 degrees from the wind angle.

theta0 = np.radians(60), Initial angle of system (in radians)
omega0 = 0, Initial angular velocity (in radians per second)
Va-magnitude = 5, Apparent wind speed magnitude
wind-angle0 = 0, Initial wind angle
c = 0.5, Damping coefficient
beta = np.radians(20), Angle between theta (the whole system) and the tail wing - set between -20 and +20
Constants:
A = 0.02, Area
rho = 1.225, Density
m = 1, Mass
r = 0.5, Radius of rotation

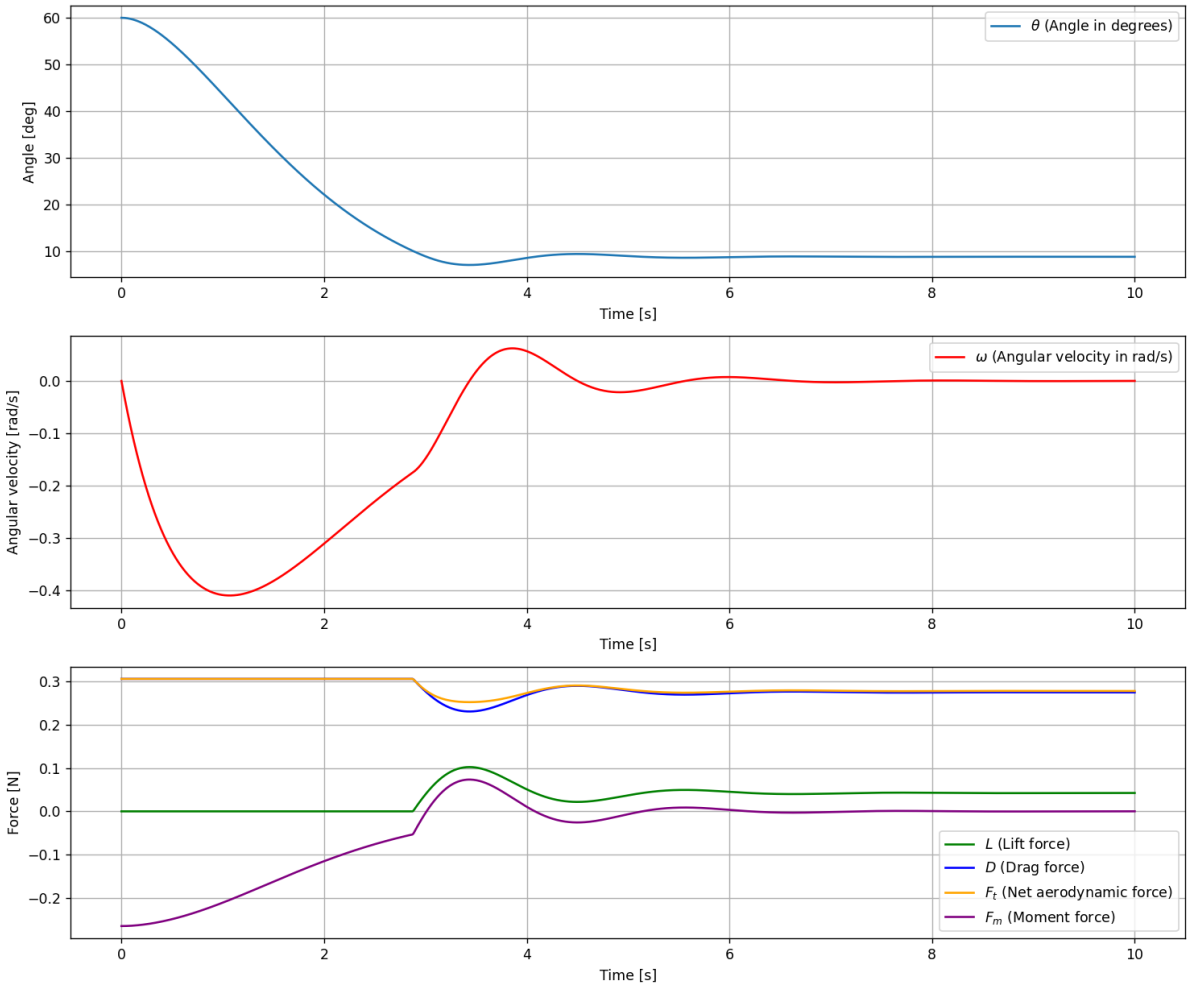

Figure E.2: The result of the solving the dynamics model.

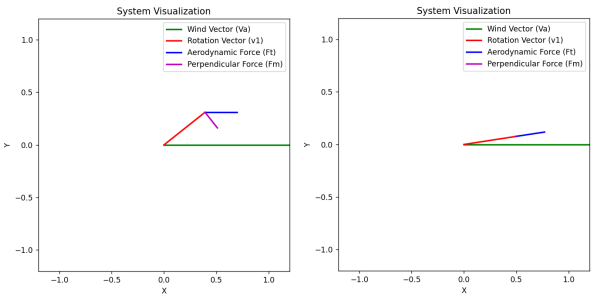

Figure E.3: Two images of the animation. On the left, the wing is moving, while on the right, the system has reached equilibrium. This is a top-view, just as Figure E.1b.

E.3. Code

```
import numpy as np
import pandas as pd
import matplotlib.pyplot as plt
from scipy.interpolate import interp1d
from scipy.integrate import odeint
from matplotlib.animation import FuncAnimation

# Initial conditions / things to change
theta0 = np.radians(60)  # Initial angle of system (in radians)
omega0 = 0  # Initial angular velocity (in radians per second)
Va_magnitude = 5  # Apparent wind speed magnitude
wind_angle0 = 0 # Initial wind angle
c = 0.5  # Damping coefficient
beta = np.radians(20)  # Angle between theta (the whole system) and the tail wing - set
    between -20 and +20

# Constants
A = 0.02  # Area
rho = 1.225  # Density
m = 1  # Mass
r = 0.5  # Radius of rotation


# Load the Xfoil data
xfoil_data = pd.read_csv('xf-naca0015-il-500000.csv', skiprows=10)
xfoil_data = xfoil_data[['Alpha', 'Cl', 'Cd']]  # Keep only relevant columns

# Create interpolation functions for Cl and Cd
alpha_data = np.radians(xfoil_data['Alpha'])  # Convert Alpha to radians
cl_interp = interp1d(alpha_data, xfoil_data['Cl'], bounds_error=False, fill_value="
    extrapolate")
cd_interp = interp1d(alpha_data, xfoil_data['Cd'], bounds_error=False, fill_value="
    extrapolate")

# Function to compute time-dependent gamma (wind angle)
def gamma(t):
    baseline = np.radians(wind_angle0)  # Baseline wind angle
    amplitude = np.radians(5)  # Maximum variation
    frequency = 0  # Frequency of oscillation
    return baseline + amplitude * np.sin(2 * np.pi * frequency * t)

# Calculate lift and drag forces as vectors
def forces(t, theta):
    # Wind vector components (wind comes from the gamma(t) angle)
    wind_angle = gamma(t)
    wind_vector = np.array([Va_magnitude * np.cos(wind_angle), Va_magnitude * np.sin(
    wind_angle)])

    # Angle of attack
    alpha = theta + beta - wind_angle
    Cl = cl_interp(alpha)  # Interpolated lift coefficient
    Cd = cd_interp(alpha)  # Interpolated drag coefficient

    # Magnitudes of lift and drag forces
    L_magnitude = 0.5 * rho * Va_magnitude**2 * A * Cl
    D_magnitude = 0.5 * rho * Va_magnitude**2 * A * Cd

    # Drag vector (aligned with wind direction)
    drag_vector = D_magnitude * (wind_vector / np.linalg.norm(wind_vector))

    # Lift vector (perpendicular to wind direction)
    lift_vector = L_magnitude * np.array([-wind_vector[1], wind_vector[0]]) / np.linalg.norm(
    wind_vector)

    # Net aerodynamic force, Force on tail
    Ft = lift_vector + drag_vector

    # V1 vector, and the vector Fm that is perpendicular and responsible for acceleration.
    v1 = np.array([r * np.cos(theta), r * np.sin(theta)])  # V1 vector
```

```
    v1_perp = np.array([-r * np.sin(theta), r * np.cos(theta)])  # Rotate v1 by +90 degrees
    Fm = np.dot(Ft, v1_perp) / np.linalg.norm(v1_perp)  # Scalar projection

    return L_magnitude, D_magnitude, Ft, Fm

# Define the system of equations (theta and omega) with damping
def dynamics(state, t):
    theta, omega = state

    # Compute aerodynamic force component responsible for the acceleration
    Fm_value = forces(t, theta)[3]  # Only Fm is needed for the dynamics

    # Moment of inertia (I = m * r^2 for point mass model)
    I = m * r**2

    # Angular acceleration with damping
    angular_acceleration = (Fm_value / I) - (c * omega / I)

    # Equations of motion
    dtheta_dt = omega
    domega_dt = angular_acceleration

    return [dtheta_dt, domega_dt]

# Initial conditions
initial_conditions = [theta0, omega0]

# Time array
t = np.linspace(0, 10, 1000)  # 10 seconds, 1000 time steps

# Solve the differential equations
solution = odeint(dynamics, initial_conditions, t)

# Extract results
theta_solution = solution[:, 0]
omega_solution = solution[:, 1]

# Arrays to store lift, drag, Ft, and Fm over time
L_magnitude_arr = np.zeros_like(t)
D_magnitude_arr = np.zeros_like(t)
Ft_arr = np.zeros_like(t)
Fm_arr = np.zeros_like(t)

# Calculate lift, drag, Ft, and Fm for each time step
for i, ti in enumerate(t):
    L_magnitude_arr[i], D_magnitude_arr[i], Ft, Fm_arr[i] = forces(ti, theta_solution[i])
    Ft_arr[i] = np.linalg.norm(Ft)

# Plot the results
plt.figure(figsize=(12, 10))

# Plot angular position (theta)
plt.subplot(3, 1, 1)
plt.plot(t, np.degrees(theta_solution), label=r'$\theta$ (Angle in degrees)')
plt.xlabel('Time [s]')
plt.ylabel('Angle [deg]')
plt.grid(True)
plt.legend()

# Plot angular velocity (omega)
plt.subplot(3, 1, 2)
plt.plot(t, omega_solution, label=r'$\omega$ (Angular velocity in rad/s)', color='r')
plt.xlabel('Time [s]')
plt.ylabel('Angular velocity [rad/s]')
plt.grid(True)
plt.legend()

# Plot Lift, Drag, Ft, and Fm
plt.subplot(3, 1, 3)
plt.plot(t, L_magnitude_arr, label=r'$L$ (Lift force)', color='g')
plt.plot(t, D_magnitude_arr, label=r'$D$ (Drag force)', color='b')
```

```
plt.plot(t, Ft_arr, label=r'$F_t$ (Net aerodynamic force)', color='orange')
plt.plot(t, Fm_arr, label=r'$F_m$ (Moment force)', color='purple')
plt.xlabel('Time [s]')
plt.ylabel('Force [N]')
plt.grid(True)
plt.legend()

plt.tight_layout()
plt.show()

# Visualize System with Wind Angle, v1 (rotation vector), Ft (net aerodynamic force), and Fm (perpendicular force)
fig, ax = plt.subplots(figsize=(6, 6))
ax.set_xlim(-1.2, 1.2)
ax.set_ylim(-1.2, 1.2)
ax.set_aspect('equal')
ax.set_title('System Visualization')
ax.set_xlabel('X')
ax.set_ylabel('Y')

# Line for gamma (wind direction)
gamma_line, = ax.plot([], [], 'g-', lw=2, label='Wind Vector (Va)')

# Line for v1 (rotation vector)
v1_line, = ax.plot([], [], 'r-', lw=2, label='Rotation Vector (v1)')

# Line for Ft (net aerodynamic force)
Ft_line, = ax.plot([], [], 'b-', lw=2, label='Aerodynamic Force (Ft)')

# Line for Fm (perpendicular force)
Fm_line, = ax.plot([], [], 'm-', lw=2, label='Perpendicular Force (Fm)')

# Add legend
ax.legend()


def init():
    gamma_line.set_data([], [])
    v1_line.set_data([], [])
    Ft_line.set_data([], [])
    Fm_line.set_data([], [])
    return gamma_line, v1_line, Ft_line, Fm_line


def update(frame):
    theta = theta_solution[frame]  # Get current angle theta
    gamma_angle = gamma(t[frame])  # Get current wind angle gamma
    Va = Va_magnitude  # Apparent wind speed magnitude

    # Va vector (wind vector)
    Va_x = [0, Va * np.cos(gamma_angle)]
    Va_y = [0, Va * np.sin(gamma_angle)]
    gamma_line.set_data(Va_x, Va_y)

    # v1 vector (rotation vector with magnitude r)
    v1_x = [0, r * np.cos(theta)]
    v1_y = [0, r * np.sin(theta)]
    v1_line.set_data(v1_x, v1_y)

    # Calculate forces (lift, drag, Ft, and Fm) from the forces function
    L_vector, D_vector, Ft_vector, Fm_value = forces(t[frame], theta)

    # Ft vector (net aerodynamic force) origin at the end of v1
    Ft_x = [r * np.cos(theta), r * np.cos(theta) + Ft_vector[0]]
    Ft_y = [r * np.sin(theta), r * np.sin(theta) + Ft_vector[1]]
    Ft_line.set_data(Ft_x, Ft_y)

    # Now calculate Fm, which is the projection of Ft onto the direction perpendicular to v1
    # Unit vector along v1
    v1_unit = np.array([np.cos(theta), np.sin(theta)])

```

```
    # Direction perpendicular to v1 (rotated 90 degrees)
    v1_perpendicular = np.array([-np.sin(theta), np.cos(theta)])

    # Projection of Ft onto the perpendicular direction
    Ft_projection = np.dot(Ft_vector, v1_perpendicular) * v1_perpendicular

    # Fm vector is the projection of Ft onto the perpendicular direction
    Fm_x = [r * np.cos(theta), r * np.cos(theta) + Ft_projection[0]]
    Fm_y = [r * np.sin(theta), r * np.sin(theta) + Ft_projection[1]]
    Fm_line.set_data(Fm_x, Fm_y)

    return gamma_line, v1_line, Ft_line, Fm_line


# Animate
frames = len(t)
ani = FuncAnimation(fig, update, frames=frames, init_func=init, blit=True, interval=20)

plt.show()
```

Listing E.1: Code of the dynamics model.